PHASE TWO

FINAL TECHNICAL REPORT

RCSR GUIDELINES HANDBOOK

EES/GIT Project A-1560-001

By

E. F. Knott

Prepared for

DEPARTMENT OF NAVY
NAVAL ELECTRONIC SYSTEMS COMMAND
WASHINGTON, D. C. 20360

Under

Contract N00039-73-C-0676

April 1976

1976

ENGINEERING EXPERIMENT STATION
Georgia Institute of Technology
Atlanta, Georgia 30332

ENGINEERING EXPERIMENT STATION
Georgia Institute of Technology
Atlanta, Georgia 30332

(6) RCSR GUIDELINES HANDBOOK.

Phase Two Final Report on

EES/GIT Project A-1560-001

(9) Final technical rept. on Phase 2,

by

(10) E. F. Knott

(12) 152

Prepared for

DEPARTMENT OF THE NAVY
NAVAL ELECTRONIC SYSTEMS COMMAND
WASHINGTON, D. C. 20360

(11) 1 Apr 76

(14) GIT-A-1560-001-TR-P2

(15) Under

Contract N00039-73-C-0676

April 1, 1976

FOREWORD

This handbook was prepared by the Engineering Experiment Station at the Georgia Institute of Technology for the Department of the Navy, Naval Electronic Systems Command, under Contract N00039-73-C-0676. The Contracting Officer was R. M. Hill and the Technical Monitor was J. Foote, both of the Naval Electronic Systems Command.

For the purposes of internal control at Georgia Tech, the effort was designated Project A-1560-001. The Project Director was M. T. Tuley.

Although the bulk of this handbook is unclassified, some classified information has been used in order to show examples of radar cross section (RCS) and radar absorbing materials (RAM). In order to facilitate accessibility and handling, this classified information has been collected into Appendices B and C, which are bound together under separate cover.

Contract N00039-73-C-0676
Department of the Navy
Naval Electronic Systems Command
Washington, D. C. 20360

A-1560-001-TR-P2
Engineering Experiment Station
Georgia Institute of Technology
Atlanta, Georgia 30332

RCSR GUIDELINES HANDBOOK

by

E. F. Knott

ABSTRACT

This handbook is intended as a primer for people involved in ship architecture and design but who are not necessarily familiar with radar detectability factors. Its scope is therefore broad, but its depth is limited. Methods for reducing radar ship echo are described and demonstrated.

Modern surface ships are far from optimum shapes from the radar echo standpoint. They typically have many flat horizontal and vertical surfaces meeting at right angles, all of which constitute strong radar reflectors. Major improvements (reductions) in detectability can be made using a few simple techniques:

1. replacing flat surfaces with curved surfaces;
2. tilting upright surfaces away from the vertical;
3. angling intersecting flat surfaces at other than 90 degrees;
4. using screens;
5. installing radar absorbent materials.

Although these concepts are simple, we realize that incorporating them in ship design is not so simple. Each imposes its own brand of penalty, not the least of which is cost. Nevertheless, if detectability is to be reduced, the penalties must be paid.

ACKNOWLEDGMENT

The author is grateful for the encouragement of Mr. F. B. Dyer in preparing this document and to Mr. M. T. Tuley who reviewed the manuscript and made many valuable suggestions. The editorial comments of Mr. B. O. Pyron are also appreciated.

Mr. J. A. Koenig of the Naval Electronic Systems Command was particularly helpful in pointing out recent measurements and providing useful contacts during the project.

Special mention should be made of Mr. L. E. Carter of the Air Force Avionics Laboratory, Wright-Patterson Air Force Base, Ohio, who suggested important sources of information as well as supplying Figures C-1 and C-2 (Appendix C) for this handbook.

TABLE OF CONTENTS

*Appendices B and C have been separately bound and are classified CONFIDENTIAL.

LIST OF FIGURES

LIST OF FIGURES - Continued

LIST OF FIGURES - Continued

I. INTRODUCTION

A. Scope and Purpose

The successful execution of the mission of a modern warship or combatant vessel depends upon many factors, among them the fitness of the ship, the experience of her skipper, the effectiveness and maintenance of her equipment, and so on, but not least, her vulnerability to detection. It has become apparent in the last few years that the development of increasingly effective hostile detection systems threatens to reduce the mission effectiveness of a wide class of ships, and attention is now being given to methods of increasing survivability by reducing the probability of detection. Since the specific configuration of any vessel is determined by many factors involved in its mission, the final design represents a compromise between conflicting requirements. It is the purpose of this handbook to supply information and concepts leading to intelligent decisions in the resolution of conflicts involving radar detectability.

The handbook is intended primarily for people who, while competent in their own fields, are not necessarily familiar with electromagnetic theory. It addresses the radar cross section reduction (RCSR) problem of surface ships at sea, a class of targets particularly suited to the following techniques:

1. replacement or shielding of flat surfaces by curved surfaces
2. tilting upright surfaces away from the vertical
3. angling flat intersecting surfaces at other than 90 degrees
4. deployment of screens
5. application of radar absorbent materials (RAM)

The first four will be recognized as target shaping methods and guidelines are developed and explained in Section III. Although these methods are familiar to RCSR experts and are by no means new, quantitative results never before published are given (e.g., Figures 29 and 48). The use of radar absorbent materials, the fifth method listed above, is a broad topic that cannot be treated in depth in a book of this size, consequently the discussion of RAM in Section IV is restricted to an overview. Shaping and RAM can be applied simultaneously to achieve RCS reductions that neither could provide if applied separately.

Extensive mathematical derivations and equations are minimized, and much of the information is presented in the form of charts and graphs that can be understood and interpreted with a minimum of "homework." Many of these are generated with the aid of theoretical approximations because the theory is often sufficiently developed to give quite good results. In other cases the theory may not be perfect but is acceptably accurate to illustrate underlying concepts and principles. Occasionally we present empirical data which, by their nature, are the results of great quantities of experimental observations and measurements. A selection of experimental RCS patterns of simple targets is given in Section II and of ships in Appendix B (bound separately) in order to acquaint an unfamiliar reader with the radar characteristics of these targets and typical methods of displaying them.

It should be emphasized at the outset that radar cross section reduction is a study of compromises in which virtues are balanced against limitations, and this fact should become apparent in later sections. A reduction in RCS at one viewing angle is usually accompanied by an enhancement at another when target surfaces are re-shaped or re-oriented to achieve the reduction. However, if radar absorbent materials (RAM) are used, the reduction is obtained by the dissipation of energy within the material, thus leaving the RCS levels relatively unchanged in other directions. On the other hand, the use of RAM is a compromise paid for with added weight, volume and surface maintenance problems. Thus each approach involves its own form of trade-off.

The virtue of target shaping is that the penalties of added weight are low, and if certain viewing angles are unlikely, dramatic reductions can be achieved. On the other hand, the volume or distribution of stowage space may not be optimum, or the resulting shape may be weaker than the original, pound for pound, depending on the particular case. These remarks apply only to outer surfaces of hull, deck and superstructure, since the incident radar energy does not penetrate appreciably into the ship's interior spaces.

No matter which technique is employed, each decrement in RCS is obtained at successively higher cost. The first 10% reduction is usually quite inexpensive, while the next 10% is a little more expensive, the next more costly still, until a 95% total reduction may be prohibitively costly, in terms of dollars as well as trade-offs in weight, size and configuration. The cut-off point--deciding how much RCS reduction to incorporate--depends on a host of variables such as relative effectiveness, incremental cost, the ship's mission and so on, and since each class of vessel poses its own particular problems, this handbook cannot establish the optimum RCS design for the general case. However, the concepts and principles illustrated herein should make it easier to arrive at such a decision when specific ships are considered.

B. A Preview of the Handbook

"Round your plates, tilt your bulkheads and use absorbers in the flare spots."

This succinct bit of advice might constitute a 13-word RCS reduction handbook were it not for the uncertainties of which ones, how far, what kind and how much. The answers to some of these are provided in Sections III and IV, and where specific answers cannot be provided, guidelines and concepts are given as suggestions. Shaping is an attractive way to reduce RCS without adding much weight to the vessel, but its full effect is difficult to recover if a ship has been built without regard for RCS considerations. Because of the powerful influence of the sea surface, purely vertical surfaces should be avoided if at all possible and Section III tells how to select optimum tilt angles. The interaction of a vertical surface with the sea surface in the elevation plane is much like the interaction between a pair of mutually perpendicular vertical surfaces in the azimuth plane, hence surfaces should never intersect or meet each other at right angles. A method for selecting optimum angles of intersection is given by a simple mathematical formula. Section III also discusses the advantages of rounding otherwise flat surfaces and the analysis suggests that some, in fact, should not be rounded.

Section IV is devoted to radar absorbent materials and although some are discussed which may not be well suited to the shipboard environment, they are included for completeness. A list of commercial producers was solicited for product information but since many have gone out of business or discontinued their product lines, the sources of supply are disappointingly few. Some even declined to respond, even though they are still in business.

The principles laid down in Sections III and IV are utilized in a ship modeling program developed at Georgia Tech, which is described briefly in Section V. The individual and collective application of several techniques to an actual surface vessel configuration is tested by way of demonstrating their effectiveness.

While Sections III and IV represent the most direct and useful information in the handbook, Section II provides the basic background and concepts for more complete understanding of the RCS reduction problem. The nature of the echo properties of simple shapes is discussed and some experimental RCS patterns are displayed showing how they differ. The particular influence of the sea surface is described, since it acts like a rough mirror and tends to emphasize the effects of target reflections.

Section I offers even more basic information. Since the ship designer cannot be expected to be familiar with the terms, notation and language of the radar expert, such definitions are given in subsection C. The reader is free to skip that subsection, of course, but he may find himself referring back to it occasionally. Similarly, the principle of operation of radars is described in elementary terms in subsection D; in essence, a radar is a timer, and since the velocity of propagation of a radio wave is known, time can be converted to distance.

A bibliography is included in Appendix A, and only the more pertinent references have been chosen. Some of the documents are classified and we have attempted to assess their value to the typical reader by including comments in the bibliography.

C. Conventions and Definitions

1. Time Convention

Radio waves and signals vary harmonically with time and because of the mathematical convenience of representing sinusoidally varying functions as exponentials, the notion of phasors and complex numbers has become ingrained in electrical engineering. A phasor is a "snapshot" of a time-varying complex number taken at some reference time (usually at time zero), in which the time dependence is assumed to be either $e^{-i\omega t}$ or $e^{i\omega t}$, where $\omega = 2\pi f$ is the radian frequency in radians per second and f the actual frequency in Hertz (cycles per second). Actual field strengths and alternating signals consist of real quantities, of course, and the phasor notation is merely a mathematical convenience.

The assumed time dependence automatically implies that distance variations are given by the phasor e^{ikr}, where k is a propagation factor along the direction in which the distance r is measured. Therefore the function $e^{-i(\omega t - kr)}$ describes the temporal and spatial variation of electromagnetic fields. The product kr represents a phase angle which can be resolved into a unique angle between zero and 2π radians after all necessary multiples of 2π have been removed. The variation e^{ikr} implies that an increase in r produces an increase in the phase angle.

Surfaces of constant phase angle are planes for plane waves (hence the name), the planes being perpendicular to the direction of propagation. For waves emanating from a point source the surfaces of constant phase are concentric spheres and at distances far from the source, the local deviation of a spherical wave from a plane wave is small. For waves propagating in an unbounded vacuum the wavenumber $k=2\pi/\lambda$ radians per wavelength, where $\lambda = c/f$ is the free space wavelength and c is the velocity of light. The speed of light is taken to be 29.97925 cm per nanosecond or, equivalently, 11.80285 inches per nanosecond, a nanosecond being one billionth (10^{-9}) of a second. Note that one foot per nanosecond is a close approximation, being only 1.6% higher than the actual value.

2. Far Field Criterion

A common approximation made in considering the reflection or scattering of high frequency waves is that the distance from radar to target is much larger than any target dimension. This is the so-called far field approximation and it allows the incident wave in the vicinity of the target to be represented as a plane wave. Since the incident field phase fronts can never be planar unless the distance tends to infinity, there will always be some phase variation over the transverse target dimension. If this phase deviation is limited to $\pi/8$ radians then the familiar far field range criterion is the result:

$$R = 2D^2/\lambda \qquad (1)$$

This criterion has been a standard for many years for RCS measurements and a detailed critique of such standards is given by Kouyoujiam and Peters [27]. The criterion is commonly felt to give measurement accuracy better than 1 dB (26%), assuming perfect instrumentation.

By virtue of the appearance of the wavelength in equation (1), the standard far field range depends on frequency: the higher the frequency, the greater the range. This is illustrated in Figure 1, a plot of the far field distance as a function of target size for a selection of frequencies. Note, for example, that a target whose greatest dimension is 100 ft should be measured at a distance of 11.5 miles or better at a frequency of 3 GHz (3×10^9 cycles per second). It is difficult and often impossible to meet this criterion for ships because of their size, however, consequently the range is usually mentioned in the presentation of ship RCS data.

3. Relative Phase

The notion of phase is extremely important in the study of RCS and methods of RCS reduction. By way of example, consider a point target located a distance R from the radar. The phase of the return echo signal varies as e^{i2kR}, the factor 2 accounting for the double traverse of the path from radar to target and back. If another point

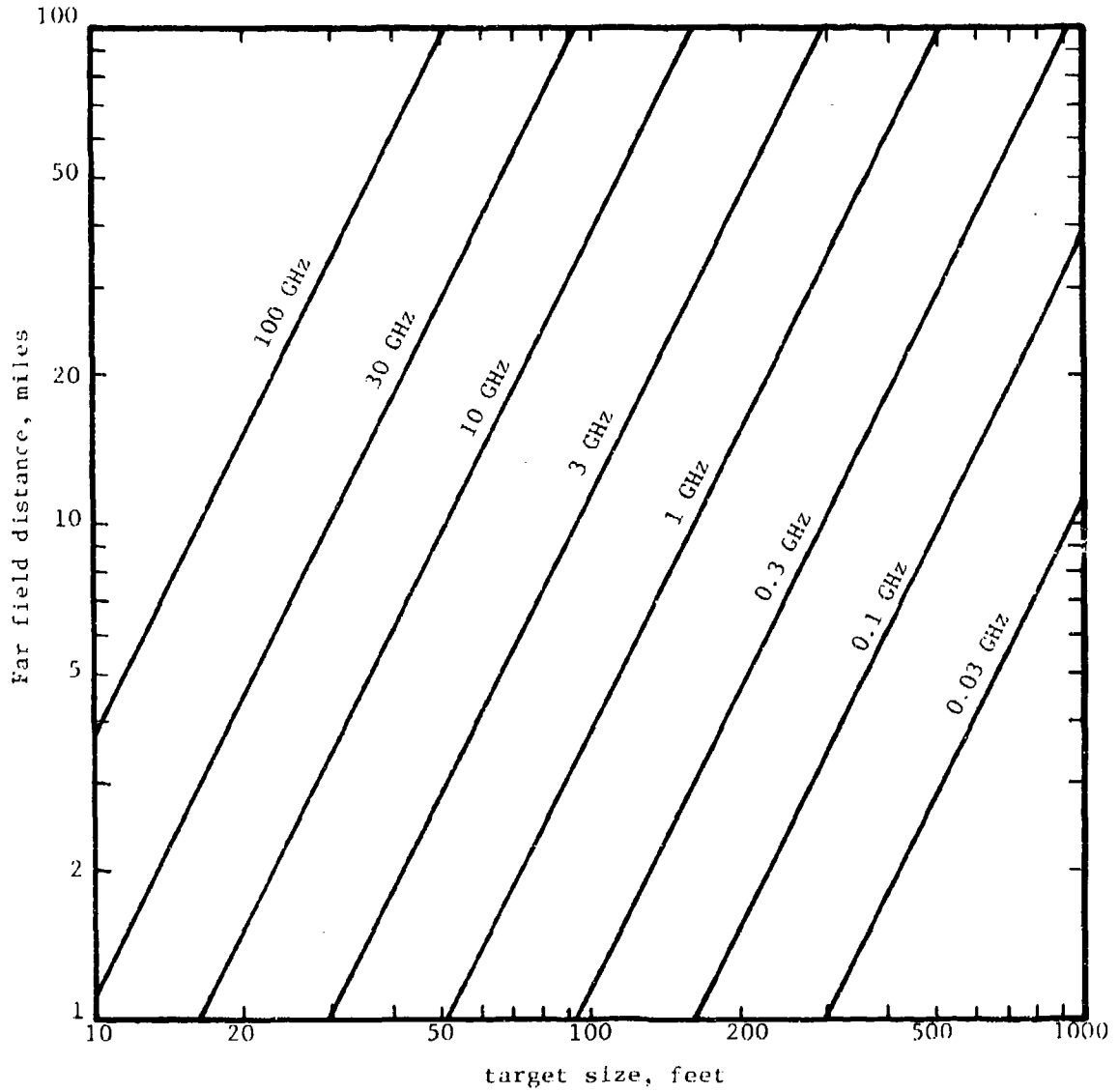

Figure 1. Far-field range criterion.

target is installed some distance d behind the first, the phase of its return is $e^{i2k(R+d)}$, since the energy propagates an additional distance of 2d. If we designate the amplitudes of the two signals by A and B, the receiver signal voltage will consist of the phasor sum

$$V = Ae^{i2kR} + Be^{i2k(R+d)} = (A + Be^{i2kd})e^{i2kR} \qquad (2)$$

Typically it is the received power that is recorded or displayed somewhere in the receiver circuits and this is proportional to $|V|^2$. Consequently, under steady state, continuous wave conditions,

$$|V|^2 = A^2 + B^2 + 2AB \cos(2kd) \qquad (3)$$

Therefore the received power depends on the relative spacing between the targets, as indicated by the cosine term, and will attain minimum and maximum values

$$|V|^2_{min} = (A-B)^2, \quad |V|^2_{max} = (A+B)^2 \qquad (4)$$

If the two targets have identical characteristics, say A=B, then it is possible for the receiver to sense no signal whatever from the two targets. This occurs whenever $2kd = n\pi$, where n is an odd integer, and is an example of one signal precisely cancelling another. The variation with distance is shown in Figure 2 for the simple case of two point targets for three amplitude selections.

Typical targets are obviously far more complicated than this and the effective separation between targets or target elements along the line of sight changes with viewing angle. Moreover their amplitudes (the coefficients A and B in the example above) themselves vary with viewing angle instead of being simple constants, hence the received signal from an obstacle such as a ship will change in a complicated manner with time or the relative motion of radar and target. This variation is due to the simple mechanism of relative phase variations, and is often called scintillation.

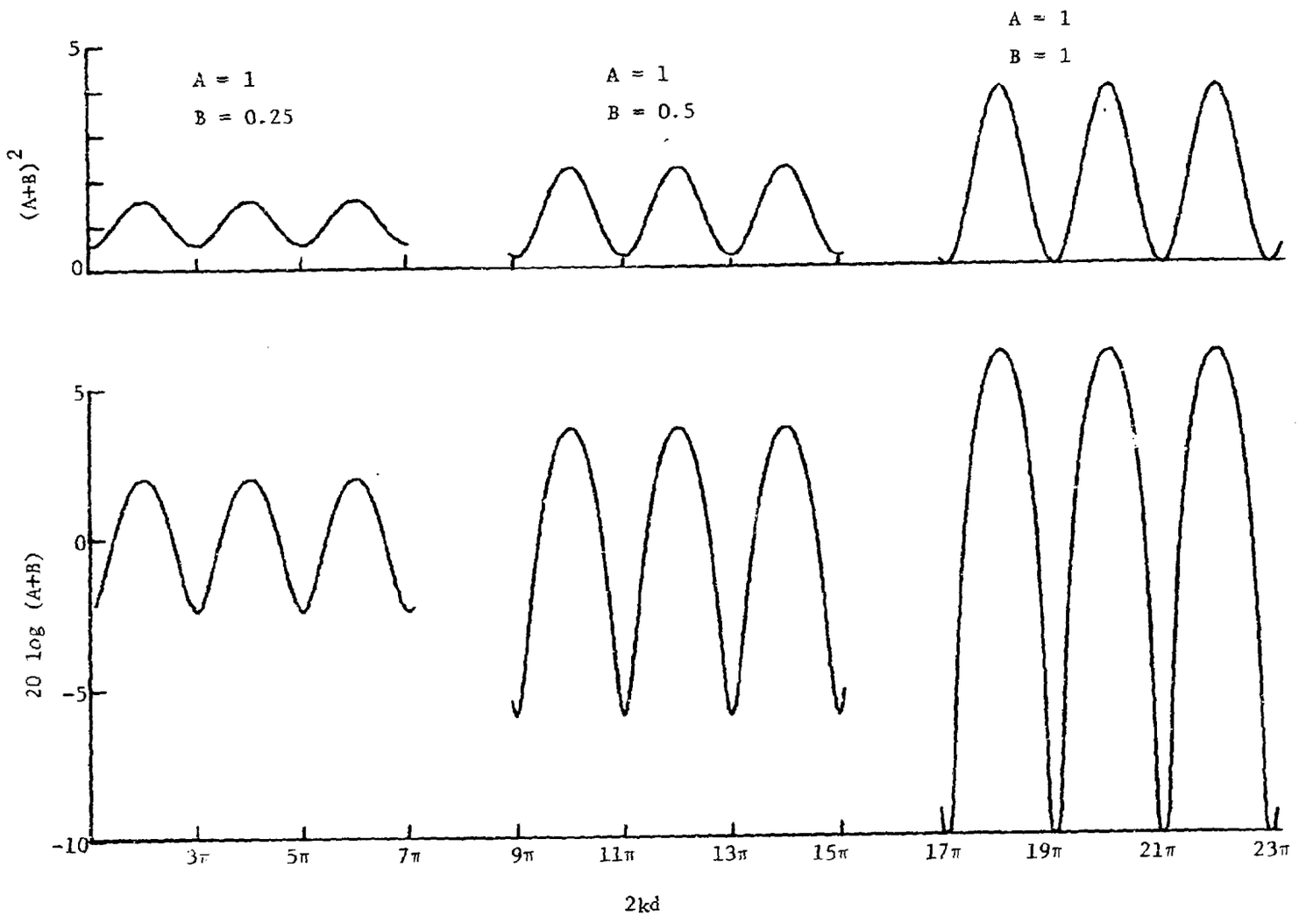

Figure 2. Variation in signal strength as a pair of targets move apart along the line of sight. Individual signal strengths are A and B, and the lower set of curves illustrate the effects of using the logarithmic decibel scale.

The concept of relative phase is also important in the design of radar absorbent materials intended to minimize surface reflections. When an incident electromagnetic wave strikes the outer surface of an absorbent layer, some energy is reflected and some is transmitted into the layer. The transmitted portion is attenuated as it travels through the material and will be reflected by whatever metallic bulkhead lies under the coating. This reflected wave will travel back to the surface, part being transmitted through the interface and part being reflected back toward the bulkhead again. The process continues indefinitely and as a result, the net reflection at the outer layer is due to a primary reflection of the incident wave plus contributions of an infinity of internal reflections, each smaller than the previous one. If the absorber layer is now adjusted so as to be a quarter wavelength thick, as measured within the material, then the fields reflected from the metal bulkhead will be out of phase with the primary reflection at the outer surface of the layer. Thus, in addition to the dissipation of energy in the coating, further reduction is obtained by "tuning" the electrical thickness of the layer, an exploitation of the notion of phase.

4. Scattering, Reflection and Radar Cross Section

The terms scattering, reflection and radar cross section are all related, but each has a distinct meaning. Scattering is the resulting spatial disposition of electromagnetic fields when an obstacle (a "scatterer") is inserted in an otherwise uniform field such as that of a plane wave. Energy from the incident field is "scattered" in all directions by the obstruction and since the scattered fields must obey well-known laws of physics, the resulting field distribution is deterministic and ordered. For high enough frequencies, implying objects large enough in terms of wavelengths, the fields can be found by applying the laws of optics, thus leading to the concept of "reflection." A reflection is understood to mean the process by which waves bounce off surfaces mirror-fashion according to Snell's law, which states that the angle of a reflected ray equals the angle of the incident ray. A reflection is therefore a high frequency (large object) specialization of the more generalized phenomenon of scattering.

Radar cross section is an effective area, as its name implies, but the area is a fictitious one that may or may not be closely related to

the physical area of the target. It is a measure of how big or how bright the target appears to the radar. It represents the area that would have to be carved out of an incident wavefront such that the power streaming through the cut-out would exactly match the power scattered back to the source by the target. The incident wavefront is customarily, but not necessarily, taken to be planar so that the power density is constant over the wavefronts, implying that the source is infinitely far away.

If the scattered fields are known for directions other than back toward the source (radar), the power can be calculated for these directions, too, and an equivalent area can again be specified. Thus a cross section can be determined for any scattering direction, but if the direction is back toward the radar, then the area is commonly called the radar cross section. A less frequently used term, but one that more accurately describes the process, is called the "backscattering cross section." Another is "echo area."

5. The Decibel Scale

Being an area, RCS can be expressed in any of several units, including square inches and square meters, or some other unit depending how the information is to be used. System designers prefer square meters while physicists like square wavelengths; occasionally a characteristic dimension of the target, such as length or diameter, may be squared and used as the unit of reference. Whatever unit is chosen, however, convention has established the decibel as the basic format for presenting or otherwise displaying radar cross sections. Borrowed from the field of acoustics, the decibel is ten times the logarithm (base 10) of the ratio of two numbers, in this case two areas. Thus if A is a radar cross section and A_o is the unit reference area,

$$\text{RCS in decibels} = 10 \log_{10} (A/A_o)$$

The square meter and the square of the wavelength are the two most common reference units for A_o. The notation "dBsm" is read "decibels

above a square meter" and "$dB\lambda^2$" is read "decibels above a square wavelength." Note that a cross section of zero implies $-\infty$ decibels, an unplottable number. The symbol dB is the standard abbreviation for the decibel.

The logarithmic scale has the effect of suppressing small numbers in favor of large ones, since the logarithm of a small number is a large negative number. Invariably the RCS of even simple objects is due to localized scattering centers on the object and as these scatterers change position along the line of sight due to changing aspect angle, sinusoidal variations in the net return occur as described above. As shown in Figure 2, the logarithmic presentation of such sinusoids has a distinct and recognizable form. Note that as the minimum values get closer to zero, the nulls in the decibel form of presentation become sharper and deeper. These sharpening characteristics have become familiar to engineers who routinely work with RCS data and we shall see other examples of them in later sections. Since RCS is proportional to power, and power to the square of a voltage or field strength, it is not uncommon to find data expressed as 10 log (P/P_o), where the P's are power levels or power densities or as 20 log (V/V_o), where the V's are voltages or field strengths.

6. Polarization and Impedance

Since an electromagnetic field describes the force that an electric or magnetic particle would experience when exposed to such a field, the fields have the vector properties of both magnitude and direction. The polarization of an electromagnetic wave is commonly referenced to the orientation of the electric vector and for most radars, horizontal and vertical are the two principal polarizations used. The electric field of a horizontally polarized wave lies completely in the horizontal plane, and that for a vertically polarized wave lies completely in a vertical plane. Some radars are circularly polarized, with the electric vector rotating as a function of space and time; a circularly polarized wave can be created by adding together two linearly polarized waves (one horizontal polarization and one vertical polarization) of equal amplitude but 90 degrees out of phase.

Large smooth surfaces do not significantly depolarize linearly polarized waves; the echo signal from such a target has essentially the same polarization as the transmitted wave. Circularly polarized waves tend to be converted from right circular to left circular upon reflection, or vice versa, hence circularly polarized radars are typically designed to receive the sense opposite to that transmitted. Some sophisticated systems transmit left and right circular on alternate pulses and resolve the received signal into its linear horizontal and vertical components. The purpose of such complex processing is usually to improve the signal-to-clutter ratio or to extract more information about the target than simply its location.

The concept of impedance has carried over from circuit theory to wave theory, because it is a concept usually acquired early in an engineer's education. It is usually defined as the ratio of the electric field strength to the magnetic field strength with both vectors being perpendicular to each other as well as the direction of propagation. It is a natural choice, since the units of electric and magnetic field intensities are volts per meter and amperes per meter, respectively, and the ratio has the units of ohms. The impedence of a wave traversing free space is 377 ohms and waves traveling in materials typically have lower impedances. The utility of the impedance concept will become more apparent in Section IV in connection with radar absorbent material design.

D. Basic Radar Principles

It is not the purpose of this handbook to review the principles of radar design, since such a task could easily consume several feet of library shelf. However, it does seem appropriate to mention some of the basic features of radar systems for the benefit of those readers who are not familiar with them. The limitations of time and space permit only a very brief discussion here.

The fundamental physical principle of radar is that a finite and measurable time elapses while an electromagnetic wave propagates between two points in space. A modern radar measures the time between the emission of a pulse of radio frequency (RF) energy and the reception of a target echo. Since the velocity of propagation is known with high accuracy, the measurement of elapsed time can be converted into a distance measurement along a radial path. The geometry of the path, and therefore the location of the target, can be estimated from a knowledge of the direction in which the emitter (the antenna) is aimed, this information typically being derived from angular position sensors attached to the antenna positioning mechanism.

The range of the system -- how far it can "see" -- depends on the amount of power transmitted, the directivity or gain of the antenna(s), the intensity of the target echo and the sensitivity of the receiving circuits. Some parameters can be adjusted to compensate for others; for example, the use of more directive antennas can reduce the amount of RF power that must be generated, but this requires larger antennas. The radiated power can range up to the megawatt region and frequencies may run from only a few MHz to tens or even hundreds of GHz.

In practice radars emit repetitive bursts of energy such as depicted in Figure 3, with the "off" time being much greater than the "on" time. The interpulse period is used for "listening" for return signals and the length of this inactive period is determined by such considerations as range ambiguity and total energy incident on the target. The pulse repetition frequency (the PRF or "rep rate") is typically hundreds of pulses per second or more and the pulse

duration can range from a fraction of a microsecond to hundreds of microseconds, depending on the particular design. Unsophisticated radars emit narrow band signals (i.e., nearly one frequency) while others have the capability to change frequency from pulse to pulse, or to vary the frequency within a given pulse. These schemes are usually designed to extract additional information about the target, to increase sensitivity or to overcome some countermeasure environment.

Figure 3. Example of emitted waveform. The interpulse period has been greatly compressed for display purposes.

The received signals often contain reflections from the sea or terrain in the vicinity of the target and tend to obscure the desired target reflections. Undesired signals are called "clutter" regardless of their origin, and even the returns from birds and insects have been known to confuse or obliterate target signals.

The target echo signal can be amplified and displayed for visual inspection in any of a variety of forms. The most familiar is the plan position indicator (PPI) in which the signals are superposed on a cathode ray tube along with a coarse, recognizable map of the topology surrounding the radar site. Other types of display include the amplitude of the return as a function of range or time or both. Often, as with synthetic aperture radars (SAR's), the signals are recorded for processing at a later time with special equipment. In this case the results of a regional mapping, say for the purpose of crop control or assessment, cannot be evaluated until the processing is complete, which could be several days after the data were recorded.

Moving targets shift the frequency of the return signal by an amount proportional to the radial component of the relative velocity between radar and target. Some systems exploit this basic phenomenon (the Doppler effect) to discriminate between stationary and moving targets. This is possible by the use of filters and signal processing techniques that extract the frequency "offset" of the Doppler spectrum. It should be noted that clutter may also have a Doppler characteristic by virtue of the real or apparent motion of a myriad of scintillating elements.

As suggested by Figure 3, a pulse can contain hundreds of cycles of the RF carrier wave and once the pulse has been emitted it can span thousands of feet of space as it propagates, the precise span depending, of course, on the pulse duration. For the purposes of this handbook it may be assumed that a pulse of radar energy completely brackets the target. Then for a substantial length of time (a few microseconds) the target return behaves as though the incident field had never been turned off and can be described as if it were a continuous wave (CW). This behavior makes it possible to analyze and predict the nature of the target scattering (reflection) properties, and even in those cases where the pulse is short, CW concepts can still be applied. For example, a reduction of the CW return of a target also reduces its short pulse return if pure cancellation methods are avoided.

II. RADAR CROSS SECTION

A. Basic Concepts

The interaction of an obstacle with an impinging electromagnetic wave is a phenomenon of academic interest in its own right as well as being one of the basic factors influencing radar design and operation. The incident field induces charges and currents on the surface of a metallic object, and inside a non-metallic body as well, which in turn radiate new fields to all points in space. These current and charge distributions satisfy well-established boundary conditions and the fields they radiate back toward the radar constitute the radar "echo."

From the standpoint of wavelength, electromagnetic scattering problems fall into three natural categories, depending on whether typical obstacle dimensions are much less than, comparable to, or much greater than the wavelength. These are called the Rayleigh, resonant, and optics regions, respectively. By virtue of the sizes of targets and the wavelengths involved in the typical marine environment, it is the optics region that will command our attention. The optics range of scatterer-to-wavelength dimensions is commonly called the high frequency range, but it should be emphasized that "high frequency" does not refer to actual frequencies; more precisely, it describes the condition that a scattering obstacle is many wavelengths in size.

High frequency scattering can be calculated or measured, and many studies of RCS make use of both approaches. Analytical methods represent approximate solutions of the wave equation (a second order partial differential equation), while any experimental apparatus required for a measurement constitutes an analog computer that solves the same equation. Each has its virtues, of course; a carefully controlled and instrumented experiment is likely to yield more accurate results, yet a calculation can be performed at low cost. On the other hand, each suffers its limitations; experiments can be very costly and

cannot be used at all if there is no target to measure. And while calculations can be applied to objects and targets that exist only in the mind or on paper, they can be inaccurate and cumbersome to implement.

The high frequency techniques most useful in the study of radar cross section are geometric optics, physical optics and the geometrical theory of diffraction (GTD), the latter being a relatively new theory introduced in the 1950's by J. B. Keller [29]. Geometric optics and physical optics have been used for many years as the basic tools for designing optical systems and studying diffraction, and many of the terms and notation have carried over into the microwave spectrum. Geometric optics is also known as "ray tracing" and most people are familiar with the diagrams given in elementary physics showing how light rays progress through a system of lenses. Geometric optics describes reflection and refraction of waves from an interface separating two media of different indices of refraction, as well as the reflection of waves from perfectly conducting surfaces. At microwave frequencies the reflection of radio waves from metallic surfaces takes place much as does the reflection of light from highly polished surfaces, even if not perfectly conducting.

These methods can be, and have been, used to predict the radar cross section of very complicated targets such as ships and aircraft, but only insofar as the target can be represented as an idealistic shape or collection of composite scatterers. In principle any target can be handled numerically by simply adding up the contributions of the returns from all illuminated parts, but since the elemental surface patch must typically be less than 0.1λ on any side, such a process is not feasible for objects more than a few tens of wavelengths in extent. Moreover, implementing a simple shadowing test to ascertain if a given patch of surface is shaded by any other patch is in itself a major undertaking. Thus, at least for the purpose of radar cross section control, it is often best to examine the behavior of a few classes of scatterers, or to model the target at only a handful of aspect angles, in order to judge how best to implement radar cross section control.

Since the energy emitted by a radar or scattered by an obstacle spreads away from the source, the field intensity decays with increasing distance. Field intensity is measured in units of volts per meter if the electric field is being measured, or amperes per meter if the magnetic field is being measured; power density is the product of the two in watts per square meter for example. It is customary to remove this dependence on distance by speaking of an equivalent area obtained by dividing scattered power by a power density; the definition of radar cross section is therefore commonly taken as

$$\sigma = \lim_{R\to\infty} 4\pi R^2 \left|\frac{E_s}{E_o}\right|^2 = \lim_{R\to\infty} 4\pi R^2 \left|\frac{H_s}{H_o}\right|^2 \qquad (5)$$

where E_s and H_s are the electric and magnetic field strengths of the wave scattered by the target and E_o and H_o are the corresponding field strengths of the incident wave at the target. This ratio, which is much like finding an area by dividing a force by a pressure, is therefore a measure of scattered power and the definition serves to shift the range (distance) dependence to the measurement system so that RCS becomes strictly a characteristic of the target and not the parameters of the system used to measure the echo.

This method of characterizing the target simplifies the job of radar design. The design problem itself invariably involves the radar range equation at one stage or another, which establishes the relation between echo power received, power transmitted, range and the nature of the obstacle giving rise to the echo. The relation is

$$P_r = P_t \frac{G^2\lambda^2\sigma}{(4\pi)^3 R^4} \qquad (6)$$

where P_r and P_t are the received and transmitted powers, respectively, G is the gain of the transmit/receive antenna, σ is the radar cross section of the target and R is the range (the distance between target

and radar). Note that because R is raised to the fourth power, the received power decays rapidly with increasing range.

The antenna gain G is a measure of how effectively the radiated energy can be concentrated along the desired line of sight: the higher the concentration, the greater the gain. Gain is a dimensionless quantity and can be as large as 1000 or more for large dishes and perhaps as small as 10 or less for small antennas. The radar range equation can be expressed completely in terms of dimensionless ratios by dividing numerator and denominator by the fourth power of the wavelength,

$$P_r/P_t = \frac{G^2}{(4\pi)^3} \frac{\sigma/\lambda^2}{(R/\lambda)^4} \qquad (7)$$

Since only dimensionless quantities are involved, the decibel (logarithmic) form of representation is particularly useful. This form also shows why it is convenient to express radar cross section in terms of square wavelengths.

The radar designer may now make some appraisals of how his system must perform for a given target (σ/λ^2) detectable at a given range $(R/\lambda)^4$. How much should he increase his P_t for a reasonable G? Or how sensitive must his receiver be (P_r) for fixed G and P_t? The design problem must also include many other factors, such as weight and size, the effects of clutter, the variations in operator performance and so on, but the radar range equation is the only way that RCS can enter his design considerations. Therefore the designer needs to know something about expected radar cross sections of anticipated targets.

B. Examples of RCS Measurements

Although a ship is a very complicated structure from the standpoint of electromagnetic scattering, it can be represented as a collection of relatively simple scatterers. Even if the number of

scatterers is large, there are only a few classes of shapes, hence it is of interest to show the RCS characteristics of common shapes found on ships. Several such patterns are presented in Figures 4 through 14.

These patterns were recorded on Georgia Tech's Compact Indoor Measurement Range, which makes use of a paraboloidal dish to generate a plane electromagnetic wave in a relatively short space[36]. Since the incident field is uniform even near the dish, the customary far field requirement is avoided and the target can be placed quite close to the dish. A CW cancellation system is used for the measurements, in which a sample of the transmitted signal is adjusted in both phase and amplitude, and then added to the return signal so as to cancel residual reflections from the walls and nearby objects. The received signal is calibrated by the substitution of a known object in place of the test target, the known object typically being a metallic sphere or cylinder whose radar cross section is known theoretically to a high degree of accuracy. The calibrated target return is recorded as a function of aspect angle using a conventional pattern recorder.

Figure 4 is the RCS pattern of a square metallic plate six inches on a side. The measurements were carried out at a frequency of 9.40 GHz, for which the wavelength is 1.255 inches. The theoretical broadside echo is 8.2 dBsm and the measured peak is not too far from this value. The incident electric polarization was vertical and the plate was rotated about a vertical axis, with one pair of plate edges being in a vertical plane. The series of peaks and nulls on either side of the main lobe are due to the echoes of the edges going in an out of phase with each other due to the changing aspect angle. The pattern in Figure 5 is of the same plate but oriented with its edges angled 45 degrees from the vertical (i.e., the axis of rotation lay on a corner-to-corner diagonal). In this orientation there are no edges parallel to the incident polarization and the sidelobes drop off much more rapidly. This is an example of the difference between cases 4 and 8 of Table I (page 37) and shows how target orientation affects the RCS pattern.

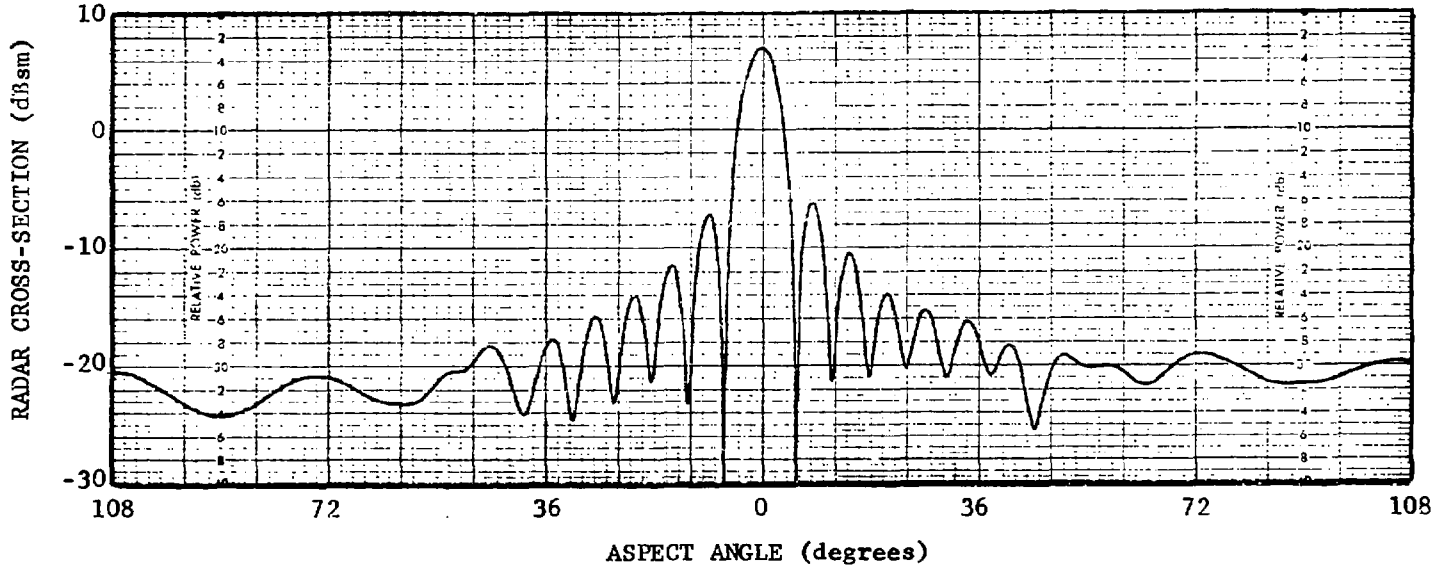

Figure 4. RCS pattern of a square plate with one pair of edges in the measurement plane.

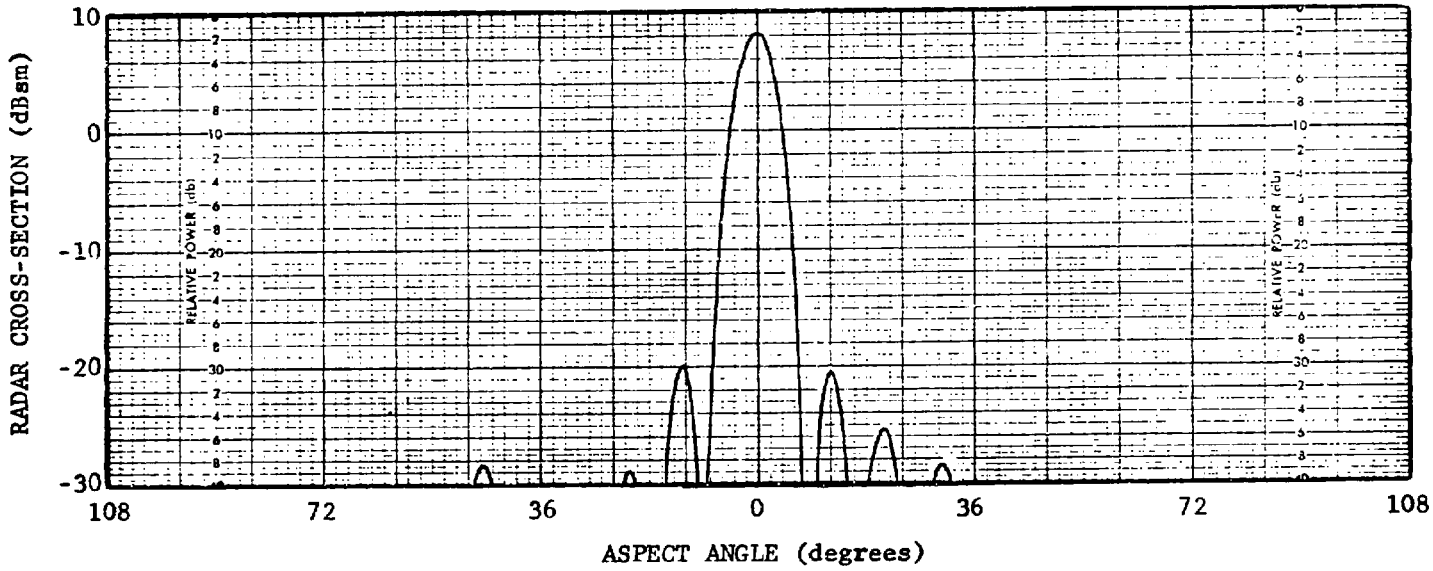

Figure 5. RCS pattern of a square plate with the plane of the measurements containing diagonal corners.

Figure 6 is the pattern of a solid right circular cylinder 9.5 cm in diameter and 31 cm long. The sharp, narrow lobes on either side of the pattern are due to the broadside reflection and the broad lobe in the center of the pattern is due to the flat disk presented by the cylinder when seen end-on. Because the end dimensions are much smaller than the length, the pattern features are much broader. Figure 7 is the pattern of a hollow cylinder 10.2 cm in diameter and 30.2 cm long. Note that because the lengths of the solid and hollow cylinders are comparable, the lobe structure in the broadside regions are similar. However, the patterns are different in the end-on region. The end-on return from the hollow cylinder is complicated by the fact that energy can be reflected from the far end as well as the near end, and the energy may flow through the inside as well as the outside. On the other hand, if the cylinder had been of small enough diameter, no energy would have propagated down the inside because the dimensions would not have been great enough to support the wave structure inside.

Figure 8 is the RCS pattern of a 90-degree dihedral corner reflector with square faces 17.9 cm along a side. The broad central part of the pattern is due to the interaction of the two faces, with the incident wave being reflected twice, once from each face. The peaks at either side of the pattern are the returns from the individual faces and the ripples in the central part of the pattern are due to the sidelobes of the individual face patterns.

The broad double-bounce return can be reduced by angling the two faces of the dihedral at some angle other than 90 degrees, and Figures 9 and 10 are the results for acute and obtuse dihedral angles, respectively. The angle of the dihedral for Figure 9 is 80 degrees; note that the specular face returns have moved outward from the center of the pattern. The broad double-bounce contribution has been substantially reduced and, because of partial shadowing, so have the specular face returns. The acute angle, however, gives rise to a triple-bounce component that produces minor peaks at $\pm$ 30 degrees aspect. Opening the dihedral angle to 100 degrees produces the pattern of Figure 10 which is

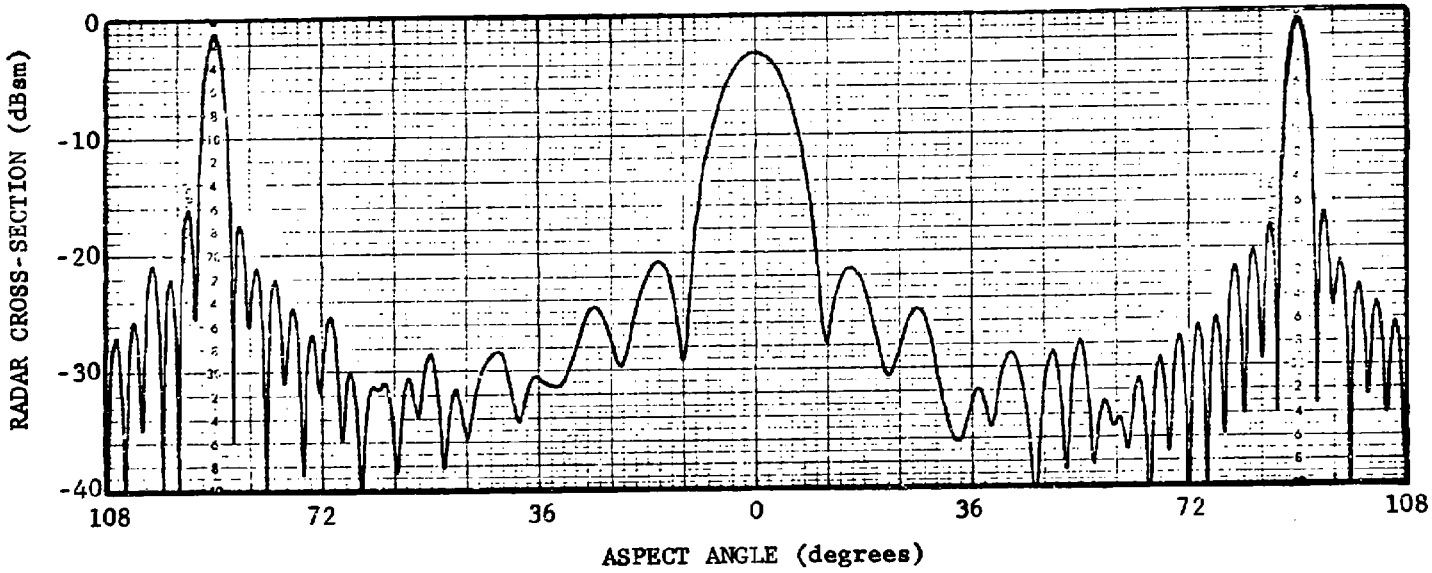

Figure 6. RCS pattern of solid cylinder 9.5 cm in diameter and 31 cm long at 9.4 GHz.

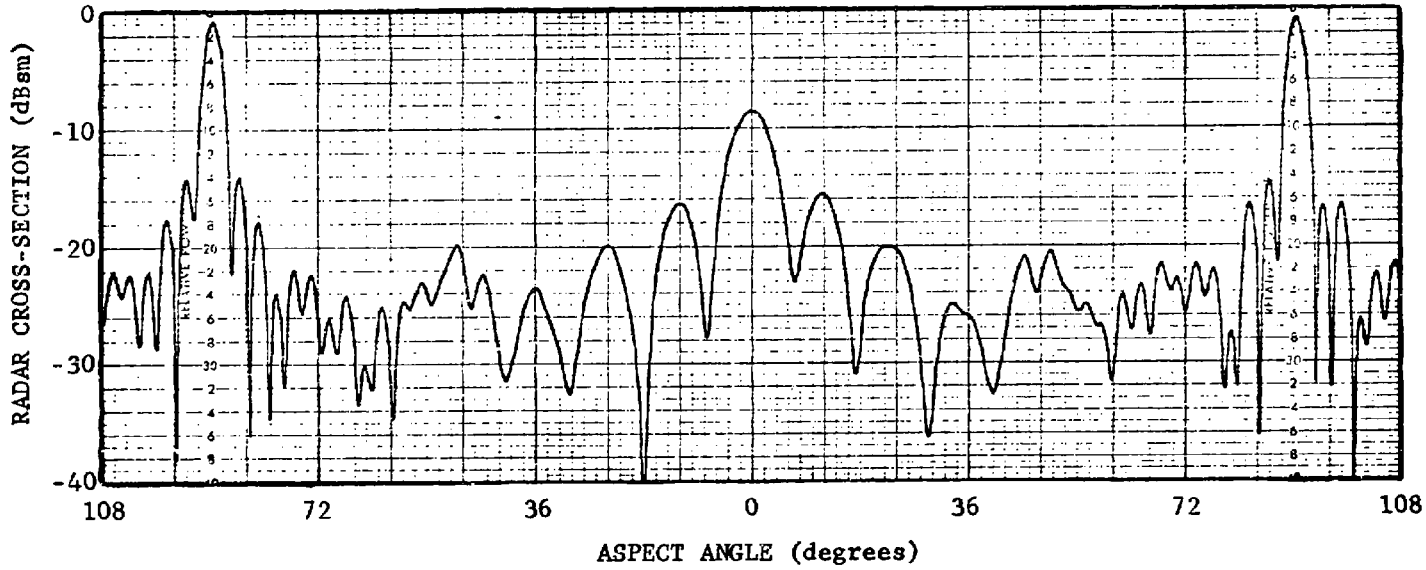

Figure 7. RCS of hollow cylinder 10.2 cm in diameter and 30.2 cm long at 9.4 GHz.

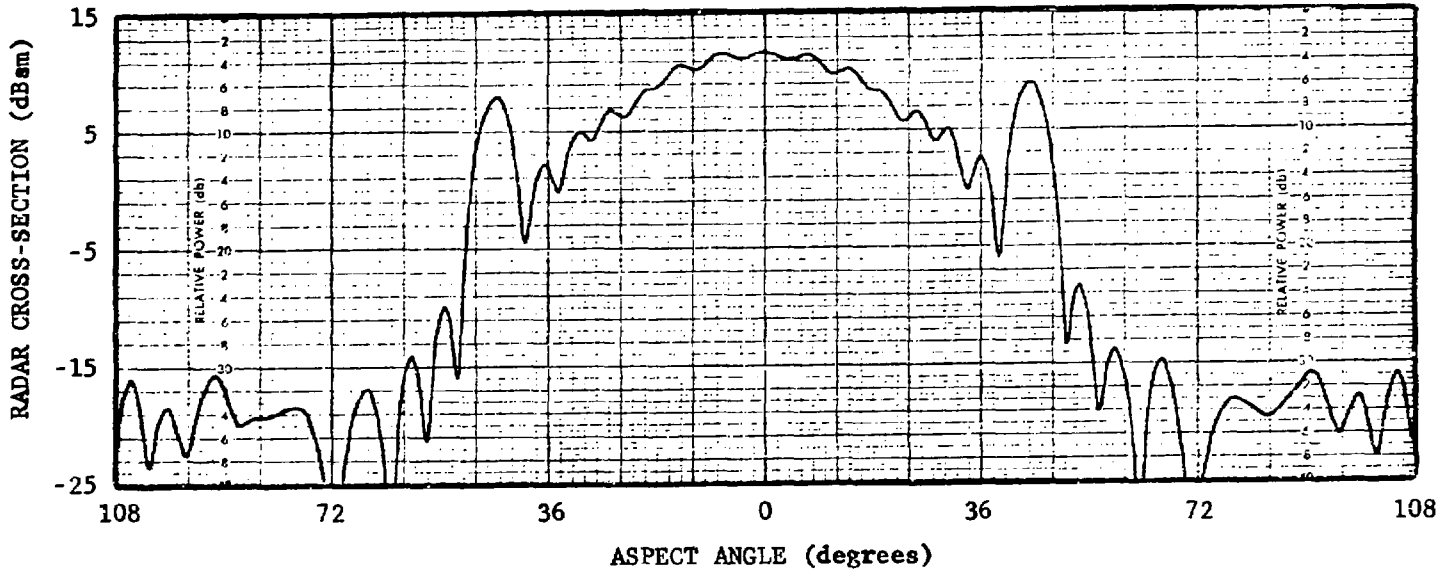

Figure 8. RCS pattern of a 90-degree dihedral corner with square faces 17.9 cm along a side.

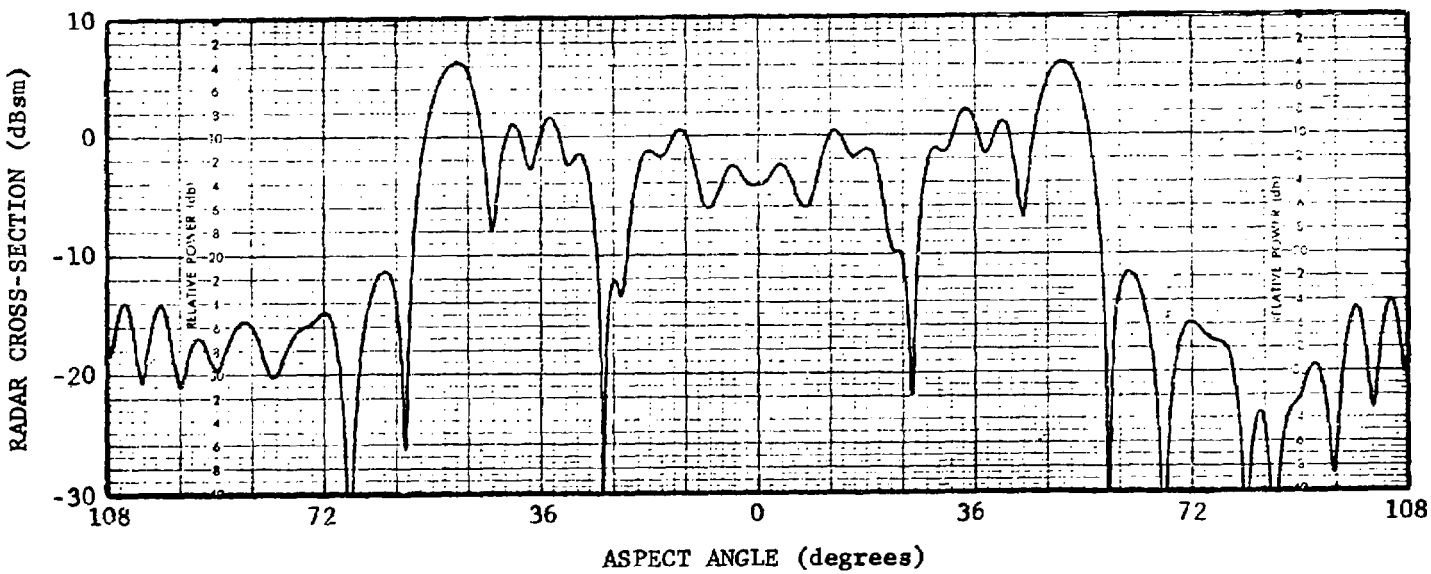

Figure 9. RCS pattern of an 80-degree dihedral corner with square faces 17.9 cm along a side.

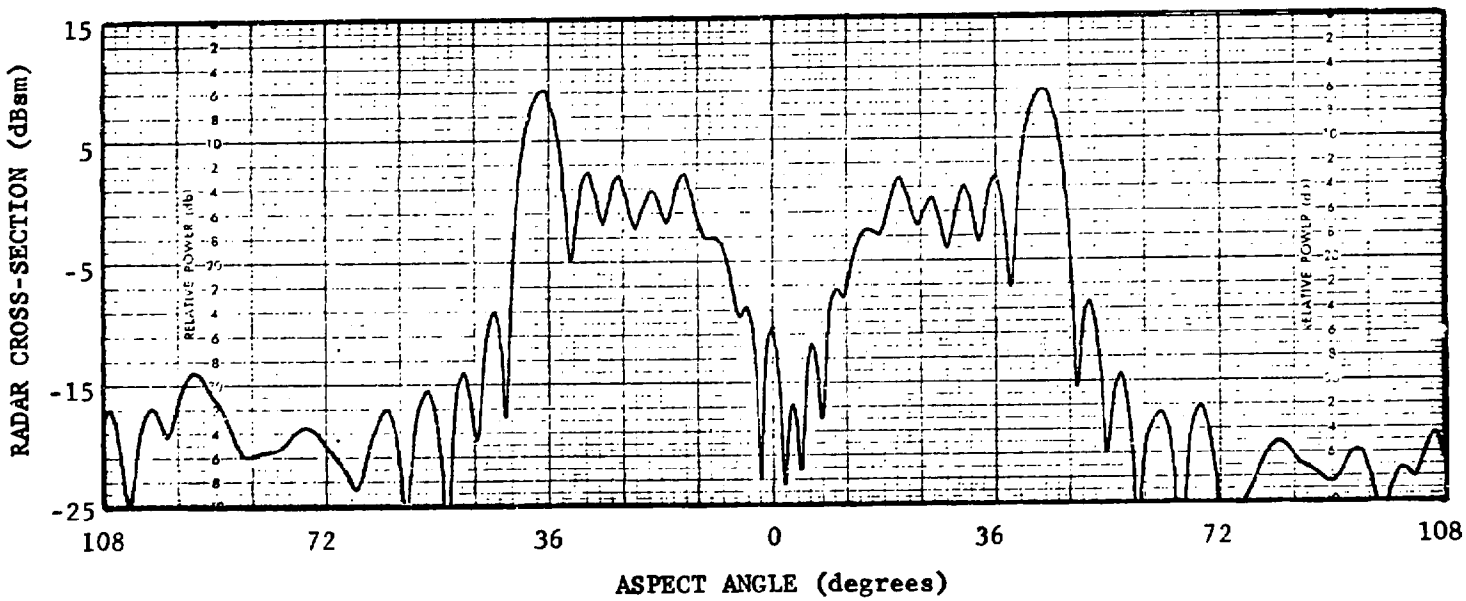

Figure 10. RCS pattern of a 100-degree dihedral corner with square faces 17.9 cm along a side.

not dissimilar to that of Figure 9, but has a much reduced double-bounce component around 0 degrees and lacks a triple-bounce component. Reducing the echoes of dihedral corners is considered in more detail in Section III.

Figure 11 is the RCS pattern of a trihedral corner formed by the intersection of three mutually perpendicular faces. Each face is a right isosceles triangle with leg lengths of 14.5 cm. The perpendicularity of the faces is responsible for the very broad pattern and an incident wave suffers three internal bounces before being reflected back to the radar. Figure 12 is also a trihedral corner pattern, but one whose faces are angled only 80 degrees apart. The faces are again isosceles triangles, but with leg lengths 11.9 cm long. Although the smaller leg length is partly responsible for the lower RCS level of Figure 12, the primary reason for the reduction is the non-perpendicularity of the faces. The pattern level of Figure 12 is about 12 dB lower than that of Figure 11, but only 1.7 dB of this difference is due to the smaller size of the 80-degree trihedral. The remaining 10.3 dB difference is because of the reduced angle between the faces. Thus the reduction available from tilting the faces is applicable to trihedral as well as dihedral corners.

Figure 13 is the pattern of a right circular cone 19.63 cm long and 5.11 cm in diameter. The broadside flashes on either side of the pattern occur at an aspect angle corresponding to incidence at right angles to the slanted surface, hence they do not lie at the 90-degree aspect angle. The broad lobe at the center of the pattern is actually due to the base of the cone, even though the tip is pointed toward the radar. The scattering due to the tip itself is very small. Even though the "nose-on" return is due to the base, objects like cones have smaller cross sections than cylinders of approximately the same size. See Figure 6, for example.

Figure 14 is the pattern of an ordinary corrugated cardboard carton, 19 cm wide by 19 cm long by 12 cm tall. This figure shows that the echoes from non-metallic objects, although smaller than metallic objects, are not necessarily negligible. The pattern is complicated by partial reflection from surfaces and corners, along

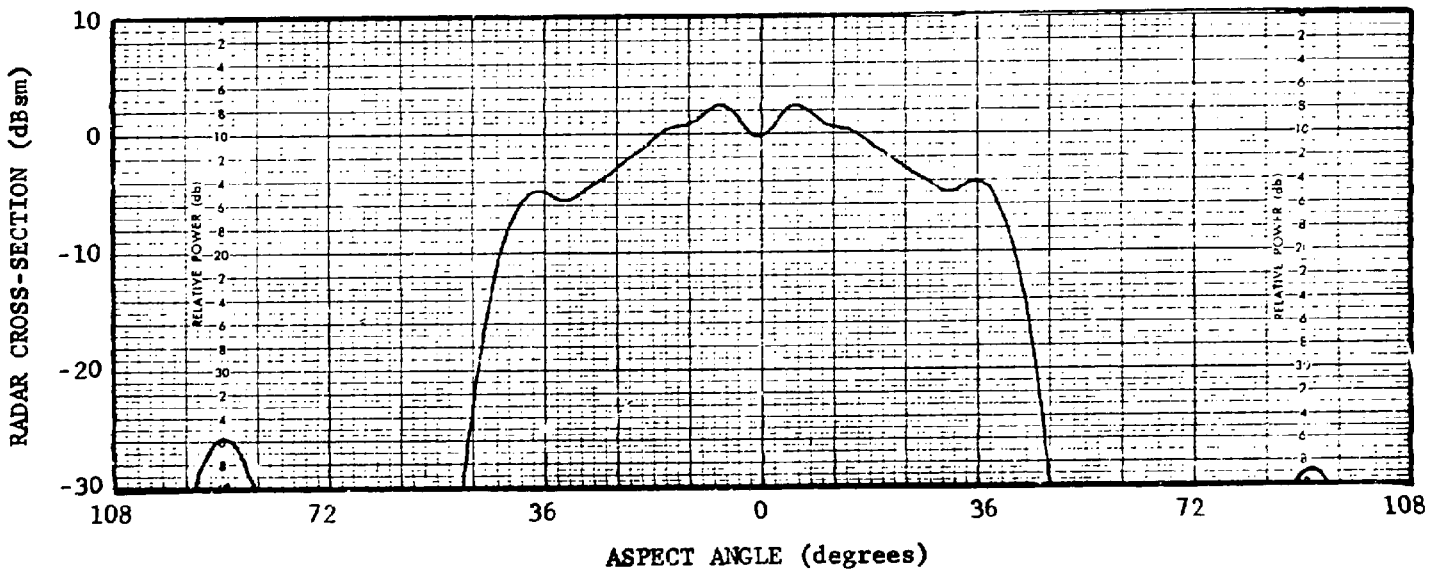

Figure 11. RCS pattern of a 90-degree trihedral corner with a leg length of 14.5 cm.

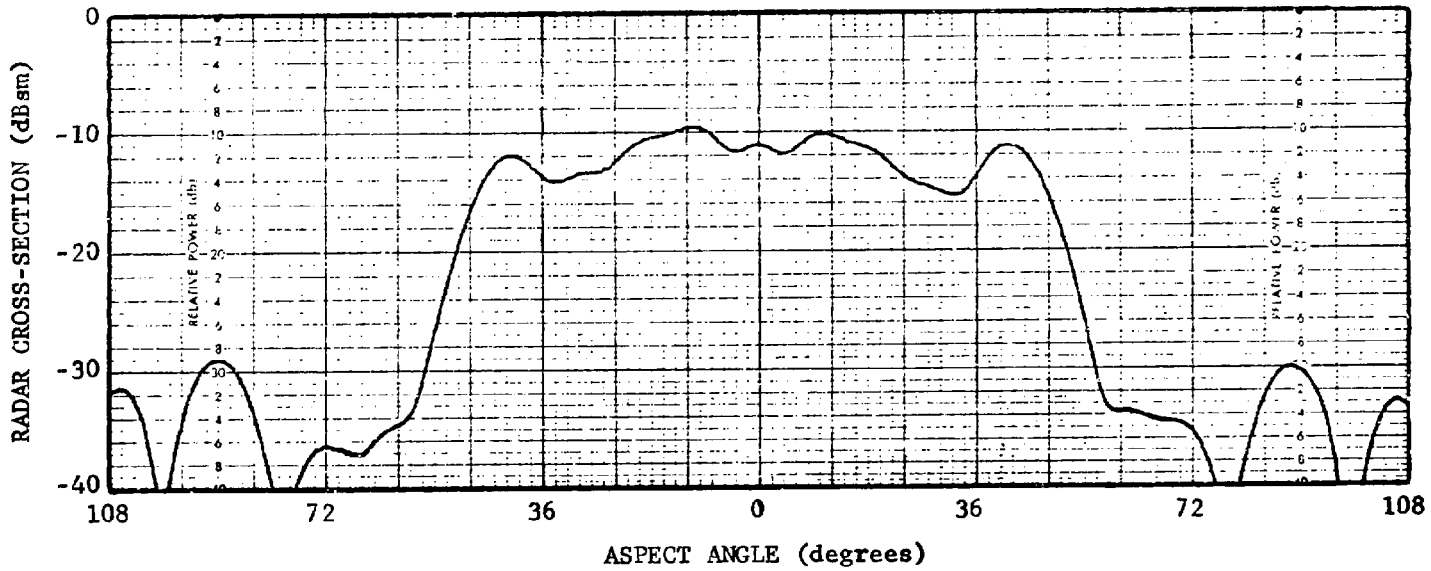

Figure 12. RCS pattern of an 80-degree trihedral corner with a leg length of 11.9 cm.

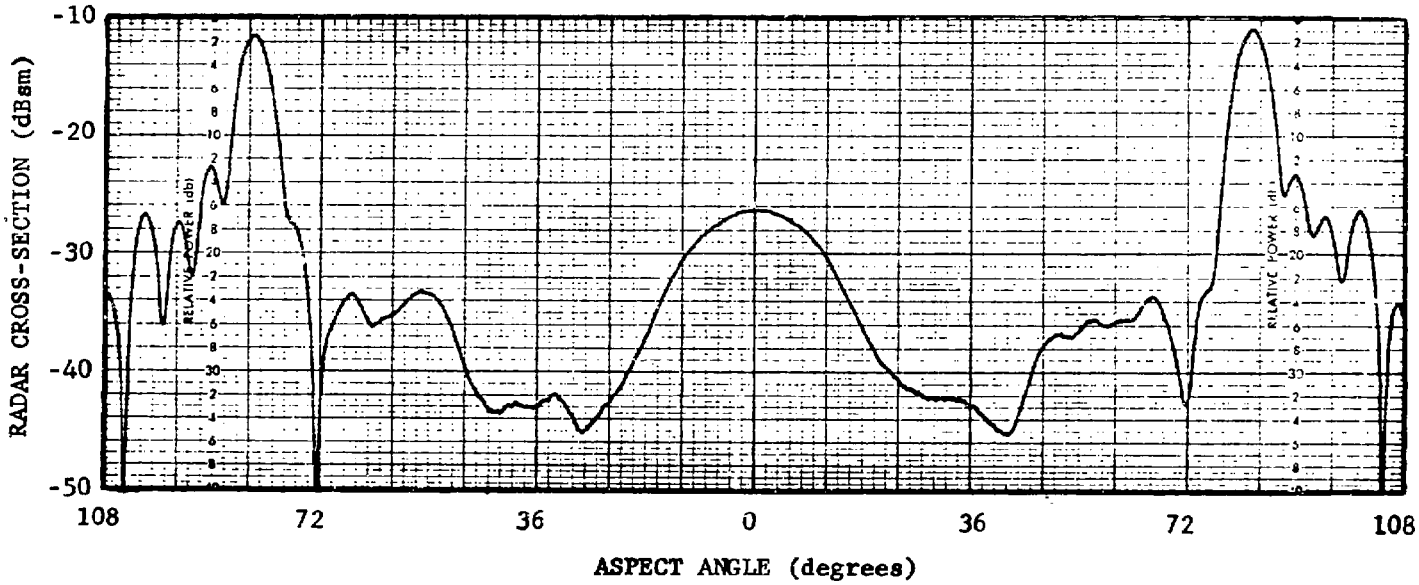

Figure 13. RCS pattern of a right circular cone 19.63 cm long and 5.11 cm in diameter at 9.4 GHz.

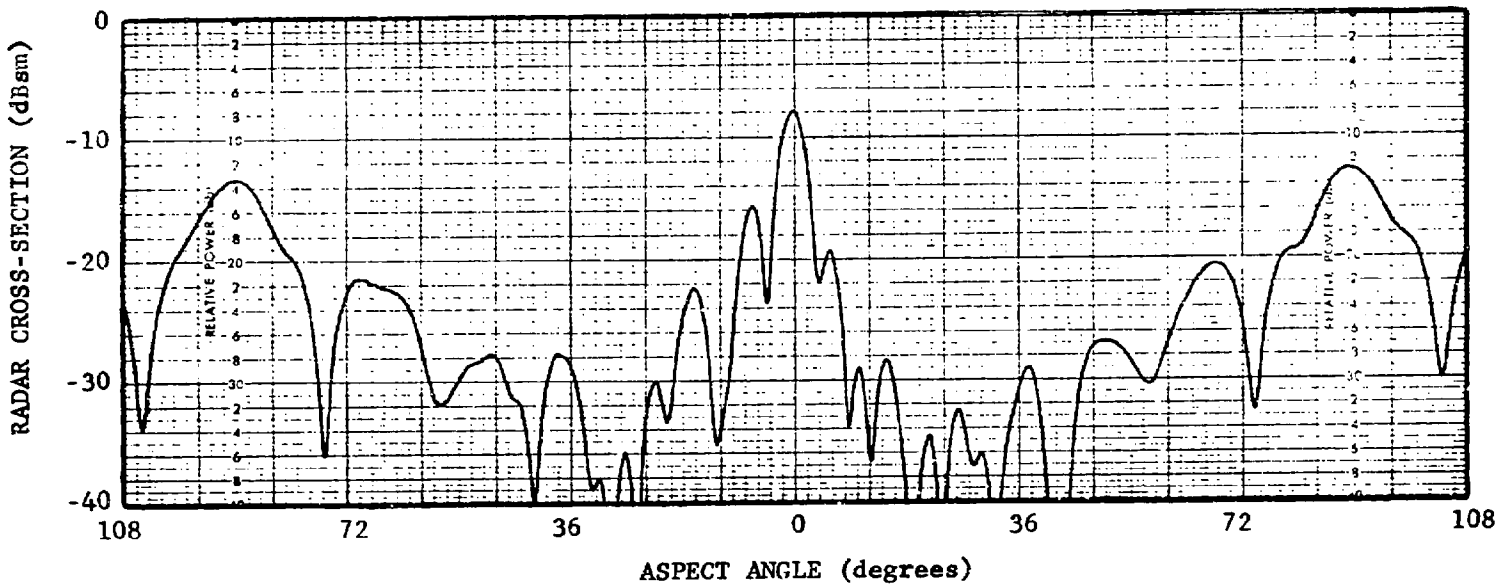

Figure 14. RCS pattern of cardboard carton 19 cm wide, 19 cm long and 12 cm tall at 9.4 GHz.

with partial transmission of the incident wave through the inside of the box, which thus illuminates internal surfaces. It is of interest to note that the RCS is greater than that of the metallic cone of Figure 13 at almost all aspect angles.

Figures 4 through 14 thus represent the RCS pattern characteristics of some of the scattering shapes that may be found on ships. These patterns were taken under static conditions in which the distance to the target is held fixed and the target orientation and aspect angles are derived from simple position indicators (selsyns) mounted in the target rotating mechanism. The situation is quite different under dynamic conditions in which an actual vessel is to be measured in its ordinary environment. Firstly, due to the presence of innumerable scatterers going in and out of phase with each other as relative position changes, with some popping into or out of view behind others, the total target echo executes many oscillations or scintillations, even with very small changes in viewing angle. Moreover, even if the ship is moored in a fixed position, the echo signal will still fluctuate in time due to the influence of the sea surface. Consequently it is only some average value, either in time or angle, that conveys any useful information.

In addition, there is no simple mechanism attached to the ship that allows a direct read-out of orientation or aspect angle. The task is complicated if the moving ship is viewed from a moving platform (e.g., an aircraft), and is only a little less complicated when the radar is fixed in an attempt to measure the RCS dynamically. In its ship RCS measurement program, the Naval Research Laboratory (NRL) uses a shore-based radar and time recordings are made of the target coordinates (range, azimuth and elevation) and the ship's gyro reading. These data allow the relative aspect angle of the target ship to be computed in subsequent data processing. Example of dynamic measurements of ship RCS are in Appendix B and were abstracted from Reference [10], which reports measurements of seven classes of ships.

C. Hierarchy of Scattering Classes

Elementary scatterers can be listed or arranged according to the frequency dependence of their scattered fields, and such a list

is highly illustrative. The amplitude of the scattered field depends not only on the shape of the body, but on its orientation with respect to the radar as well. Thus the list suggests which shapes ought to be considered in devising a low RCS design either for retrofitting an existing structure or for designing one yet to be built. The heirarchy of scattering types is listed in Table I and sketched in Figure 15, and represents an extension of the abbreviated list of Crispin and Moffett [30].

The last column of Table I displays the frequency dependence of the scattering types and since high frequency conditions have been assumed (i.e., scatterer dimensions large compared to the wavelength), flat structures are the least desirable and vertices are the most desirable. Flat plates viewed at normal incidence have the largest radar cross sections of any shape in the list, with the return varying with the square of the frequency. Thus, if the frequency is doubled, the RCS of a flat structure viewed at normal incidence will quadruple, an increase of 6 dB. Singly curved surfaces show a linear dependence on frequency while doubly curved surfaces have none. That is, the RCS of doubly curved surfaces such as spheres and ellipsoids tends to remain constant (at constant viewing angles) as the frequency is varied. The return from vertices varies inversely as the square of the frequency, hence these might be classed as the most desirable shapes as long as they can be oriented for non-specular conditions. However, an assembly of vertices is always interconnected by edges and surfaces, and it is impossible to meet the non-specular requirements. Thus the vertex, although an inherently low RCS shape, is idealistic and not at all suited for practical applications to ships.

In attempting to reduce the RCS of a structure, its shape and orientation should first be examined to see if it can be replaced by one appearing somewhere below it in the list, preferably one as low as possible. Since the table includes the effect of orientation as well as the class (or type) of obstacle, the reduction may

Case	Surface class or Type of scatterer	Examples	Orientation	Frequency dependence of RCS (exponent of frequency)
1	flat surface	plates, disks	normal incidence	2
2	singly curved surface	cylinders, cones	broadside, specular	1
3	doubly curved surface	spheres, ellipsoids, paraboloids	specular	0
4	straight edge	plate edge, wedge	$\perp$ to edge length	0
5	flat surface	rectangular plate	non-specular incidence, in plane $\perp$ to edge	0
6	curved edge	disks	non-specular	-1
7	singly curved surface	cones, cylinders	off broadside	-1
8	flat surface	rectangular plate	not $\perp$ to any edge	-2
9	straight edge	wedge	oblique incidence	-2
10	vertex	cone tip, corner of polyhedron	non-specular	-2

Table I. Hierarchy of scattering classes or features.

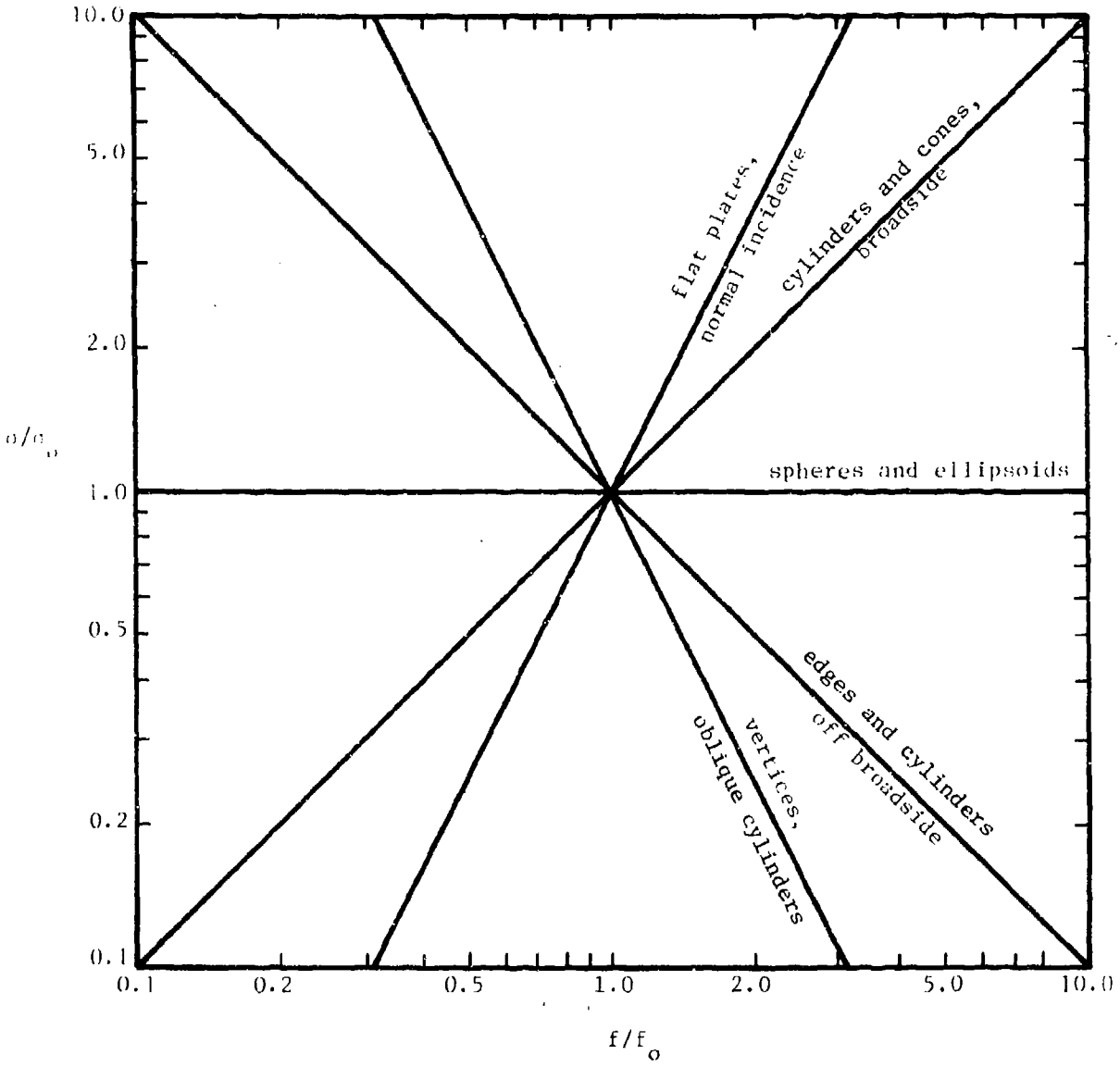

Figure 15. Frequency dependence of the radar cross sections of several scattering objects.

possibly be accomplished by a change in orientation alone. For example, a substantial reduction in the RCS of a flat plate can be achieved if the plate is swung away from normal incidence, thereby shifting the echo characteristics from case 1 down to case 5. Even greater reduction can be obtained by insuring that no plate edges are perpendicular to the line of sight, dropping the condition even further down the list to case 8. Note, however, that such changes in orientation may be fruitless if all viewing angles are equally likely, since the large specular echo is merely shifted toward some other direction in space.

In the event all viewing angles are equally likely, the surface might be reshaped or enclosed by a different surface having a lower RCS. By way of illustration, consider a square flat plate enclosed by a cylinder or sphere just large enough to accommodate the plate, as depicted in Figure 16. The echoes from these three targets can be reconstructed and compared using the theory of physical optics which, for objects of this size and shape, has been repeatedly demonstrated as a good approximation of measured results. The theoretical returns are given by

$$\sigma = \begin{cases} \frac{\ell^2}{\pi} \left[kw \cos\theta \, \frac{\sin(kw \sin\theta)}{kw \sin\theta} \right]^2 & \text{(flat plate)} \quad (8) \\ ka\,\ell^2 & \text{(cylinder)} \quad (9) \\ \pi a^2 & \text{(sphere)} \quad (10) \end{cases}$$

where ℓ is the vertical dimension of the plate or cylinder, w is the width of the plate, a is the radius of the cylinder or sphere,

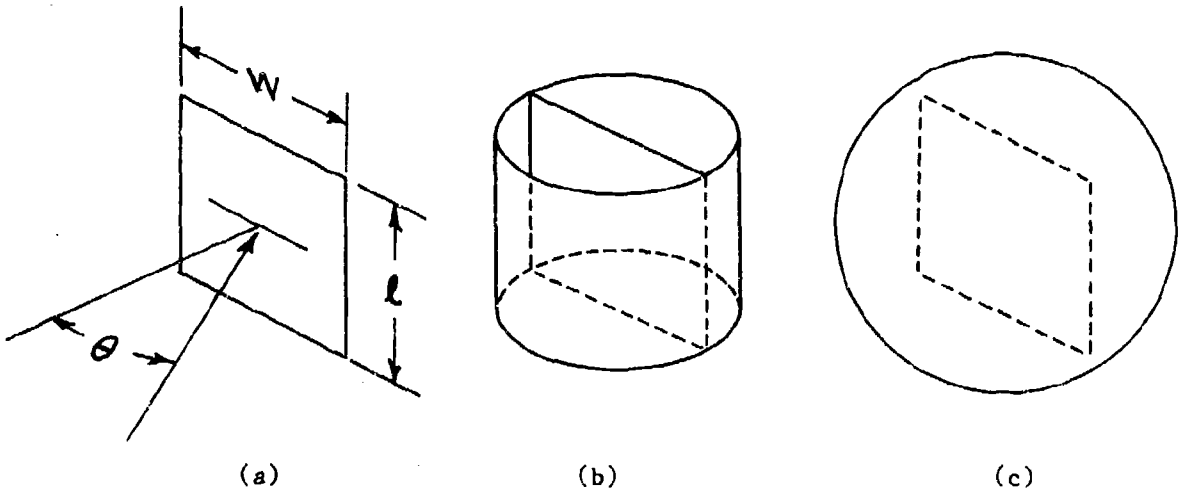

Figure 16. Radar cross section of flat plate (a) can be reduced by replacing it or enclosing it with cylinder (b) or sphere (c).

$k = 2\pi/\lambda$ is the free space wavenumber and θ is the aspect angle as shown in Figure 16. In order to enclose a flat plate whose width is equal to its length, the radius of the cylinder must be $a = \ell/2$ and the radius of the sphere must be $a = \ell/\sqrt{2}$. Note that the RCS of the cylinder and sphere are independent of θ, since these two objects are rotationally symmetric about the axis normal to the plane containing the direction of incidence.

The radar cross section patterns are plotted for an arbitrary plate length of 25 λ in Figure 17; note that the RCS has been normalized to the square of the plate length. The pattern of the flat plate shows the characteristic sin x/x behavior of uniformly illuminated apertures and has a large specular value (at $\theta = 0$) for broadside incidence. The amplitude falls off by more than 30 dB as the aspect angle swings toward $\pm$ 15 degrees, making it clear that a substantial reduction in RCS is available if the plate can be oriented so as never to be seen broadside. The cylinder return, in sharp contrast, is constant and lies some 20 dB below the specular plate return. Similarly, the return from the sphere is constant and lies nearly 30 dB below the specular plate echo. Thus, dramatic reductions in RCS are potentially available for certain target orientations.

However, the display of Figure 17 also illustrates another principle: that a reduction of RCS at one angle is usually accompanied by an enhancement at another. For example, the flat plate pattern at aspects of $\pm$ 10 degrees is 10 dB, while that of the cylinder is 19; consequently the 20 dB reduction obtained at 0 degrees is offset by a 9 dB increase at $\pm$ 10 degrees. Moreover, the plate return is reduced only over an angle (in this case) of about 4 degrees, while it is enhanced over an angle of nearly 30 degrees. Thus while the enhancement is not as great as the reduction, it is more persistent. Whether this is acceptable or not depends in large measure on the specific details of the particular RCS reduction task at hand and upon mission requirements; in some cases, it may not be at all acceptable.

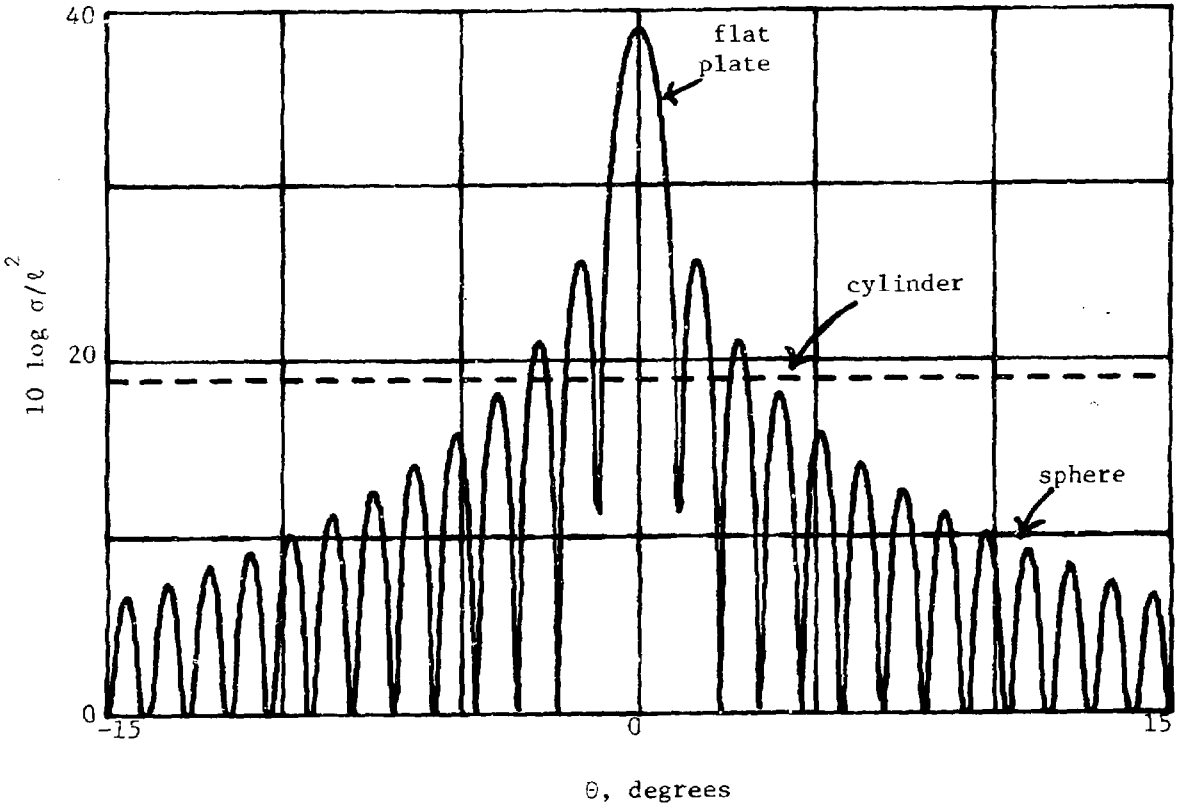

Figure 17. RCS patterns of flat plate, circular cylinder and sphere.

D. The Ship-Sea Radar Environment

The presence of the sea surface in a marine target environment is the singular feature that complicates almost all aspects of the radar-target interaction. In addition to the return from the target itself via direct illumination, energy is also scattered from its image in the sea surface via a signal bounce off the water. Moreover, the ocean waves themselves produce an echo signal which tends to obscure the target and is called by many names, including sea return, sea echo and sea clutter. Even the air above the water causes aberrations because the index of refraction varies with height and ray paths are not straight. Hence the target may not actually be where it appears to be, much as a stick, when thrust into clear water, appears to be bent.

1. Sea Clutter

Sea and land clutter are often described in terms of a dimensionless ratio, σ^o, defined as the radar cross section of the sea per unit area of illuminated surface.* Thus defined, σ^o is a radar-independent property characterizing the surface roughness, for if the sea were perfectly smooth there would be no return from it unless viewed from directly overhead. In order to estimate the sea clutter return power the illuminated area must be calculated from a knowledge of the radiation pattern of the radar antenna and its position and orientation in space. Although the parameter σ^o is independent of the radar characteristics, it does depend on at least five parameters: the angle of arrival of the incident wave, the wavelength, the polarization, the sea state (i.e., the roughness) and the relative azimuth of the radar antenna with respect to the ocean wave pattern (upwind,

*Convention has established that the "o" be superscript rather than subscript when referring to sea clutter.

downwind, etc.)

Since σ^o is a dimensionless ratio, it is commonly expressed in dB. Because of the sheer variety of the parameters involved, it is difficult to characterize for all conditions, and often for specific conditions. Even in the short time between incident pulses it changes, often by several dB from pulse to pulse, so that time averaged power is the only meaningful description. A variety of theories have been put forth which attempt to predict the magnitude of the sea clutter, but none models the return with high accuracy. An alternative to the theoretical approach is to devise an empirical model and to determine the necessary constants by systematically varying all significant parameters. This is not easy, of course, since many parameters such as wind speed, direction, sea state, etc. are uncontrollable. Thus one must be content to use experimental data when they exist and phenomenological or theoretical models when they don't. Empirical formulas have been developed that are reasonably good, although deviations of 10 dB or more may be typical.

At low grazing angles sea clutter seems to be generated by the wave crests in a moderate sea, the return increasing with the number of whitecaps and the wave height. For quiet seas the return seems to arise from capillary waves, which are small amplitude waves (of the order of an inch or less) induced by highly local wind conditions. These tend to disappear quickly when the wind abates, unlike swell. The clutter tends to be greater for vertical polarization than for horizontal, and is greater when the ocean wave crests are seen from right angles than when viewed along their length. Figure 18 (taken from Reference 26) is presented as an example of sea clutter variation with increasing grazing angle for several frequencies and wind speeds. It should be emphasized that these graphs are for illustration and that more information can be found in the citations in the Bibliography in Appendix A.

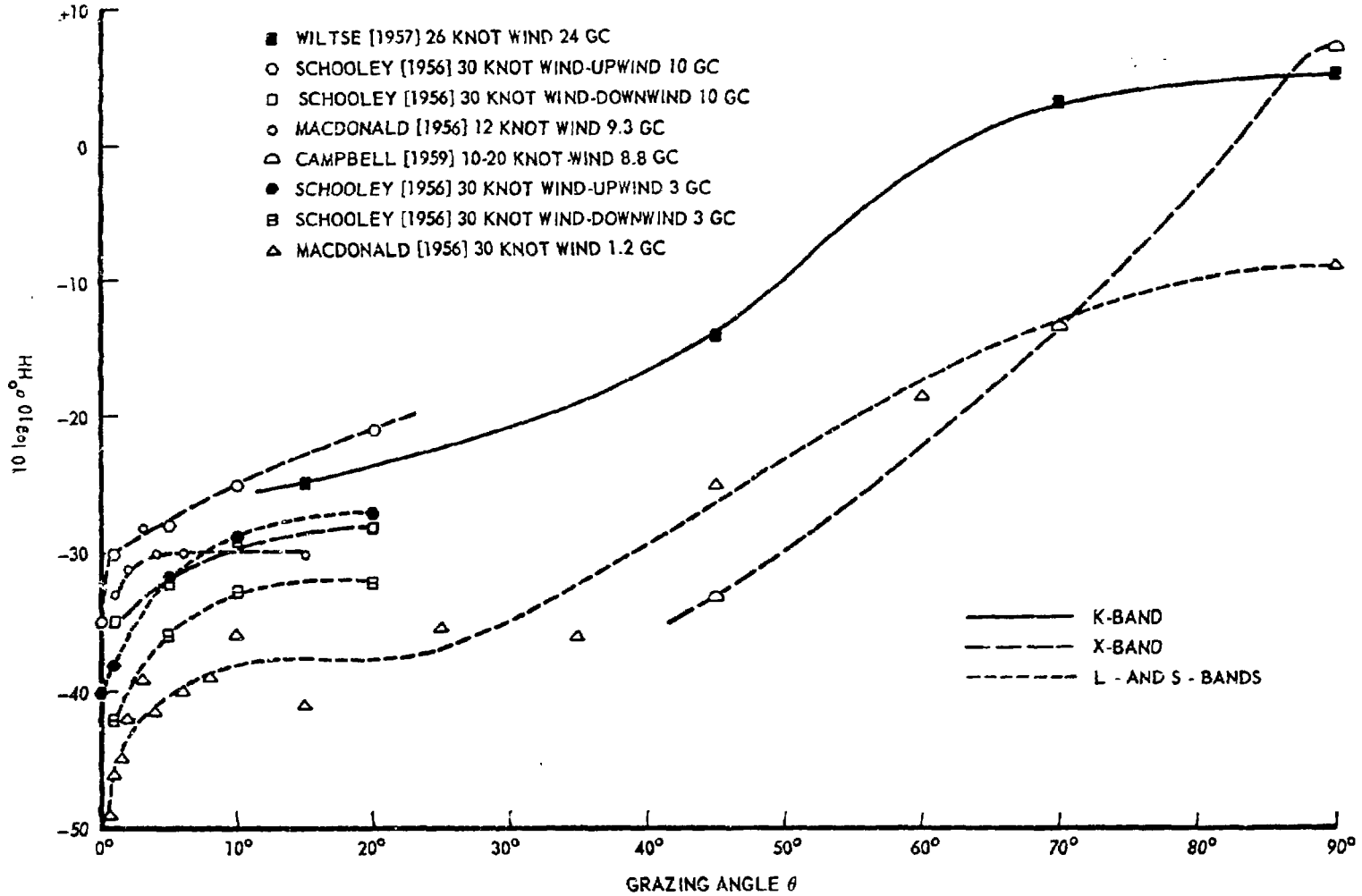

Figure 18. Measured values of σ^{o}_{HH} versus grazing angle (from Reference 26).

2. Reflection Coefficients

Sea clutter is, of course, the return from the surface in a backward direction; even for substantial grazing angles it is much smaller than the energy bounced off the surface in the forward direction. If it were not for the roughness of the surface, this forward scattering could be calculated quite accurately based on a knowledge of the dielectric constant of sea water, obtained, for example, from laboratory measurements made under closely controlled conditions. The strength of an electromagnetic wave reflected from an interface between two different media, such as the water surface, is given by the classical Fresnel reflection coefficients, one each for vertical and horizontal polarization. The Fresnel coefficients are complex numbers, implying that the phase of the wave is shifted upon reflection; for horizontal polarization, the phase shift is very nearly 180 degrees for all angles of incidence, meaning that the sense of the electric polarization vector is reversed upon reflection. The reflection coefficient for vertical polarization has a characteristic dip for low grazing angles, signifying that much of the incident energy is transmitted into the water instead of being reflected. The phase angle is near 180° for incidence angles near the horizon, 90° at the reflection coefficient null, and becomes nearly zero for angles above 20° or so. Plots of the Fresnel reflection coefficients are shown in Figures 19 and 20 for typical frequencies and dielectric properties of sea water. Such a plot implies a perfectly flat smooth surface.

As a result of the reflection, the total field structure in the vicinity of the target consists of an interference pattern produced by two signals. One signal is the incident wave, whose vertical component of incidence is toward the water, and the other is the reflected wave, whose vertical component is upward. The addition of the two produces a standing wave pattern in the vertical direction, sketched for the ideal case of a perfectly flat smooth surface in Figure 21.

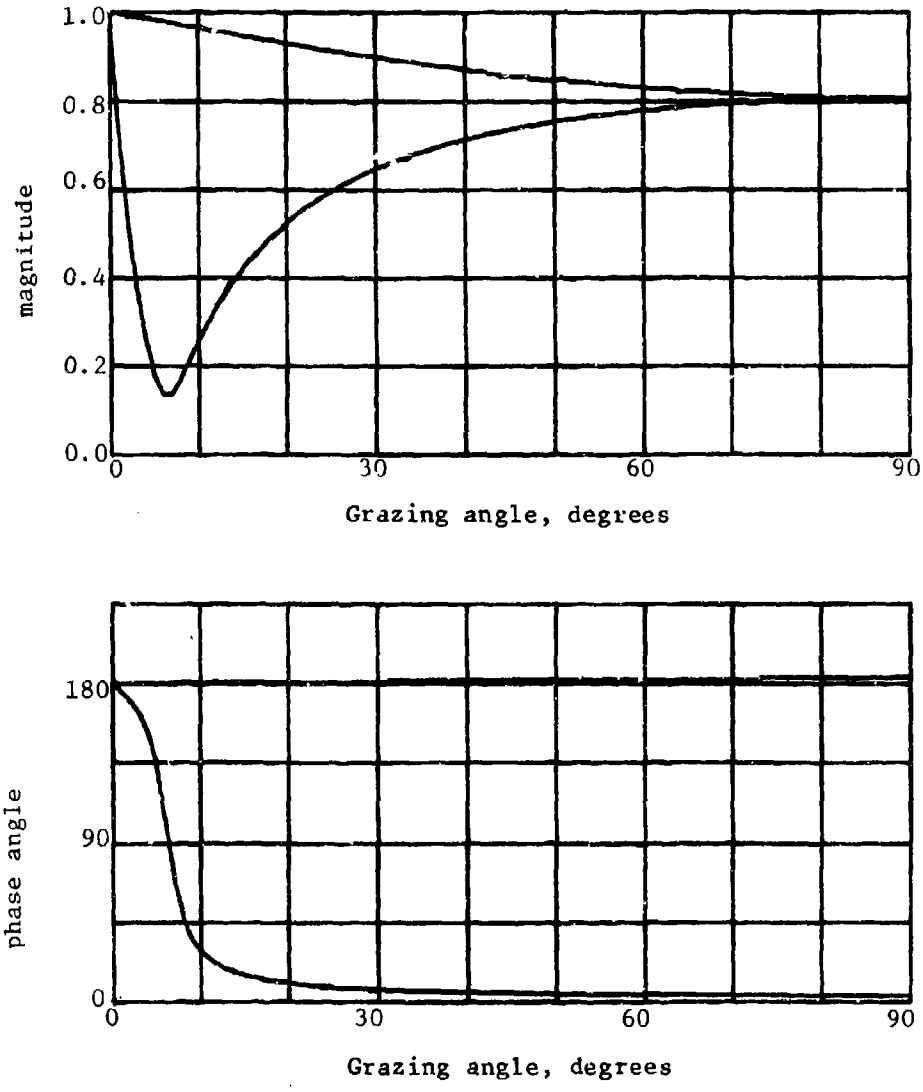

Figure 19. Fresnel reflection coefficients of sea water at 3 GHz. The upper trace in each plot is for horizontal polarization and the lower is for vertical.

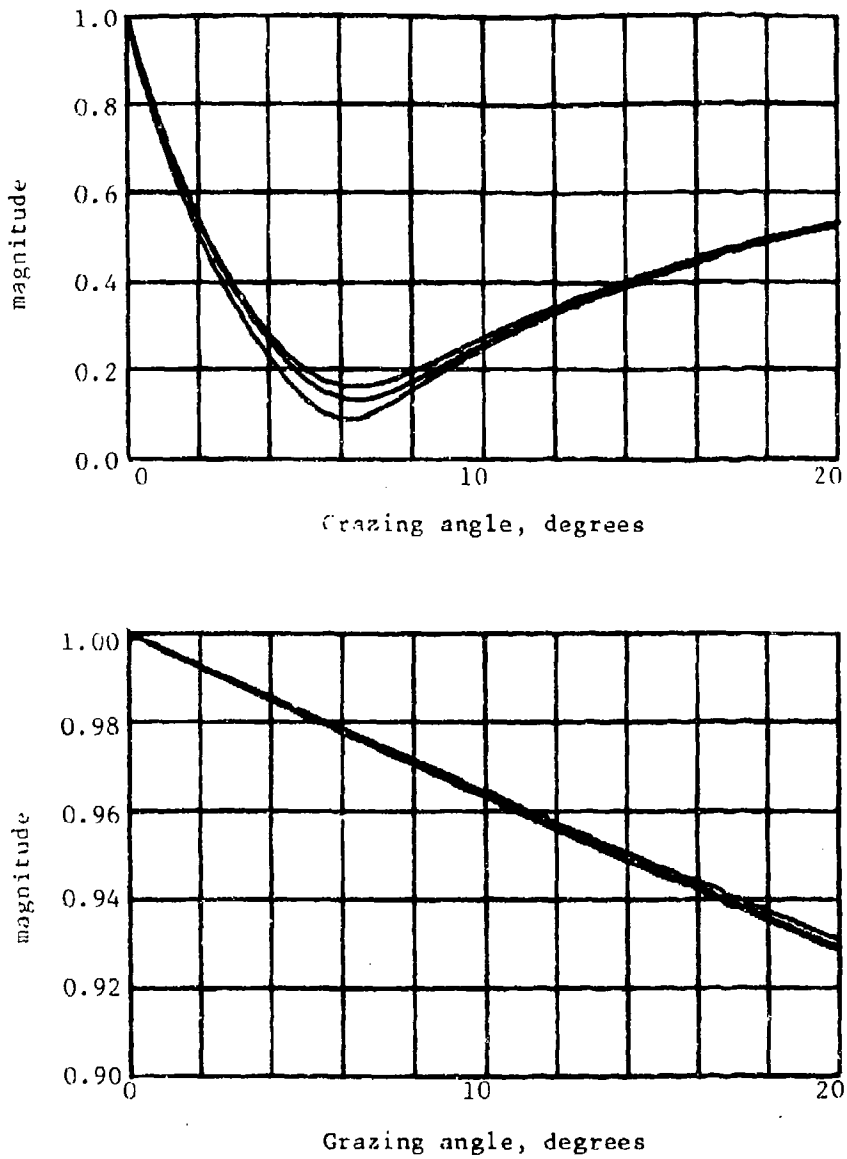

Figure 20. Fresnel reflection coefficients of sea water for 1, 3 and 10 GHz. The upper plot is for vertical polarization and the lower is for horizontal.

The periodicity of this pattern depends markedly upon the wavelength (or frequency) and the grazing angle of the incident wave, and for typical frequencies and incidence angles can amount to several hundred cycles over the vertical profile of a ship.

At an L-band frequency of 1 GHz, for example and an incidence angle of 1 degree, the periodicity is about 3.5 feet, suggesting (in this case) that the pattern in Figure 21 spans 100 feet. At 10 GHz and a grazing angle of 10 degrees, the periodicity is only 3½ inches, so that more than 300 cycles of the pattern covers a ship whose masthead is 100 feet above the waterline. Thus the incident field structure is very complex.

The sea is rarely smooth enough to produce such a regular pattern, however, and the surface roughness introduces jitter and randomness. The roughness has the effect of changing the effective reflection coefficient although the effect is more pronounced for vertical polarization than for horizontal. Figures 22 and 23 (Figs. 5.16 and 5.17 of [4]) illustrate the difference between reflection coefficients as measured and as predicted theoretically for a smooth sea. Note the wide scatter of data for horizontal polarization in comparison to that for vertical.

3. Earth Curvature and Atmospheric Refraction

Since the earth's diameter is so much larger than typical propagation paths, it is a convenience to assume that the earth is flat. Actual distances differ slightly from flat to curved earth geometries, but the difference is small enough that the decay in field strength (due to the spreading of energy away from sources of emission) is given accurately in either system. However, because the presence of the sea surface introduces an additional incident wave at the target, the path length <u>difference</u> becomes much more influential than the total path of either the direct or indirect ray. Thus, although the individual microwave field intensities are relatively

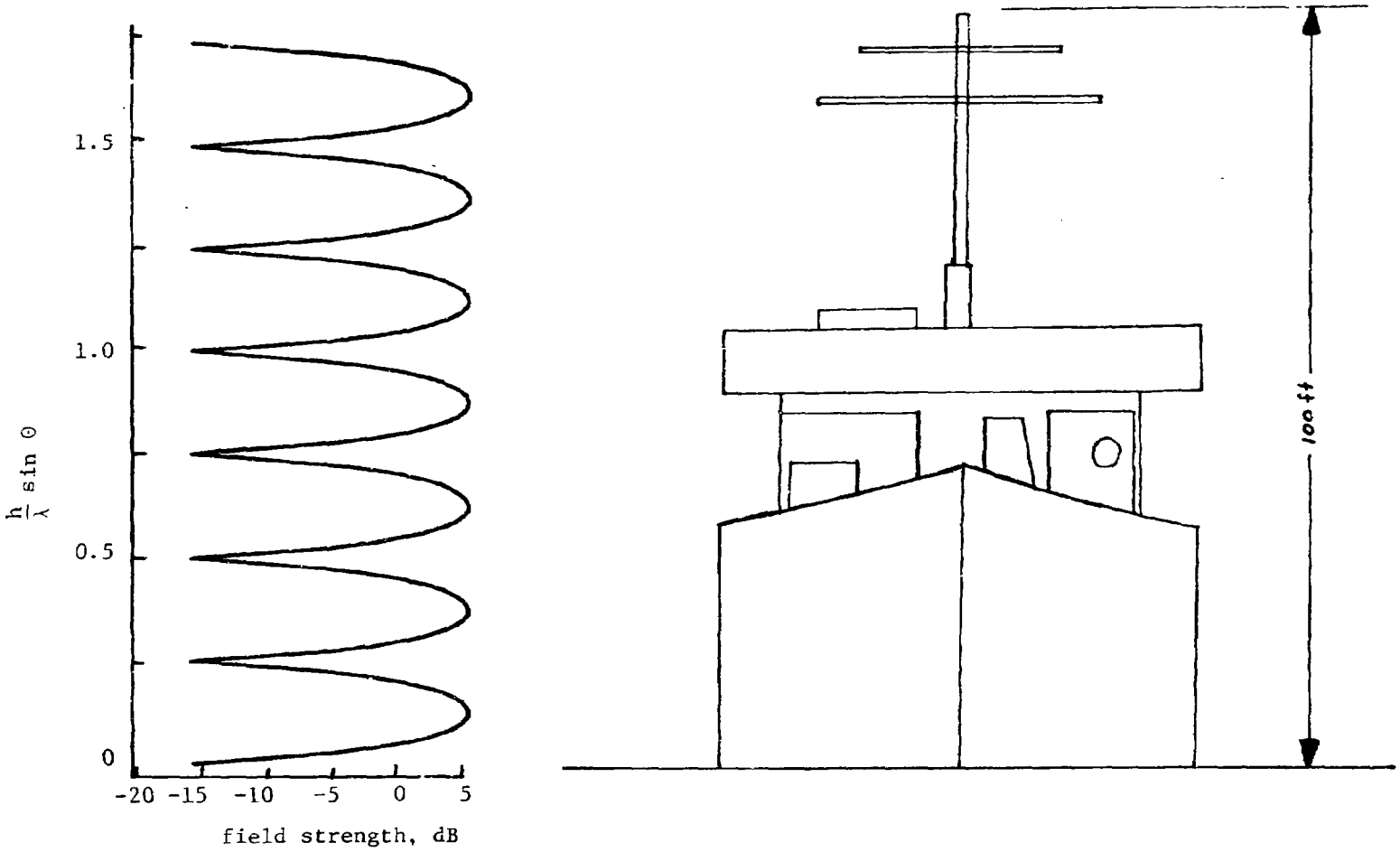

Figure 21. Incident field structure in a vertical plane. For the scale of the ship shown, a wavelength of 30 cm (frequency of 1 GHz) and an incidence angle of 1 degree are appropriate.

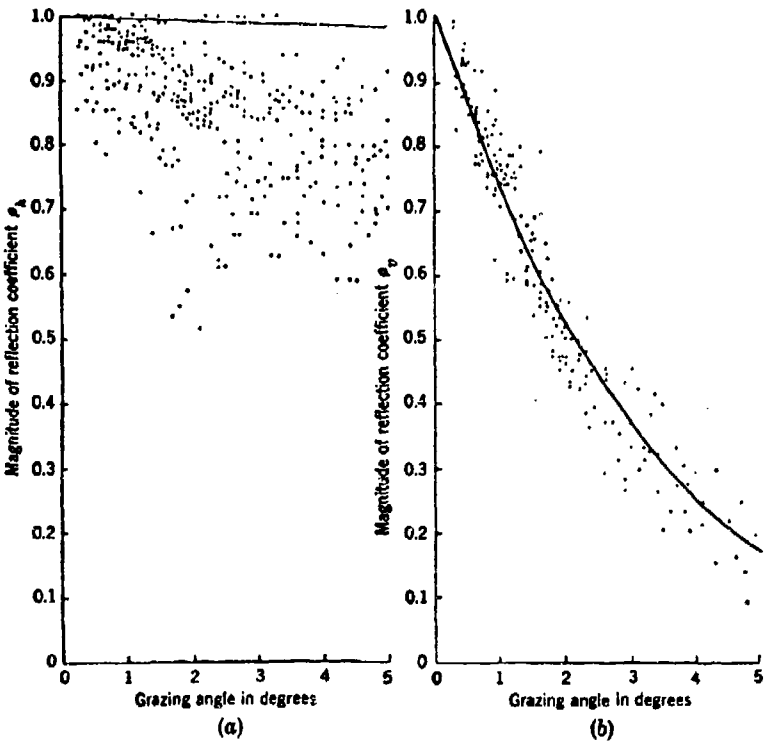

FIG. 5·16.—Values of the magnitude of the reflection coefficient observed by the Radintion Laboratory at a wavelength of 10 cm over sea water. (*a*) On horizontal polarization; (*b*) on vertical polarization.

Figure 22. Taken from Reference [4].

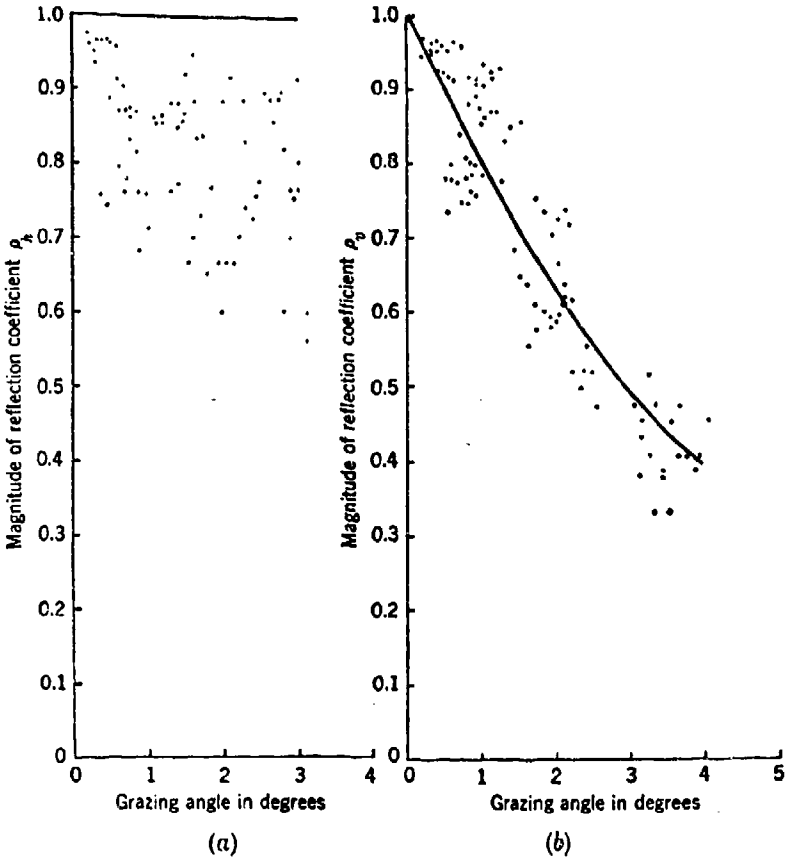

FIG. 5·17.—Values of the magnitude of the reflection coefficient observed by the Radiation Laboratory at a wavelength of 3 cm over sea water. (*a*) On horizontal polarization; (*b*) on vertical polarization.

Figure 23. Taken from Reference [4].

insensitive to the geometry used (i.e., flat or curved), the total field strength can be estimated only if the path length difference is accurately calculated. See Figure 24 for details of the geometry.

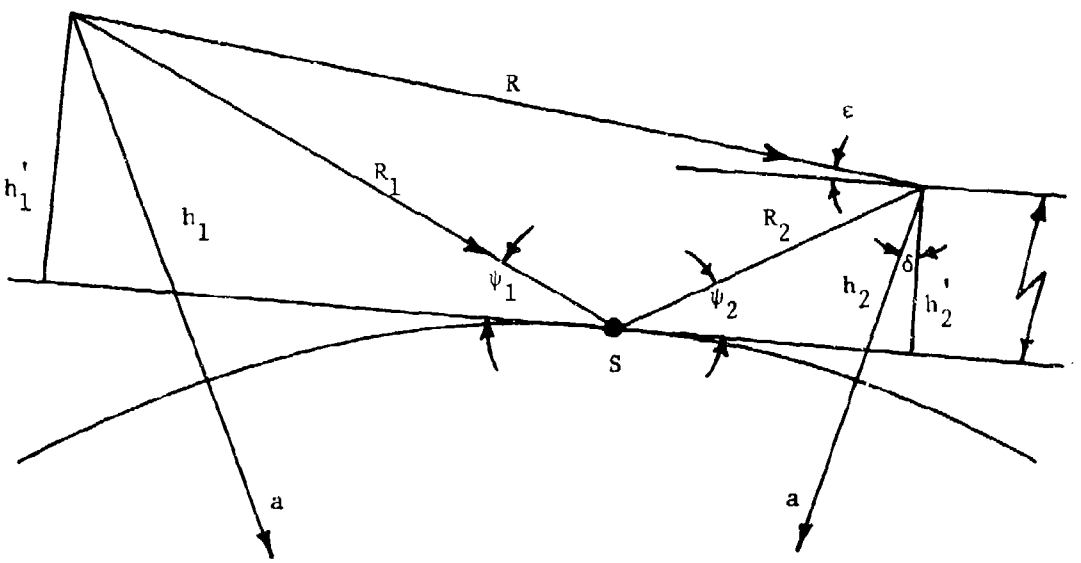

Figure 24. Multipath geometry

Achieving the necessary precision in such calculations is not a trivial task, but the problem has been solved and need not concern us here (e.g., see Kerr [4] or Durlach [28]). The primary effect of the earth's natural curvature is to shield the lowermost portions of the ship from the radar, thus reducing the strength of the echo as the vessel passes over the horizon. Therefore, which parts of a ship produce the major contributions to the echo depends upon how much of the ship is exposed, which in turn is a function of the range and the height of the radar above the sea surface. The dominant sources of ship echo when viewed broadside are the hull and superstructure, and bow-on, the superstructure alone. Therefore

the superstructure warrants serious attention, since it remains visible even after the hull has been shadowed by the earth's curvature.

The index of refraction of the earth's atmosphere is slightly greater than the free space value of unity and typically tapers from a maximum value at the earth's surface to its free space value outside the troposphere. This change in refraction causes electromagnetic waves to bend toward the earth so that propagation does not take place along straight lines, consequently a target may not necessarily lie in the direction indicated by the antenna orientation. Thus in order to determine field strengths and ray paths, an observer must account for the curvature of both the earth and the ray paths.

It turns out, however, that replacing the actual index or refraction profile with a modified one, the curved ray paths can be represented as straight lines above a flat earth. The required replacement is in the earth radius and a standard correction (modification) is to use 4/3 the earth radius in the calculations associated with Figure 24. This is about 5280 miles, but in a marine environment the index of refraction behaves differently. Thus for typical maritime conditions an equivalent earth radius of 1½ to 2 times the actual earth radius is often used instead of 4/3 the actual radius.

Often the actual index of refraction is such that, in the flat earth geometry, it decreases with altitude to a certain height, then begins increasing. This can form a "duct" such that a propagating wave bends downward sharply enough that it strikes the sea surface, is reflected up, then bends sharply down again. It continues to propagate in a sequence of hops and remains within the duct, and accounts for why a radar can often "see" well beyond the horizon. Predicting the duct characteristics requires a mathematical treatment far beyond the scope of this handbook, however, and the reader is referred to the Bibliography in Appendix A for more information.

4. Effective Angle of Incidence

The angles of arrival of both the direct and indirect rays from the radar in the flat earth geometry are slightly different from those in a curved earth representation. The difference is a small angle (δ in Figure 24) for typical slant ranges, antenna and target heights, usually much less than one degree. Thus, for all practical purposes, the angle at which the target is viewed is sensibly the same in either case and no correction need be applied.

Similarly, the effective grazing angle ε is nearly the same as the angle $\psi_1 \simeq \psi_2$ with which the indirect ray is reflected from the ocean surface. This is because the specular point S lies much closer to the target than it does to the radar, consequently both the direct and indirect rays approach the target at equal angles above and below a horizontal plane parallel to the plane representing the flat earth geometry. The grazing angle ε is shown in parametric form in the height-slant range plot of Figure 25 as corrected for the curved earth case. Note that in the curved earth geometry the curve for zero angle does not lie along the abscissa, as would be the case without the curved earth correction.

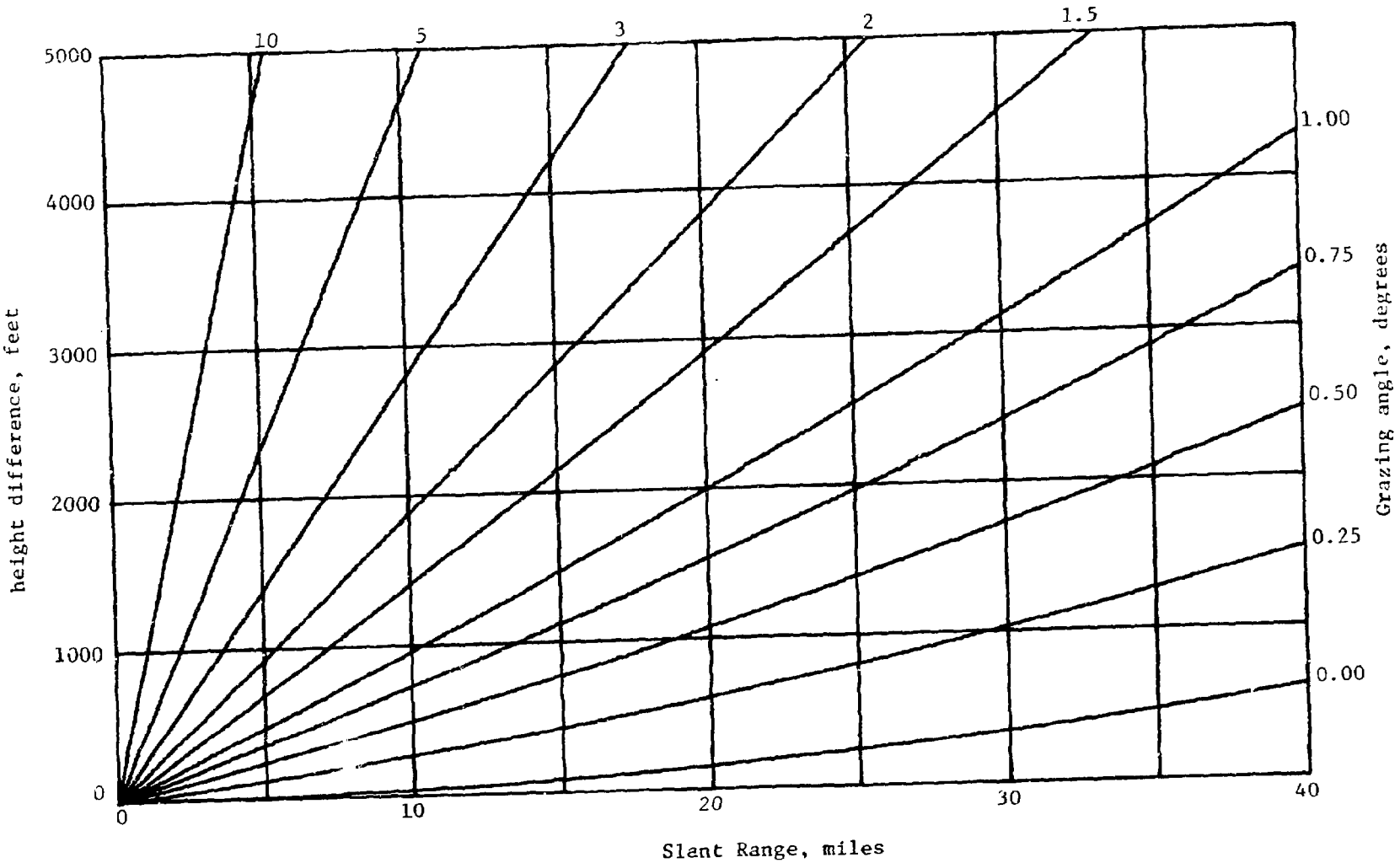

Figure 25. Difference between antenna and target heights plotted against slant range for a variety of grazing angles (effective earth radius: 6900 miles).

III. RCS REDUCTION THROUGH SHAPING

A. Rationale

The use of target shaping techniques involves assumptions about the likelihood of the angles in both elevation and azimuth from which the target vessel will be viewed. If all angles are equally likely, implying hemispherical coverage, then the ideal shape would be that of an inverted bowl, since by the "RCS conservation" principle mentioned above, reducing the RCS over one range of angles entails an increase over another. On the other hand, if the probable viewing angles are confined within a few degrees of the horizon, then the optimum shape would be a right circular cone with its tip pointed skyward. Both shapes are absurd from the practical viewpoint of course, but they represent shaping objectives from the electromagnetic standpoint under different rationales.

The rationale taken in this handbook is the second of the two, but tempered somewhat by the first. We assume that the most likely viewing angles are restricted to a region from the horizon upward to a moderate angle (say 20 or 30 degrees) above the horizon. Thus there is a favored range of angles in the elevation (vertical) plane. In the azimuth plane, however, it is assumed that all angles are equally likely, so that the objective of shaping in the horizontal plane will be to reduce the large broadside, bow and stern echoes. It might be argued that observation and detection via satellite imply that hemispherical coverage is desirable, but we assume that such observation does not constitute an immediate threat and becomes a secondary consideration. The immediate threat lies near the horizon in the form of aircraft or cruise missiles, for example; thus attention is given to this range of elevation angles.

Since the RCS of a ship is due to the sum of the returns of innumerable scatterers, successful RCS reduction is best initiated by isolating and identifying the dominant ones. For example, if one scatterer constitutes, say, 10% of the total echo, the return from the ship would be reduced by scarcely 0.5 dB even if the echo of this one scatterer could

be completely eliminated. On the other hand, if a scatterer is found whose echo contributes 50% of the total, then a 3 dB reduction can be achieved by eliminating it.

Mathematical models exist whereby the dominant scatterers can be pinpointed for a specific ship. Georgia Tech, in particular, has developed modeling techniques in which a list of the echo amplitudes of a ship's components are printed out for inspection [35]. The list quickly shows which are the dominant scatterers for a given viewing angle and facilitates the RCS reduction process. The basic model can be augmented with graphic displays and this, in fact, is currently under development. However, even though the dominant scatterers may be identified, the job of reducing their echoes is not necessarily an easy one.

The dominant sources of echo on a ship are flat vertical surfaces that intersect each other at right angles. Depending on the characteristics of the radar that scans or "sees" the ship, bending a flat surface into a curved one can be an effective way of reducing the return. However, the surface can still be a strong echo source if it remains vertical because of the presence of the sea surface as a reflecting plane. The same kind of effect is responsible for two flat surfaces that are angled 90 degrees apart to form a corner. Thus the major shaping tools available for surface ships are rounding, tilting and avoiding corners. These are discussed in more detail in sub-sections B through D below.

B. Curving Flat Surfaces

Because flat plates are among the strongest single scatterers aboard ship, it is prudent to quantitatively assess the cross section reduction available by converting them into curved surfaces, either by the substitution of a curved surface for a flat one or by the application of a curved metallic shield. As discussed in Section II, such a procedure has the potential of substantial reduction at the specular aspect (where the plate is viewed in a direction normal to its face). In the example cited (cf., Figure 17) reductions

of nearly 20 and 30 dB could be achieved by enclosing a square plate 25λ along a side within a cylinder and sphere, respectively. This potential, it should be pointed out, is available without the need for absorbent materials and even greater reduction might be achieved if the surface were to be treated, in addition, with such absorbents.

However, since a full sphere or hemisphere, or cylinder or hemicylinder, may often be undesirable in a shipboard environment, it is worthwhile examining what benefits may be derived by using incomplete segments. For purposes of analysis, a cylindrical segment such as the one shown in Figure 26 can be taken as a model, and may in fact be a more likely candidate for RCS reduction than a doubly curved surface, since a cylindrical segment can be more easily rolled or pressed from flat sheet stock. The length of the segment is designated ℓ and its edges coincide with those of the flat plate it replaces. Let the half width of the segment be d, so that the width of the flat plate being replaced is 2d. The radius of curvature is designated by the parameter a, as shown in Figure 26, the depth of the concavity by h and the angle subtended by the segment, 2γ. The plate or segment will be assumed to be scanned by a remote radar at an aspect angle θ in a plane perpendicular to the axis of the generating cylinder.

We assume that both the flat and cylindrical plates are large enough that high frequency approximations are good representations of the scattering patterns. The flat plate formula (8) therefore remains valid, but for shallow cylindrical segments equation (9) no longer holds. It can be shown, however, that a good approximation for cylindrical segments is

$$\sigma = \frac{1}{2}\, ka\ell^2 \left| F\left[2\sqrt{a/\lambda}\sin(\gamma-\theta)\right] + F\left[2\sqrt{a/\lambda}\sin(\gamma+\theta)\right]\right|^2 \qquad (11)$$

where F(x) is the Fresnel integral [28, chapter 7]

$$F(x) = \int_0^x e^{i\frac{\pi}{2}t^2}\, dt \qquad (12)$$

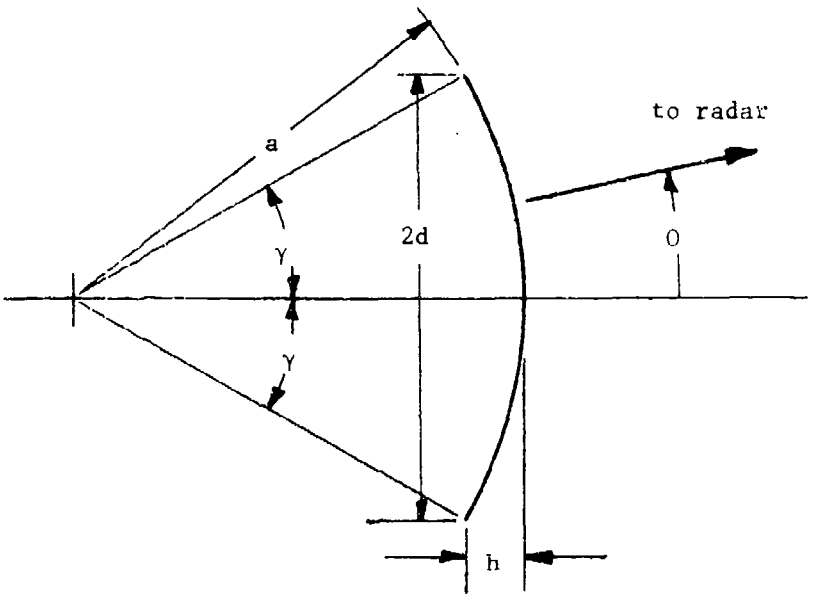

Figure 26. Geometry of cylindrical segment.

F is, of course, a complex number whose value depends on x, but for large arguments F approaches the value $e^{i\pi/4}/\pi 2$, so that equation (11) converges to equation (8).

Figure 27 is a selection of four RCS patterns of cylindrical segments for progressively deeper segments, but all for the same half-width $d = 15\lambda$. This choice of d is purely arbitrary and in a moment the influence of other values will be considered. The pattern in Figure 27(a) is actually a flat plate pattern, this being the special case of a cylindrical segment with an infinite radius. Note that as the segment becomes progressively deeper, the specular return at $\theta = 0$ decreases and the sidelobe levels rise. In the limit, if h were allowed to approach the value d, the pattern would be a flat horizontal line, such as that of Figure 17. Also note that, for a given plate, as h/λ increases, the segment half angle γ increases.

The mean levels of the patterns (c) and (d) of Figure 27 are much easier to establish on inspection than those of (a) and (b), because the variations in amplitude are smaller, at least over the initial portions of the patterns. Nevertheless a radar designer examining such patterns as bases for establishing design parameters will attempt to visually estimate the mean level despite the large variations. This is because the design cannot be based on either the specular or non-specular levels, but upon a more representative value between the two extremes. Since the probability of detection is more closely related to the mean than to detailed variations for typical tactical encounters, it is of interest to consider the mean return instead of the detailed characteristics of the patterns.

The mean return can be found for any angular base interval $\Delta\theta$ and for illustration we select intervals of 5, 10 and 15 degrees to do so. By numerically integrating patterns such as those in Figure 27, the plots of Figure 28 can be constructed. This figure shows that for whatever base interval is chosen, the mean cross section is nearly constant with increasing h until the base interval is nearly equal to the segment half angle γ. Then the mean return descends at a more rapid

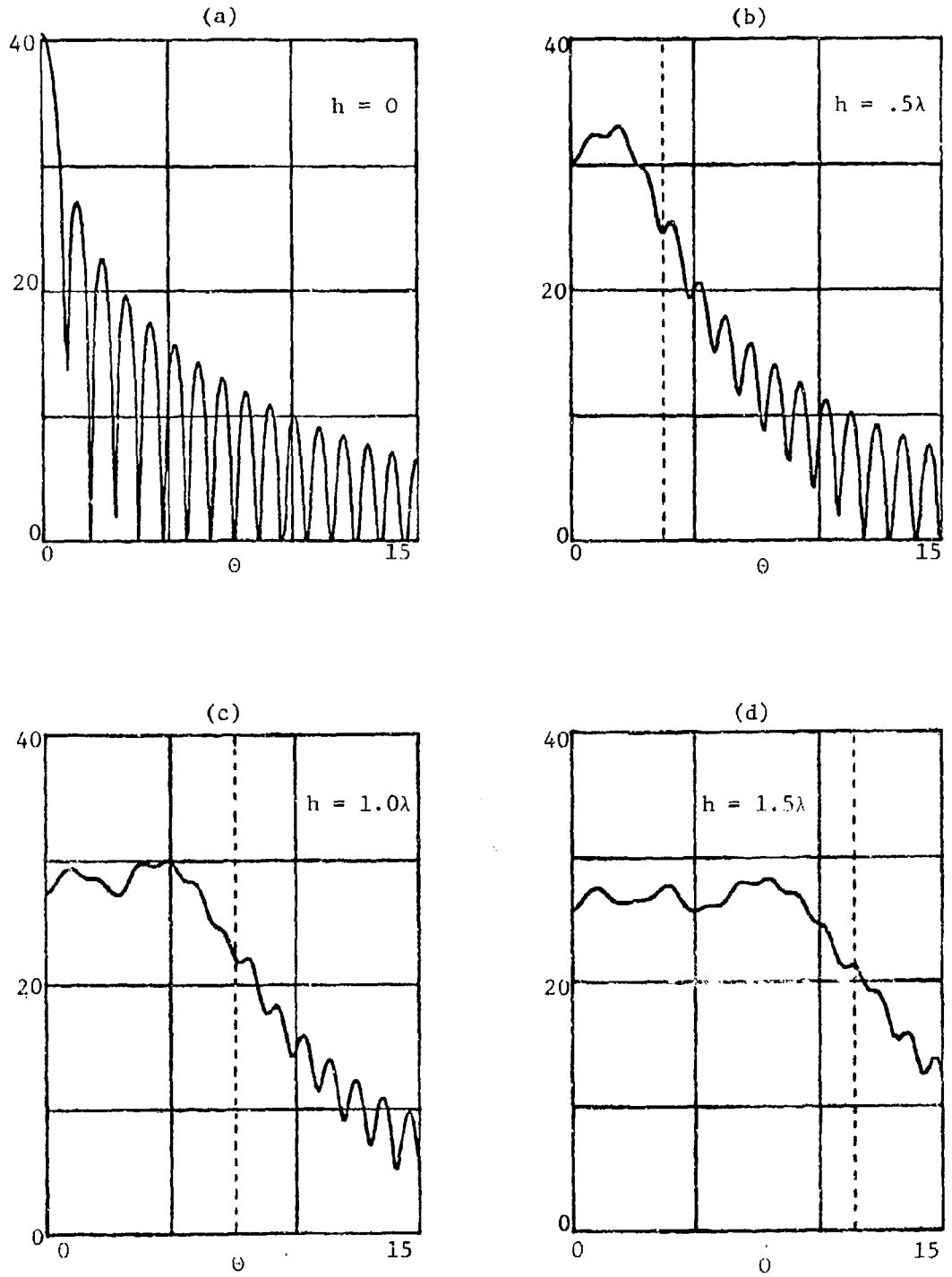

Figure 27. RCS patterns of a cylindrical segment of half width $d = 15\lambda$. The ordinate is $10 \log (\sigma/\ell^2)$ and the dashed lines indicate the segment half angle γ.

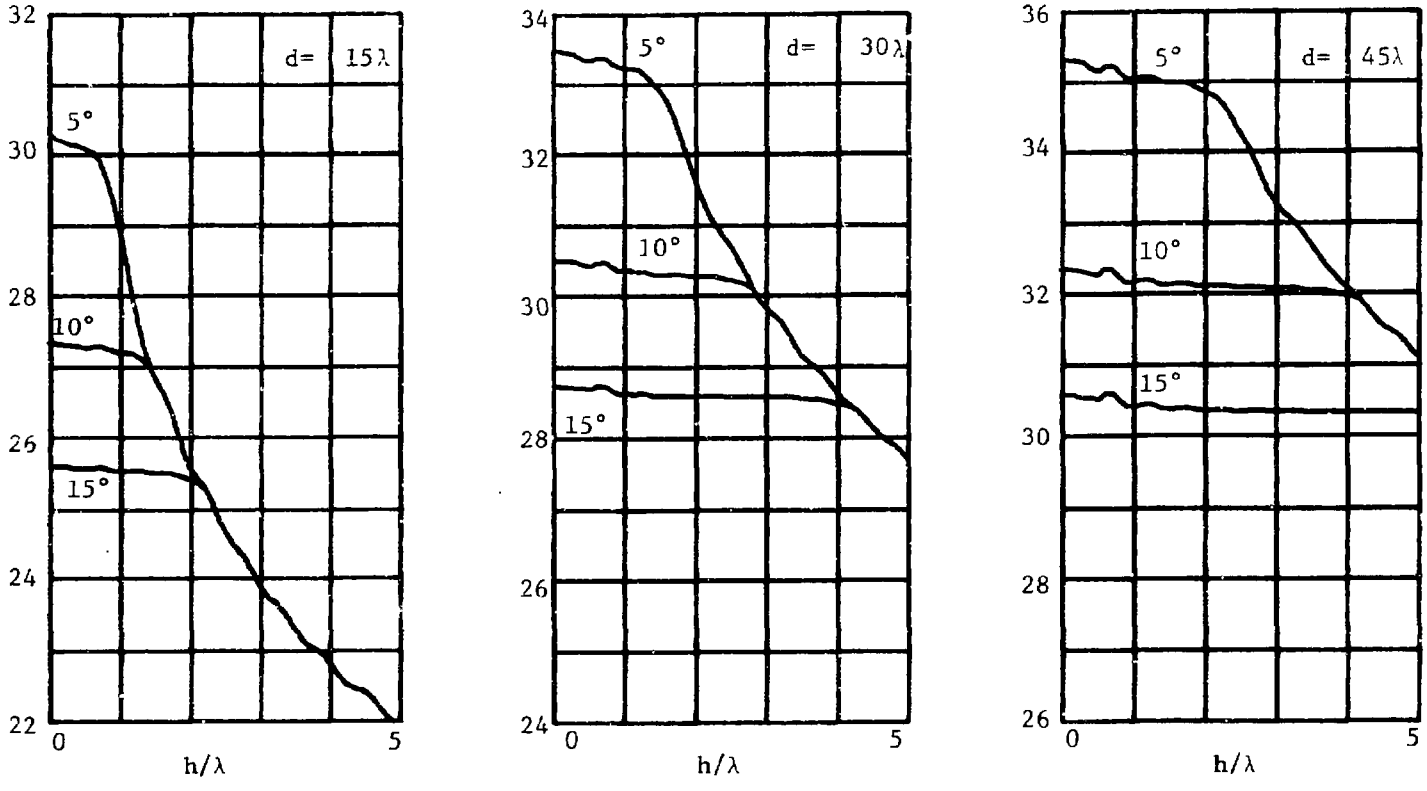

Figure 28. Mean radar cross sections of cylindrical plates for three plate half-widths and three base intervals. The ordinate is 10 log (σ/ℓ^2).

rate, the behavior being described very closely by the physical optics return of equation (9). Thus the trailing portions of the traces in Figure 28 can be represented by the broadside cylinder RCS of equation (9).

The initial portions of the traces can be estimated by integrating equation (8) over the base interval $\Delta\theta$, the result for the free space cross section being the approximation

$$\sigma_f \simeq \frac{kd\ell^2}{\Delta\theta} \tag{13}$$

This gives the initial amplitudes (for h = 0) of the plots in Figure 28 within 0.5 dB.

Based on the mean radar cross sections in equations (9) and (13), the RCS reduction available for $\Delta\theta<\gamma$ can be estimated by dividing (13) by (9); for $\Delta\theta>\gamma$ there is essentially no reduction, as demonstrated by Figure 28. Thus a radar cross section reduction factor R can be formed as an indicator of the performance of cylindrical segments,

$$R = \begin{cases} \frac{\theta}{2}\left(\frac{d}{h}+\frac{h}{d}\right), & \Delta\theta<\gamma \\ 1, & \Delta\theta>\gamma \end{cases} \tag{14}$$

Expression (14) has been plotted in Figure 29 for a selection of base intervals.

It is clear that the reduction, if any, is independent of the wavelength when the mean RCS is considered, but it does depend on the angular interval over which the mean is defined. However, it is not at all clear how $\Delta\theta$ can be chosen or specified and the estimate of equation (13) loses significance for very small $\Delta\theta$. In this case one returns to the comparison of the specular value of equation (8) with equation (9) and the reduction is

$$R = \frac{\lambda}{16h}\frac{h^2+d^2}{d^2} \tag{15}$$

which is wavelength dependent.

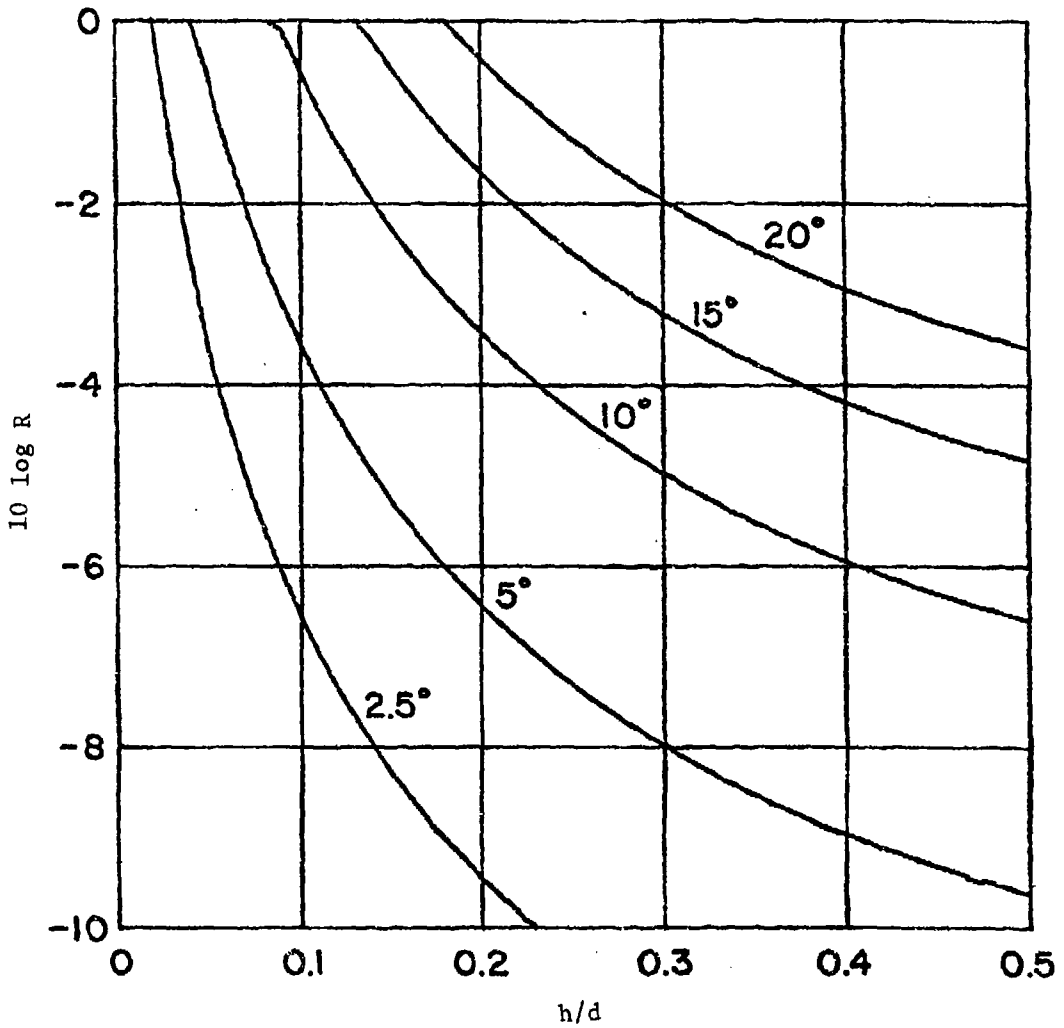

Figure 29. Approximate RCS reduction based on mean returns averaged over the indicated interval.

Therefore unless the cylindrical segment subtends an angle significantly greater than the angular averaging interval, the effective reduction is small. The maximum reduction is obtained by shielding or replacing the flat plate by a hemicylinder, for which h = d and R = $\Delta\theta$, hence the optimum selection of h might be based on non-electrical considerations, such as the constraints of space and weight in accomodating such a structure shipboard, and how well the original function of the flat surface is performed by a curved one.

In spite of the uncertainty involved in choosing a representative value for $\Delta\theta$, and therefore which value of h/d might be considered optimum, a value of $\Delta\theta = 5^{o}$ does not seem unreasonable in the light of some actual ship RCS measurements. A reasonable trade-off of RCS reduction against unmanageable shape seems to be of the order of 8 dB reduction of h/d = 0.3. Thus the "bulge" of such a singly curved surface would be 15%, meaning, for example, that a vertical plate 10 feet wide would be bulged out (or in) by 18 inches at its center (cf. Figure 26). Any more than this may become too complicated to include in the general structure of the ship.

C. The Effect of Target Tilt

As mentioned above, the sea surface has a powerful influence on the scattering characteristics of sea targets, because of the way energy is reflected from the sea. The reflection properties themselves are not subject to control, but they do depend on the roughness of the sea surface, which in turn depends on such parameters as wind velocity, wind direction and fetch. The target orientation, however, is adjustable to some degree and can be chosen so as to minimize target-sea interactions. The primary control mechanism in this case is the tilt angle of the scatterer with respect to the mean sea surface.

For the purpose of analysis and interpretation, it is sufficient to examine the behavior of a single idealistic target of simple shape. Indeed, it is virtually mandatory to consider an idealized case because the scattering by surface vessels is so complex that a detailed math-

ematical model would be unmanageable even if it could be formulated. Consequently we restrict attention to a convenient shape in order to grasp the principles involved, the precise shape being less important than the effect of the sea surface itself.

Such a target is a right circular cylinder whose length and diameter are ℓ and 2a, respectively, and floating in the water with a list or tilt much like the exposed top of a buoy, such as indicated in Figure 30. The sea surface is assumed to be perfectly flat and smooth, and characterized by a reflection coefficient ρ. The actual sea surface is not so idealistic, of course, but many of the features of actual roughness can be simulated by assigning the reflection coefficient an effective value based on sea surface measurements. As discussed earlier, ρ depends on the angle of incidence ϵ, but for simplicity it will be regarded as an adjustable constant; this will not influence the conclusions drawn, since the principles remain valid. The tilted cylinder is assumed to be viewed from an elevation angle ϵ by a remote radar, the angle being measured upward from the sea surface as in Figure 30. The cylinder axis is assumed to lie in the vertical plane containing the radar line of sight, and the tilt angle τ is assumed positive when the top of the cylinder is tipped away from the radar.

The radar cross section of the cylinder can be calculated using high frequency electromagnetic approximations, but the derivation will not be given here. The result is

$$\sigma = k\ell^2 |F|^2 = \sigma_o |F|^2 \qquad (16)$$

where the pattern factor F is the function

$$F = A + 2\rho B + \rho^2 C \qquad (17)$$

in which A, B and C represent individual patterns and are functions of the length and diameter of the cylinder, the angles τ and ϵ, and the free space electromagnetic wavelength. In this expression, σ_o is

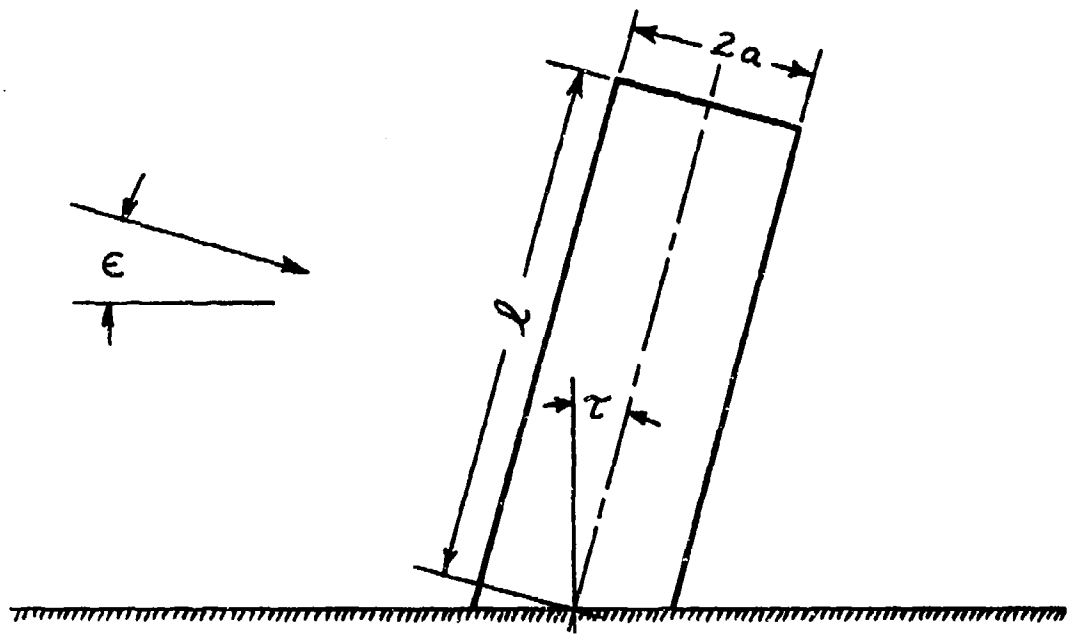

Figure 30. Geometry of tilted cylinder.

the free space, broadside cylinder RCS and the pattern factor F contains the effect of the sea surface as well as the cylinder orientation (i.e., the tilt angle).

Each of the three terms in F can be traced to one of the mechanisms sketched in Figure 31. The first term represents the pattern that should be measured had the sea not been present (Figure 31(a)) and therefore represents the free space pattern of an isolated cylinder. The third term represents the pattern of the image of the cylinder in the sea and, except for the factor ρ^2 multiplying this term, is also a free space type of pattern. The factor ρ^2 stems from a double bounce off the sea surface as depicted in Figure 31(b) and the correct angle of arrival of the incident wave can be deduced either by considering the relationship between the actual radar and the cylinder image, or between the actual cylinder and the radar image.

The second term in F includes two contributions which by reciprocity are identical (hence the factor 2), and represent the interaction of the cylinder with the sea surface as shown in Figure 31(c) and (d). This term includes a multiplicative factor ρ which, being raised to the first power, indicates a single bounce mechanism rather than the double bounce mechanism of Figure 31(b). The second term is a mathematical statement of the so-called dihedral or bi-plane effect, even though the target in this case is a cylinder.

Equation (17) can be used to investigate the influence of ρ, τ and ϵ, and Figures 32 through 39 are a collection of patterns illustrating these effects. The electrical circumference, ka, has been fixed at a value of 15 for these patterns and whether this simulates that of an actual cylinder is of little importance since it appears only in the phase factors. The cylinder length is a fixed value of $\ell = 20\lambda$, which is sufficiently long to exhibit the rapid scintillations in the patterns of electrically large targets, but yet not so long so as to obscure the interactions we seek to demonstrate.

Figures 32 and 33 are RCS patterns in which the elevation angle to the radar is held at 10 degrees while the cylinder tilt angle is varied

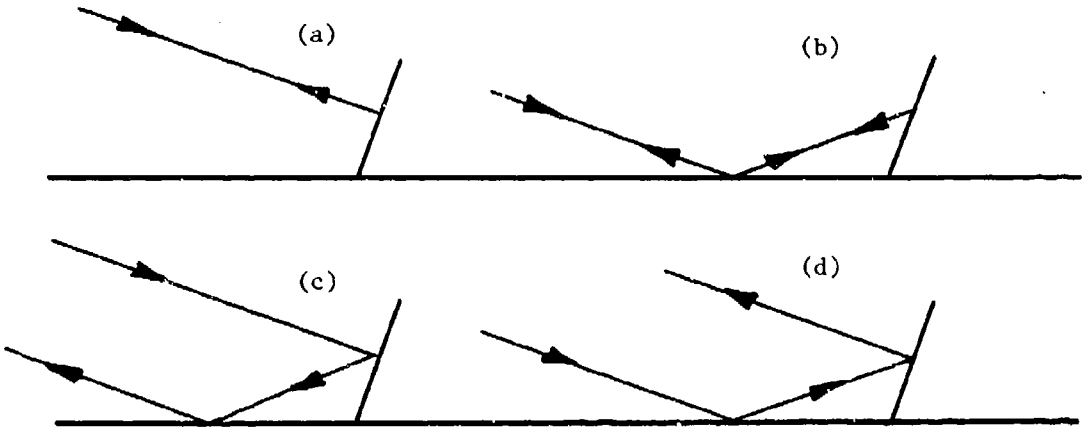

Figure 31. The four major scattering mechanisms.

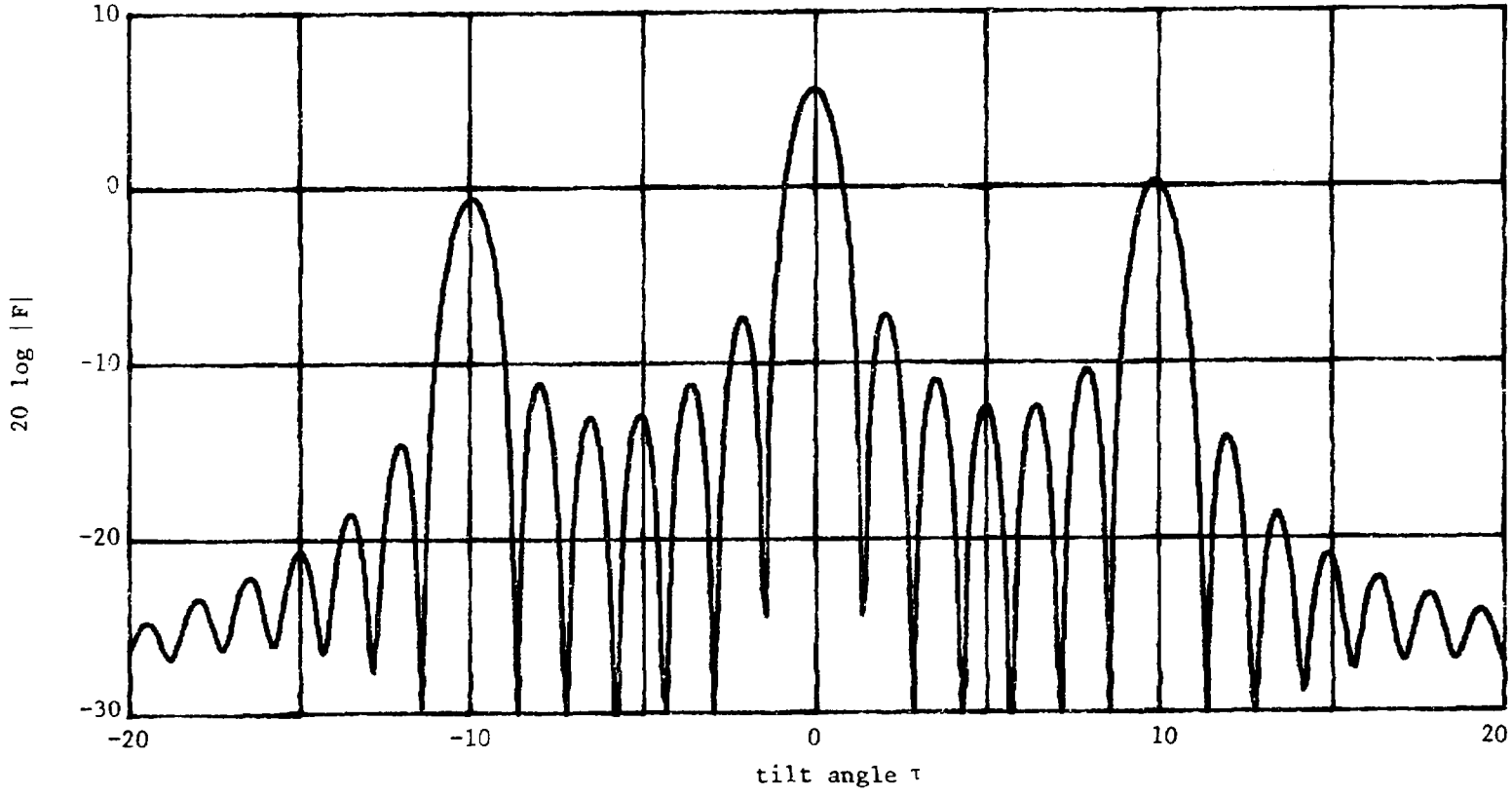

Figure 32. Pattern factor for ε = 10 degrees and ρ = -0.95.

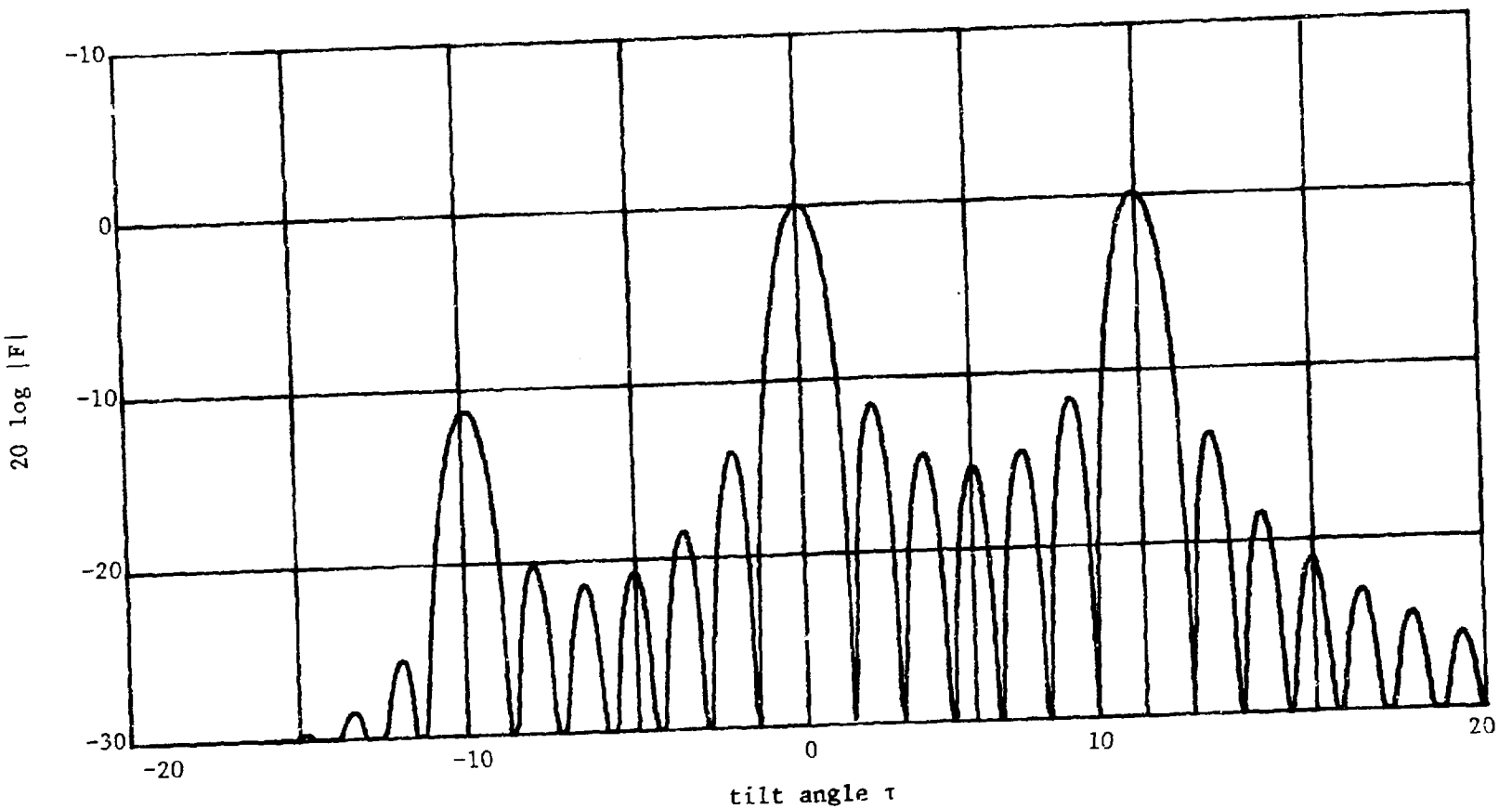

Figure 33. Pattern factor for ϵ = 10 degrees and ρ = -0.50.

by 20 degrees in both directions. The effective reflection coefficient of the sea surface was taken to be -0.95 and -0.50 respectively to illustrate the effect of this coefficient on the tilt angle pattern. By choosing an elevation angle much larger than the width of the main lobe of each of the three patterns of equation (17), the three individual contributions are separated and easily recognized, as in Figure 32. The center peak at $\tau = 0$ (i.e., for a vertical cylinder) is the strongest because it has the factor 2 mentioned earlier. The right-hand peak occurs at $\tau = \varepsilon$ and is the specular lobe of the free space cylinder pattern; since the weighting factor of this particular lobe is unity, its amplitude is always near zero on a logarithmic scale. It can never be precisely zero, since there is a small but finite contribution due to the far sidelobes of the remaining two terms in equation (17). The left-hand peak occurs at $\tau = -\varepsilon$ and is the main lobe of the image cylinder pattern; its amplitude never exceeds zero (on the dB scale) and, depending on the effective reflection coefficient of the sea surface, can be many dB less than zero.

This is in fact demonstrated in Figure 33, for which $\rho = -0.5$. Note that the left lobe has dropped about 16 dB from the corresponding amplitude in Figure 32, but that the lobe at $\tau = 0$ has decreased only about 5 dB. The right-hand lobe has changed imperceptibly in progressing from Figure 32 to 33 as expected, since this is the free space pattern level, independent of the presence of the sea surface. Thus if one were to choose an optimum tilt angle that minimizes the radar cross section, it should be approximately half the elevation angle of the radar. Moreover, the patterns suggest that the tilt angle should be negative (i.e., top of the target tilted toward the radar), because the pattern has lower amplitudes for negative than positive tilts.

The conclusion remains valid even when the elevation angle is lowered, which is shown in Figure 34 for $\varepsilon = 5$ degrees, but because the main lobes of the three individual patterns become crowded closer together, the RCS reduction may not be as great. And at even lower angles, such as in Figure 35 for a 2-degree elevation angle, the three peaks show a distinct tendency to coalesce to a single one. For low elevation angles, then, it appears that the optimum tilt angle is

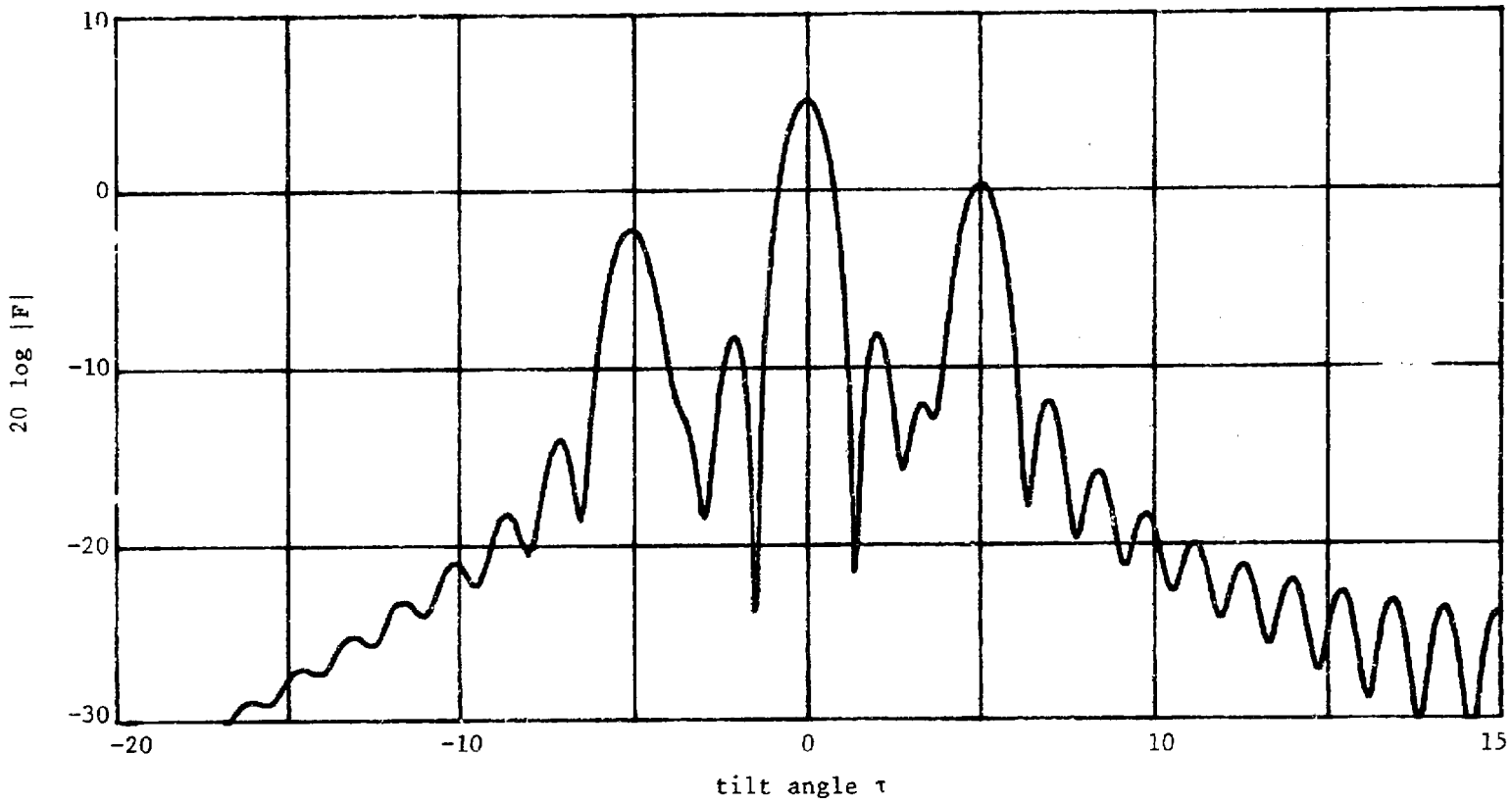

Figure 34. Pattern factor for $\varepsilon = 5$ degrees and $\rho = -0.9$.

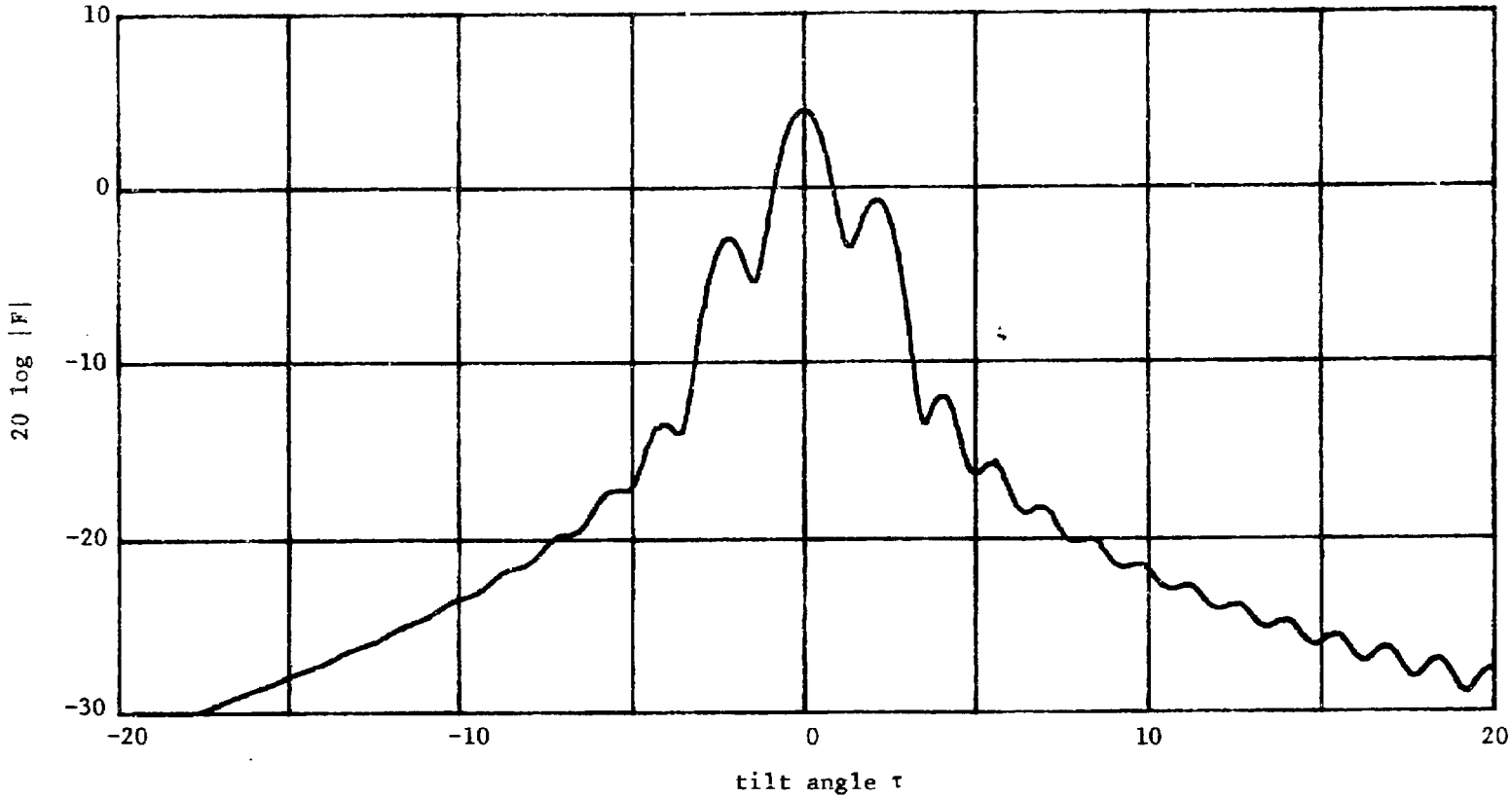

Figure 35. Pattern factor for ϵ = 2 degrees and ρ = -0.9.

at least twice the elevation angle. It should be appreciated, however, that if the cylinder were to be much longer than 20λ, the three peaks would be separated by many more pattern nulls than exhibited in Figure 35 because of the increase in electrical size, even though the angular separation would be unchanged.

Consequently we have conflicting requirements: for large elevation angles, surfaces should be tilted away from the vertical by half the elevation angle and for low elevation angles they should be tilted by twice the elevation angle or more. A more unsettling fact is that the radar will never be so cooperative as to remain obligingly at a fixed elevation angle as seen from the target; typically being airborne, the radar angle can range from zero to 90 degrees (90 degrees being overhead). Thus it seems prudent to determine the most likely angle from which the target will be viewed and then to adjust the tilt angle accordingly. Unfortunately, there are no known studies that pinpoint the most likely angle under a variety of tactical encounters.

Consequently it is of interest to impose a variety of fixed tilt angles and to then sweep the elevation angle upward from zero to well beyond the right-hand peak of Figures 32 through 35. This is illustrated in Figures 36 through 39 for several tilt angles. Observe that when the tilt angle exceeds a certain value (determined by the electrical size of the object), a sweep of the elevation angle will always include a peak whose amplitude lies close to the zero dB level. This peak is located at $\epsilon = \tau$ and the pattern levels on either side of the peak may be relatively high as in Figure 36, or lower, as in Figure 38. But small tilt angles, especially zero, should definitely be avoided since, as suggested by Figures 36 and 37, the RCS remains at high levels. In fact, although an optimum tilt angle specification depends on other considerations (of the geometry and statistics of a tactical encounter), it is clear that purely vertical surfaces must be avoided in any event.

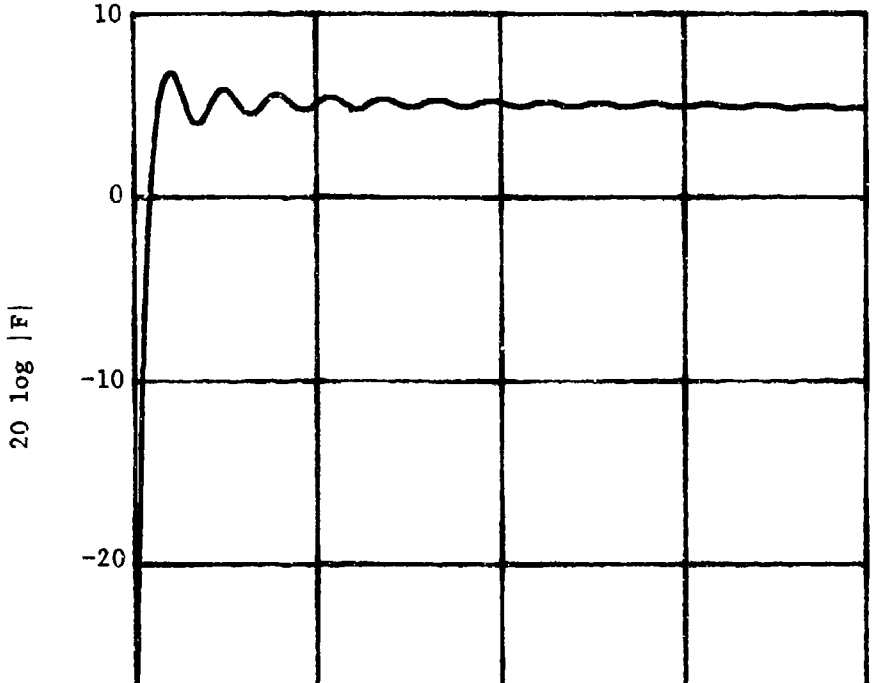

Figure 36. Pattern factor for τ = 0 degrees and ρ = -0.9.

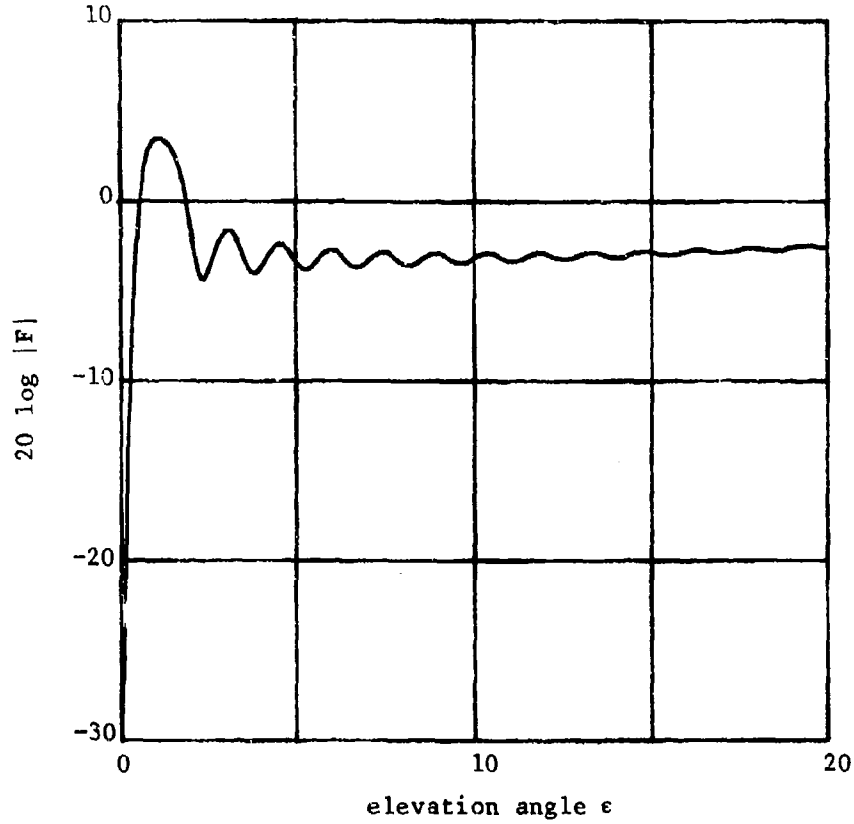

Figure 37. Pattern factor for τ = 1 degree and ρ = -0.9.

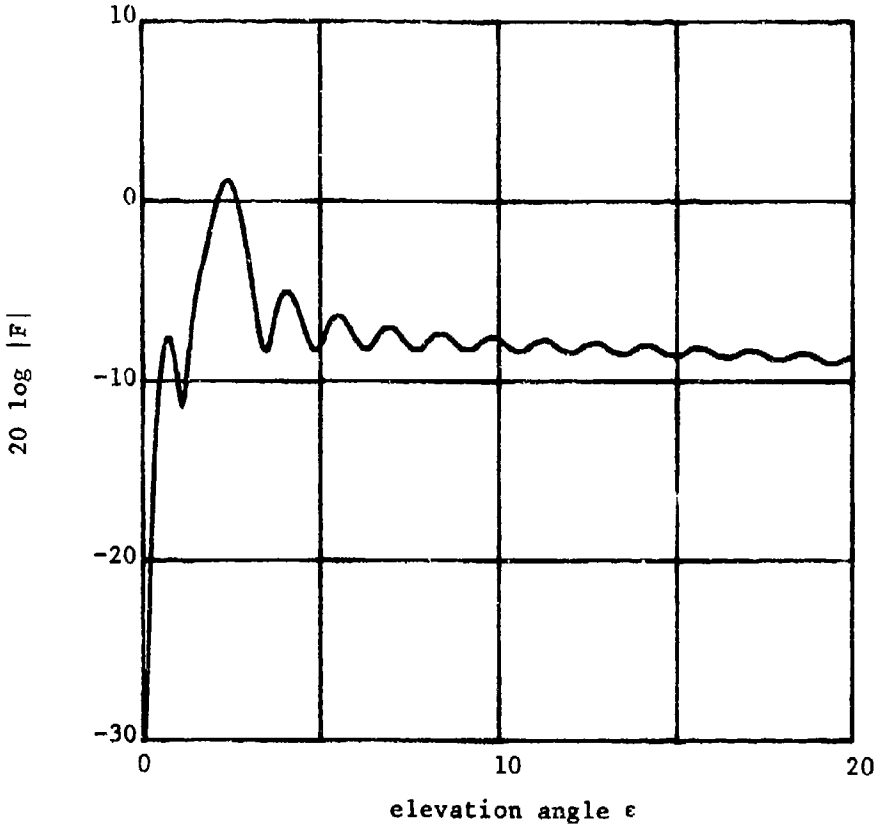

Figure 38. Pattern factor for τ = 2 degrees and ρ = -0.9.

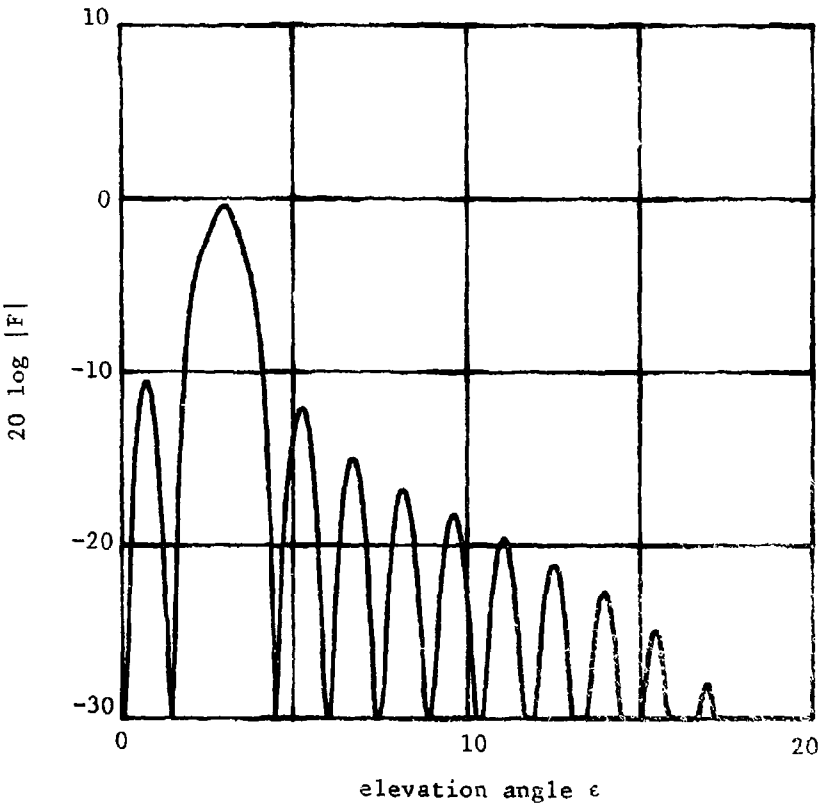

Figure 39. Pattern factor for τ = 3 degrees and ρ = -0.9.

In striking a reasonable compromise in balancing tilt angles against the functional purpose of otherwise vertical surfaces, a tilt in the range of 3 to 5 degrees would appear to be beneficial. Higher tilt angles would be more difficult to implement because of volume constraints, while lower ones do not yield the desired RCS performance. Negative tilt angles are slightly favored, but the increase in performance may be more than offset by having structures wider at the top than at the bottom. It should be borne in mind that these concepts are valid for flat plates as well as cylinders, since it is the multipath mechanisms sketched in Figure 31 that dominate the patterns. Specific target shape in the horizontal direction is less important than the fact that it is composed of straight elements extending upward more or less vertically.

The above analysis assumes that the target is in contact with the water as suggested in Figure 30, and is thereby fully exposed to both the direct rays from the radar as well as rays reflected off the surface as close as the waterline. On the other hand, many target surfaces are well above the waterline as indicated in Figure 40 and therefore the analysis does not apply in its totality to these structures. This is because obstacles closer to the waterline can block sea-reflected rays from reaching surfaces found higher on the ship, so that vertical surfaces such as B and C are only partially illuminated by the reflected ray. In order to account for these shadowing effects, an effective length should be used, possibly with a different effective length in each of the three terms due to the particular geometry of the incident and scattered ray directions in each case. Consequently the patterns associated with each term would be modified; lower amplitudes would be expected (because the effective length would be shorter than the actual length by the amount of exposed surface) and the pattern nulls would move farther apart in angle. Thus equation (17) represents a "worst case" condition.

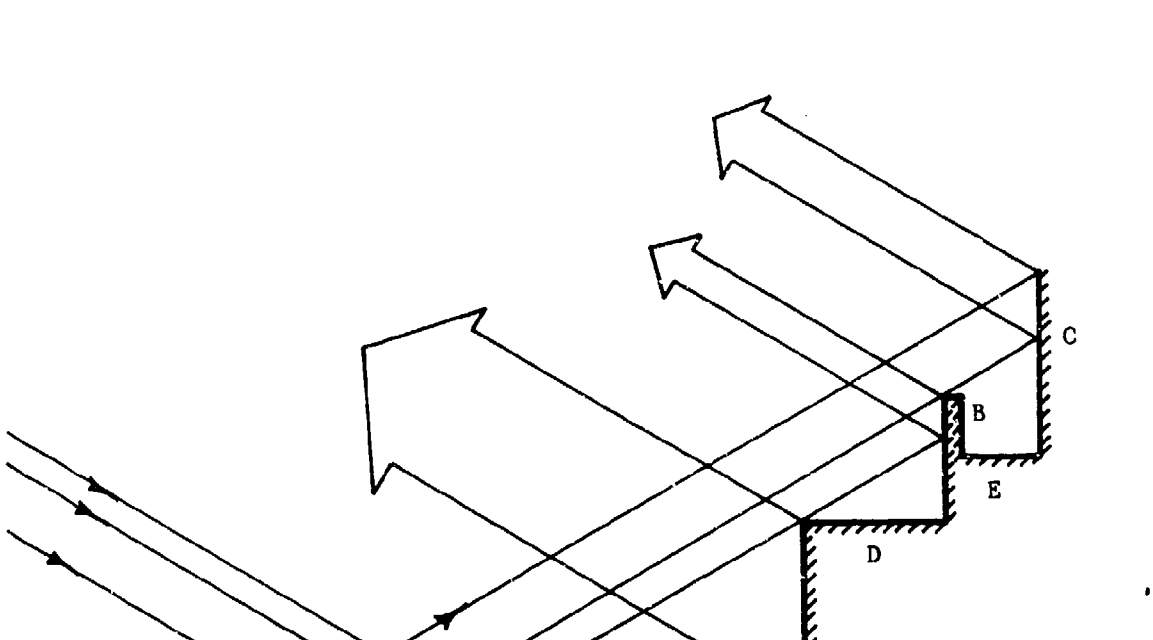

Figure 40. Surfaces not in contact with the water are partially shielded from the indirect rays by other surfaces closer to the waterline.

However, additional interactions would be introduced by horizontal surfaces D and E which in effect contribute to the return much as does the sea surface several feet below. Note that vertical surface B shields horizontal surface E from the direct ray from the radar as well as vertical surface C from indirect rays. Consequently a detailed analysis of the return from a structure such as represented in Figure 40 becomes painfully complex even though only five distinct surfaces are involved in addition to the sea surface. We must be content, therefore, to ignore the effects of blockage and shadowing and confine attention to simpler structures such as depicted in Figure 30 in order to assess the effects of tilt.

D. Deployment of Screens

It should be pointed out that the benefits of surface tilt can often be secured without tilting the actual surface itself. In many cases the offending vertical surface can be hidden behind a slanted metallic screen with essentially the same effect, provided the mesh openings are small enough. A rule of thumb is that electromagnetic waves are effectively blocked if the openings are less than $\lambda/10$ on a side, implying mesh sizes, for example, of about 1/8 inch at 10 GHz and 1¼ inches at 1 GHz. Sizes larger than this permit energy to penetrate the screen and to illuminate any surfaces behind it, although some penetration may be tolerable.

Actual selection of a screen material depends on several parameters, some of them psychological. A Navy standard, for example, is to maintain a clean, trim ship and the shrouding of a vessel with unsightly sheets of steel mesh is likely to be resisted. And as the diameter of a wire decreases (the wire used to weave the mesh), the effects of saltwater corrosion become more severe. Other mechanical factors must also be considered, such as the method of attachment and installation, susceptibility to icing and, of course, intrinsic strength and resistance to sea wash. As far as can be ascertained,

screening as a method of RCS reduction has not been extensively tested and should be viewed as a candidate for further study from the structural standpoint.

A comparison of surface tilting and screen deployment is shown in Figure 41. The original structure or design is the hypothetical profile depicted in Figure 41(a) and might represent a transverse section of the ship taken somewhere amidships. To take advantage of the benefits of slanted surfaces, the profile could have been designed and built as suggested in Figure 41(b), where only the vertical surfaces have been sloped. Note in this case that the hull of the vessel has been canted outward at the top while topside vertical surfaces have been canted inward. The use of screening to provide essentially the same effect is shown in Figure 41(c), but observe that some of the deck surfaces have been narrowed. An alternative shielding option is shown in Figure 41(d), where the point of attachment of the uppermost screen has been moved so as to provide a kind of tunnel, presumably recovering the use of the deck space that had been narrowed in Figure 41(c). Thus screening could be a convenient form of retrofit procedure for reducing RCS.

Quite often energy entering an aperture such as a ventilation duct or porthole can be reflected from interior surfaces and back out the aperture toward the radar. Screening can prevent energy from entering and can therefore help deflect the energy in some other direction. Such methods have been considered for the intake ducts of jet aircraft but the mechanical stresses from flight are too severe to allow much latitude in the design of cover screens. Aboard ships the aerodynamic problem is not as severe as it is for aircraft, but the marine environment presents its own particular problems of corrosion and sea wash. Nevertheless, portholes and ventilators should be screened to prevent radar energy from entering such openings.

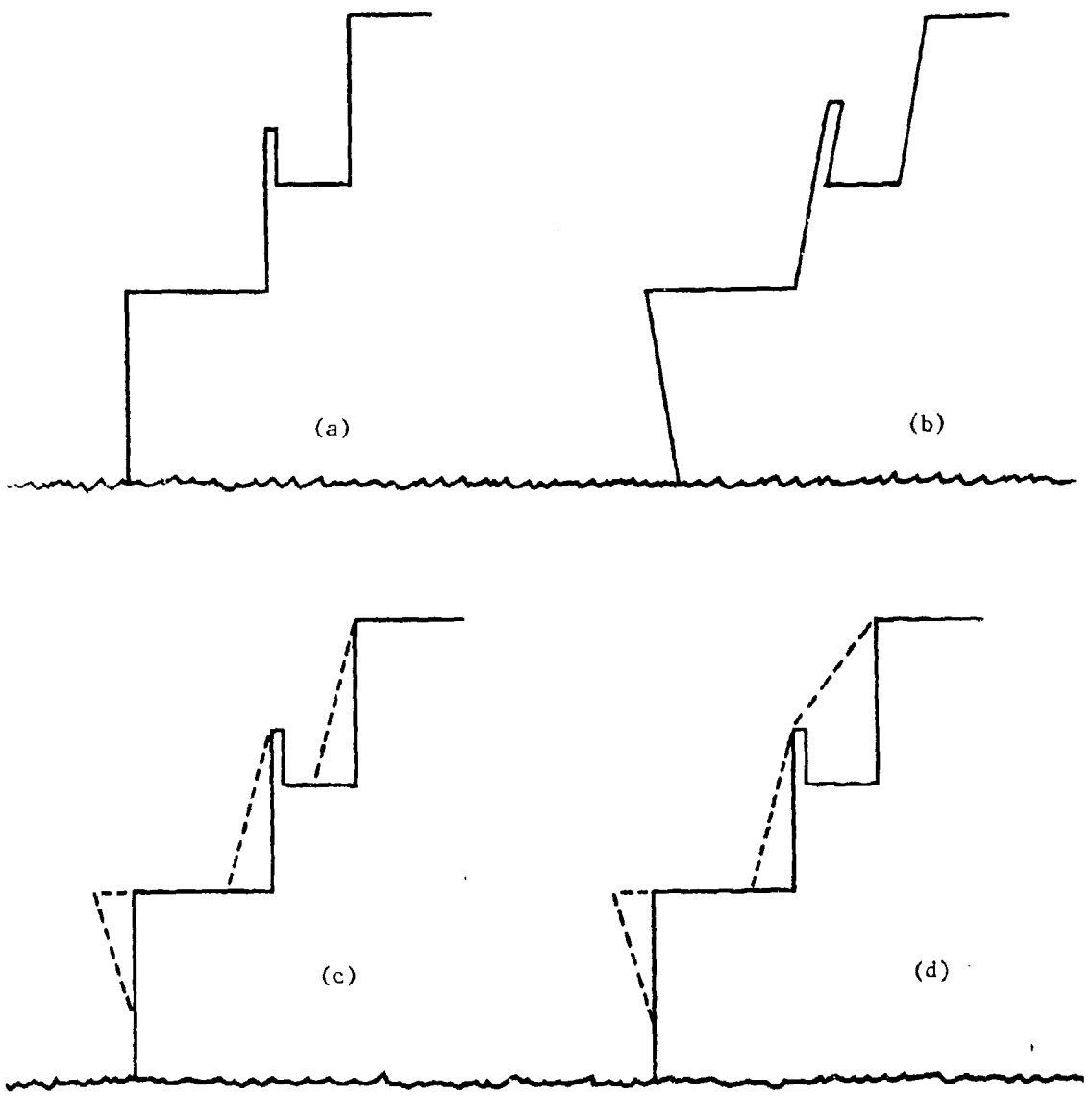

Figure 41. RCS reduction options: a) original profile; b) upright surfaces tilted away from the vertical; c) deployment of screens; d) improved deployment of uppermost screen.

E. Avoiding Internal Corners

The radar cross section of an internal corner, such as formed by the intersection of two sides of a room with its floor, is large and persists over a wide range of aspect angles. Because of the strength of the echo and the broadness of its RCS pattern, corner reflectors have been used for many years as calibration standards for patterns and gain measurements. However, even though the corner reflector is a useful device for range markers and calibration standards, it should be avoided on ships precisely because of these characteristics.

There are two dominant forms of the corner reflector depending on whether two or three surfaces are involved; a dihedral is formed by the intersection of two flat surfaces and a trihedral is formed when a third surface intersects the two that form a dihedral. The RCS pattern of a trihedral is broad in both the elevation and azimuth planes and a reflected wave generally undergoes three internal reflections, one from each face. There are a total of six possible internal ray paths representing the permutations of three bounces. The RCS pattern of a dihedral is broad in the azimuth plane (assuming the dihedral axis is vertical) but falls off in the elevation plane like the sin x/x pattern of a cylinder or flat plate. Thus the dihedral return can be reduced by tilting its axis toward or away from the radar so that the incident beam does not strike the dihedral axis at right angles. There are only two possible internal ray paths, and a reflected ray undergoes only two reflections.

Reducing the echoes from dihedral and trihedral corners found on ships can be accomplished using the tilt concept discussed earlier, since the large echoes are due almost entirely to the fact that the surfaces forming such corners tend to meet at right angles. If the surfaces can be angled slightly away from perpendicularity, then significant RCS reductions can be achieved. However, choosing the optimum angle of intersection of the surfaces is not quite as easy as in the previous case because all faces comprising the corner are finite, whereas in the previous case one of them (i.e., the sea surface) was infinite in extent.

In order to arrive at a criterion for the optimum corner angle we shall adopt as a model a dihedral corner viewed perpendicular to its axis. This is a reasonable alternative to an analysis of a trihedral corner, which is extremely complicated for non-perpendicular faces. But since a trihedral can be represented as a collection of three dihedral corners, the angles between the faces can be deduced from the analysis of the dihedral.

The geometry of the dihedral model is shown in Figure 42. The internal dihedral angle between the faces is 2β and the incident wave arrives along a direction ϕ measured from the plane bisecting the dihedral angle. The length of the dihedral (in a plane perpendicular to the plane of the figure) is ℓ and the widths of the two faces are taken to be a and b; these widths can be arbitrary, but we assume both are at least a few wavelengths wide. The analysis assumes that the scattering can be calculated by integrating the induced surface currents on each face due to a geometrical reflection of the incident wave off the other face. Depending on the dihedral angle and the angle of arrival of the incident wave, a given face may not be fully illuminated by the wave reflected off the other. Therefore effective face widths a' and b' must be used. For certain angles of arrival, it is possible that a reflected beam never strikes a face at all, and in these cases the effective face width should be set to zero.

The total return consists of four contributions, two of them being the direct single-bounce returns from each face and a pair of double-bounce contributions representing the interactions between the faces. The analysis will not be described, but the results may be computed with the aid of the formula

$$\sigma/\ell^2 = \left| \sum_{m=1}^{4} R_m \sin P_m \left(e^{-i2Q_m} - 1\right)/Q_m \right|^2 / 4\pi \qquad (18)$$

where P_m, Q_m and R_m are listed in Table II and a' and b' are effective face widths. Note that the double-bounce contribution has different

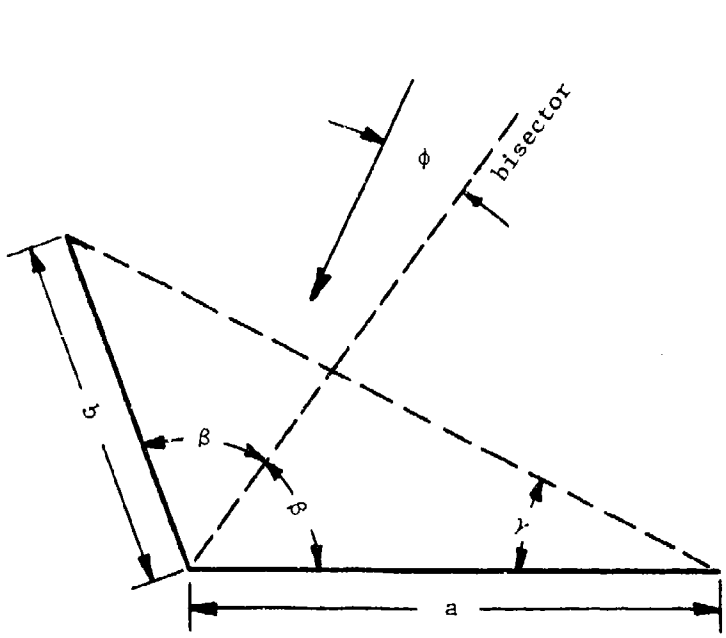

Figure 42. Generalized dihedral geometry.

terms depending whether the incident polarization is parallel or perpendicular to the dihedral axis (E- or H-polarizations, respectively).

m	P_m E-pol	P_m H-pol	Q_m	R_m
1	$\beta + \phi$	$\beta + \phi$	$ka \cos(\beta+\phi)$	ka
2	$\beta - \phi$	$\beta - \phi$	$kb \cos(\beta-\phi)$	kb
3	$3\beta + \phi$	$-(\beta - \phi)$	$kb' \cos 2\beta \cos(\beta+\phi)$	kb'
4	$3\beta - \phi$	$-(\beta - \phi)$	$ka' \cos 2\beta \cos(\beta-\phi)$	ka'

Table II. Parameters used in the RCS Formula for a Dihedral Corner Reflector

Figure 43 is the RCS pattern of a 90-degree dihedral corner having equal faces and Figure 44 is for a corner with unequal faces. The sidelobes of the m = 1,2 terms cause the ripples in the pattern and depending whether the faces are of equal width or not, the specular returns at $\phi = \pm 45$ degrees may be of unequal amplitude. Note in Figure 44 that the peak of the double-bounce contribution is shifted to one side of the pattern; this peak occurs at the aspect angle $\phi = \gamma_o - \pi/4$, where γ_o is the angle defined in Figure 45. At this particular angle of incidence both faces are fully illuminated by the beam reflected off the opposite face and the corner presents its maximum effective width to the radar. The amplitude of the double-bounce contribution at this aspect is

$$\frac{\sigma}{\ell^2} = 4(kb \cos \gamma_o)^2/\pi \qquad (19)$$

In deriving an analytical expression for choosing optimum dihedral angles, the single-bounce contributions may be ignored because their sidelobe levels will be low in the aspect angle regions where the double-bounce contributions are significant. In the analysis the dihedral angle is permitted to be some small angle τ greater than 90 degrees. Then, by fixing the aspect angle at a value near, but

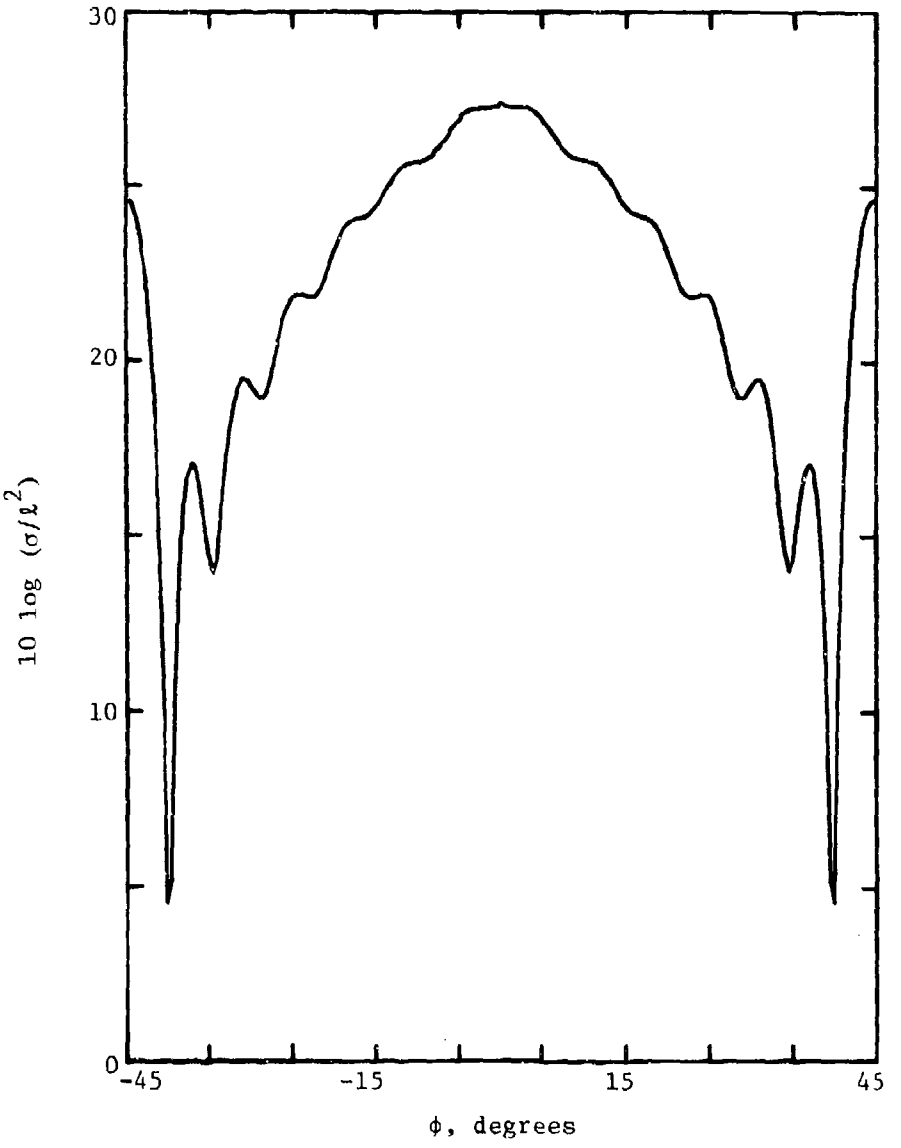

Figure 43. Dihedral corner RCS pattern for ka = kb = 30 and $\beta = \pi/4$.

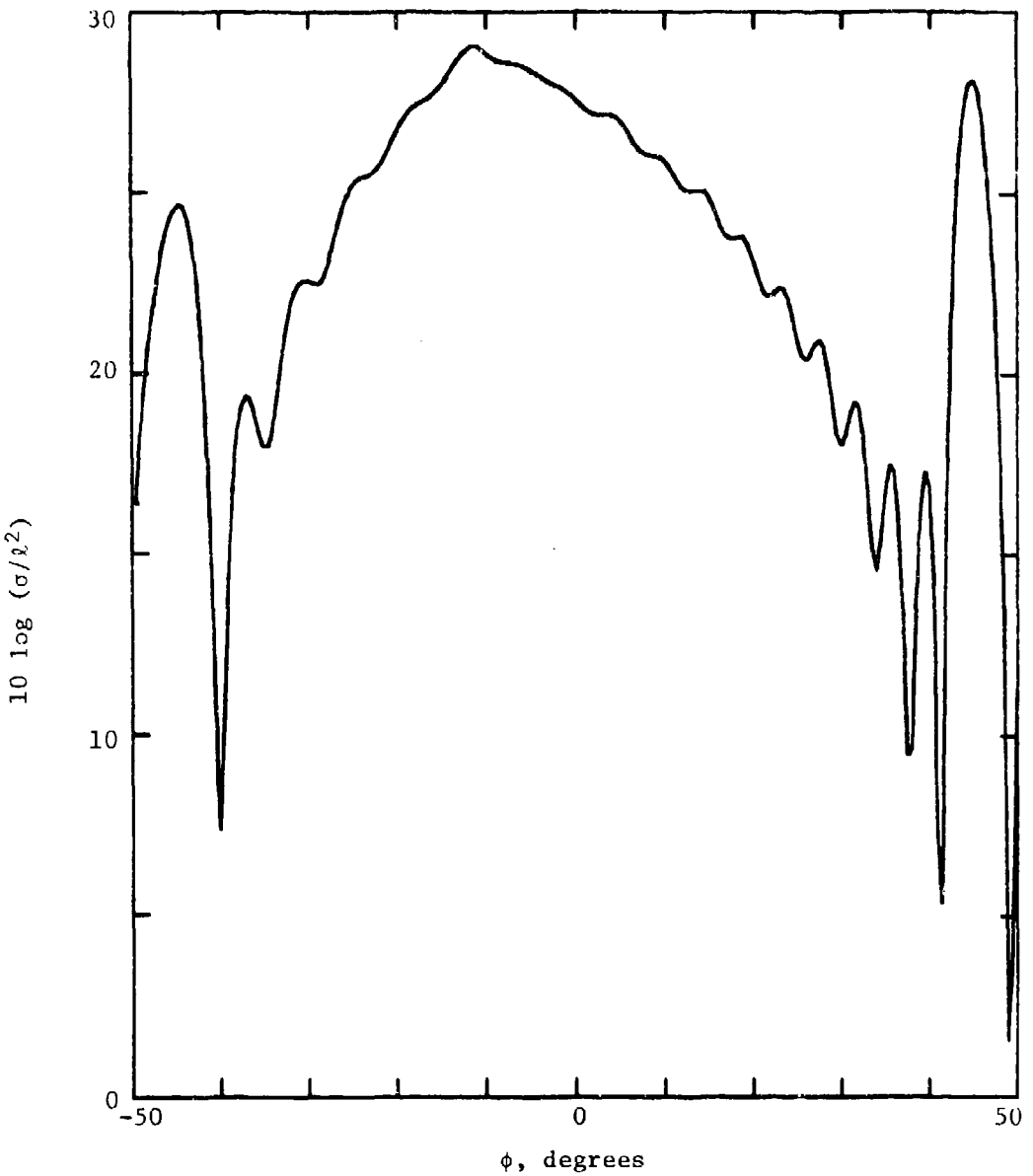

Figure 44. Dihedral corner RCS pattern for ka = 45, kb = 30 and $\beta = \pi/4$.

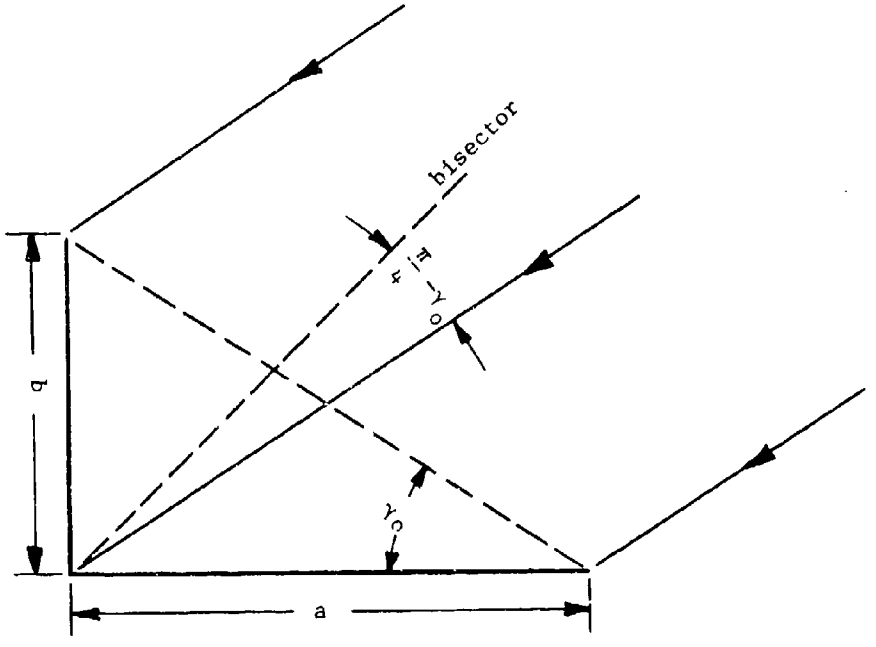

Figure 45. Maximum echo condition.

not exactly at, the angle γ_o, small-angle approximations can be made in the functions R_m, P_m and Q_m in equation (18). The resulting function is oscillatory in aspect, but attains maximum amplitudes of

$$\left.\frac{\sigma}{\ell^2}\right|_{max} = \frac{4}{\pi \sin^2 \tau} \tag{20}$$

Consequently the reduction in radar cross section can be found by dividing (20) by (19); if we denote the reduction by the symbol R, then

$$R \simeq 1/(kb \sin \tau \cos \gamma_o)^2 \tag{21}$$

Equation (21) may be solved for sin τ, and if τ is a small enough angle,

$$\tau \simeq 1/\sqrt{R}\ kb \cos \gamma_o \text{ radians} \tag{22}$$

This result shows that greater reductions (smaller values of R) require larger dihedral angles, but that higher frequencies (greater values of kb) allow similar reduction levels for smaller angles. Thus a dihedral selection based on (22) would have to include the reduction desired at the lowest practicable frequency; the reduction would then improve at frequencies higher than the lowest one, as (21) shows. A plot of equation (21) is given in Figure 46 for three values of a/b, showing greater reduction for greater dihedral angles. This figure also shows that the reduction obtained, whatever it is, will be better for unequal face widths than when the faces are equal in size. (Face b has been assumed the smaller of the two.)

If the angle of the dihedral of Figure 44 is opened up to 100 degrees from 90 degrees, implying τ = 10 degrees, then the pattern of 47 will be obtained. Figure 46 suggests that a reduction

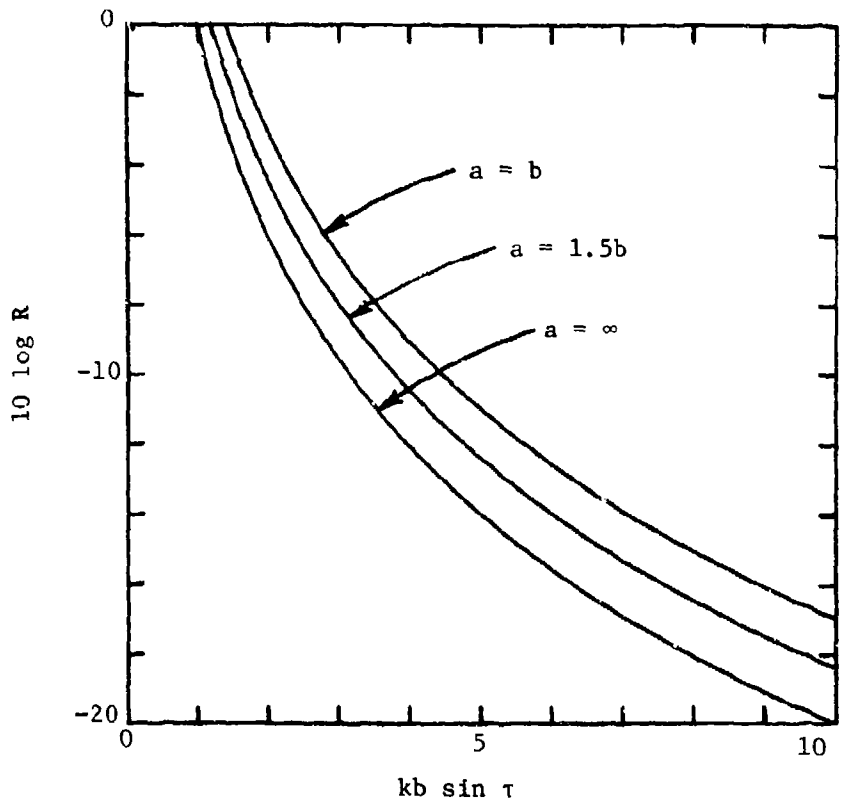

Figure 46. Optimum dihedral angle may be selected knowing kb and the reduction required.

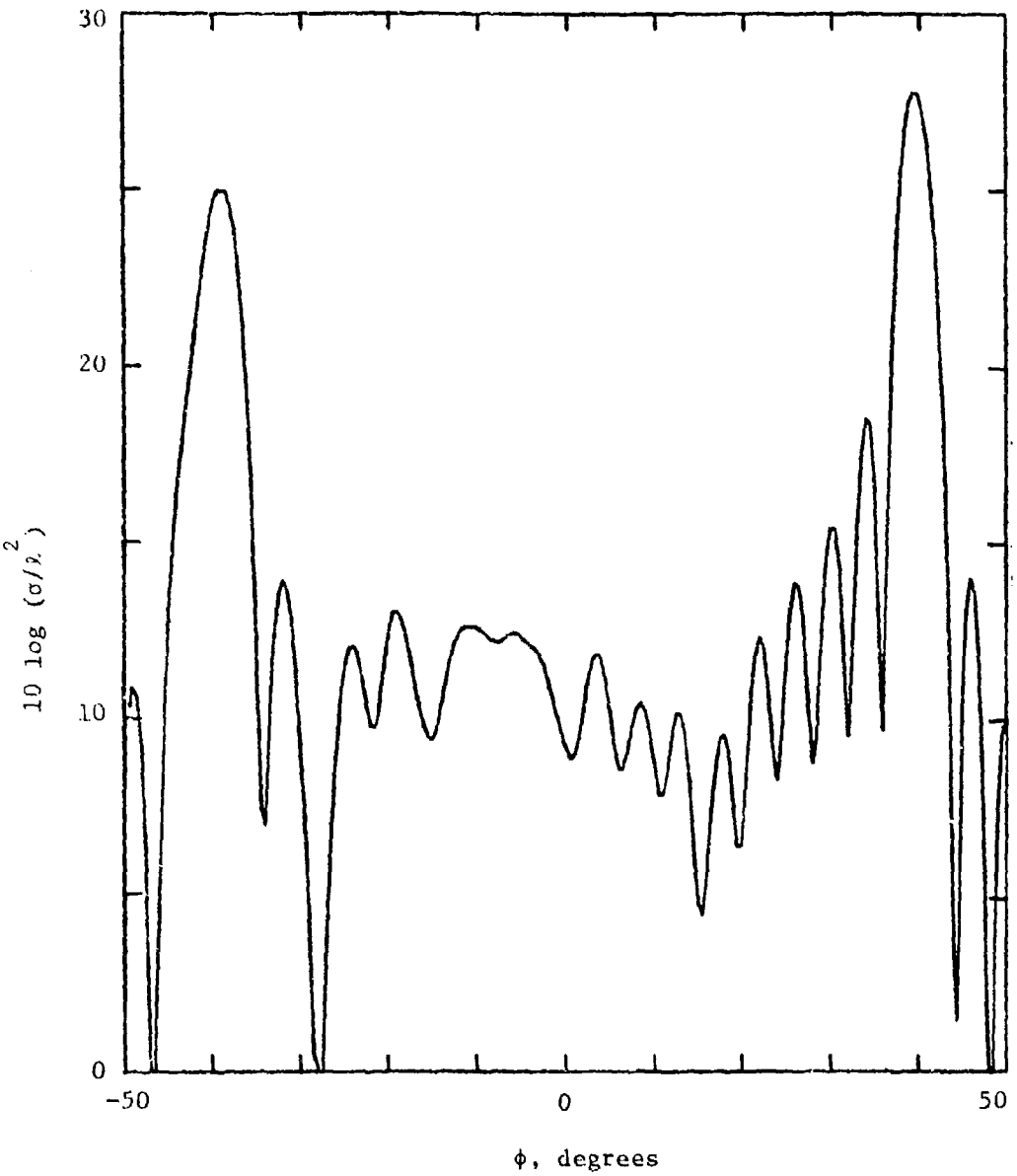

Figure 47. Dihedral corner RCS pattern for ka = 45, kb = 30 and β = 50 degrees; compare with Figure 44.

of 12.7 dB should have been obtained (for kb sin τ = 5.2) and a comparison of Figures 44 and 47 shows that this was very nearly attained over the central region of the patterns. Thus the dihedral selection criterion as represented by equation (21) or (22) is a useful one, provided the indicated angle can actually be incorporated in the structure.

Figure 48 represents another way of using criterion (22). The chart can be used as follows: first determine the lowest frequency for which the given RCS reduction must hold, thereby fixing the wavelength λ. Then find the width of the smaller face in wavelengths. Enter the chart with this value of b/λ and read the required angle for the given cross section reduction value. By way of example, assume the return from a dihedral whose smaller face is 10 feet wide must be reduced 10 dB for all frequencies above 3 GHz. At 3 GHz the wavelength is 3.94 inches, hence $b/\lambda = 30.5$. Entering the chart at $b/\lambda = 30.5$ and R = -10 dB, we read $\tau = 1.35$ degrees, whence the dihedral angle must be either 91.35 or 88.65 degrees. On some structures the construction tolerances may be such as to automatically provide a cross section reduction of this magnitude.

F. Antennas

Almost any vessel of appreciable size is fitted with dozens of antennas covering many frequencies of operation. These are associated with navigation and communications systems as well as radars; some are used for reception only, others for transmission only and still others perform both functions. Since the purpose of any antenna involves emission and/or reception of electromagnetic energy, it must be deployed and exposed, and therefore it constitutes a potential source of reflection to an incident radar beam.

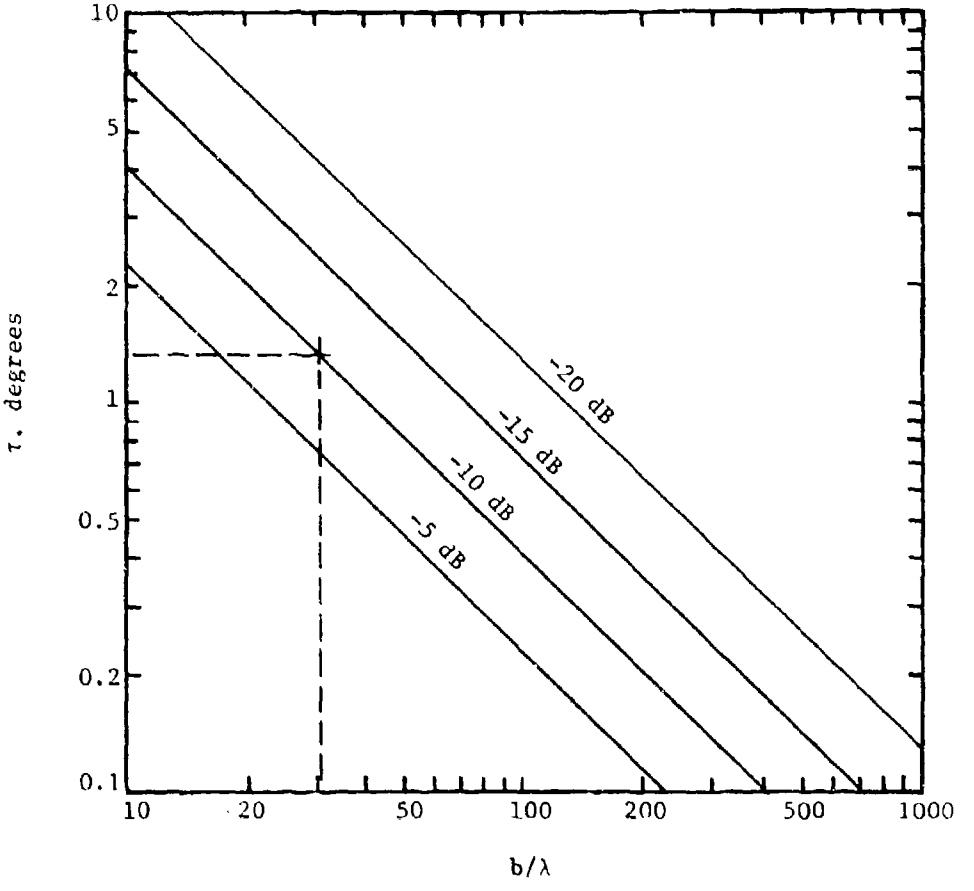

Figure 48. Dihedral corner RCS reduction chart. The dashed lines represent a specific design discussed in the text.

Reducing the echo of an antenna without impairing its performance is a difficult task, and quite often the only way to accomplish the job is simply to accept the degradation and compensate by increasing the gain or power level within some other stage of the system feeding (or fed by) the antenna. Antennas operating in the HF range tend to consist of thin elements (wires) and little can be done to shield them from radars of much higher frequencies. Occasionally increasing the output impedance of the transmitter or the input impedance of the receiver can reduce the return near the system operating frequency, but has little effect on the high frequency return. The difficulty of such problems is beyond the scope of this handbook and cannot be considered further.

On the other hand, some techniques are available for narrow band antennas that employ reflectors in the antenna design. The specular return from the reflector itself is not particularly large because it is a curved surface, and we have seen that the specular echoes from flat plates represent an even stronger source of reflection. For example, if the reflector is a paraboloidal dish of focal length f, the specular RCS is

$$\sigma = 4\pi f^2/\cos^4\alpha \qquad (23)$$

where α is the aspect angle measured from the boresight (axis of revolution of the dish). For a focal length of 0.4 meter (as might be the case for a dish 1 meter in diameter), the RCS is very nearly 2 square meters. A disk the same size, by contrast, has a cross section of nearly 800 square meters at 10 GHz. Thus the reflector itself is not necessarily a high cross section shape.

On axis, however, most of the incident beam is focused on the feed, as indicated in Figure 49, and this is, in fact, the purpose of the

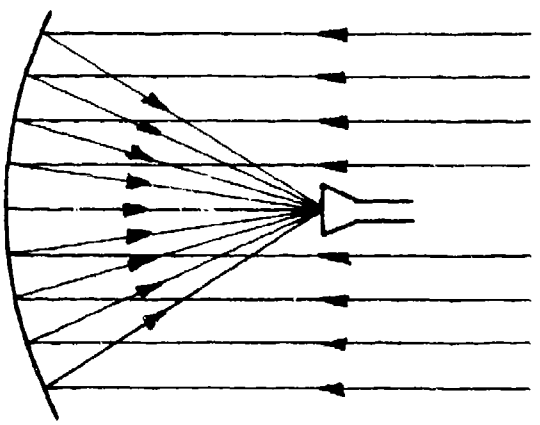

Figure 49. Focusing property of reflectors.

reflector. At the frequency of intended operation, the feed probably acts like a poorly matched load, absorbing perhaps only 50% or more of the incident energy. At other frequencies, it may be a better reflector than absorber; moreover, even if 50% of the energy is absorbed, a substantial fraction of the remainder is likely to be reflected back to the dish and thence back to the radar from whence the incident wave originated. Consequently the focusing properties of reflectors, coupled with the presence of some kind of feed structure at the focus, make high frequency antennas behave like high RCS shapes.

The effect would be most noticeable when the antenna is viewed on axis, which is precisely the case in a tactical encounter between, say, a ship and a missile. If the ship's radars have detected an approaching target (the missile), the antennas will be pointed directly at the missile while tracking it. The missile's own radar will be aimed at the ship. Each will be presenting its main beam to the other, each thus providing the other with its highest RCS for a given frequency. Depending on the precise antenna characteristics, the ship's radar antenna alone could present a radar cross section nearly as large as that of the ship itself. In particular, if the ship's hull is beyond the horizon, and the antenna sufficiently high above the waterline, the antenna might well constitute the only substantial target to be seen by the approaching missile. Thus radar antennas are potential sources of RCS vulnerability.

Two techniques have recently been developed by which the RCS of reflector antennas can be reduced; one is a band-pass metallic radome that can be placed in front of the antenna and the other is to make the reflector itself behave like a transparent surface at all but the frequency of operation. Typically both surfaces are perforated metallic sheets, with the size, shape and distribution of the perforations chosen for the mode and frequency of operation. The methods are indicated diagrammatically in Figure 50.

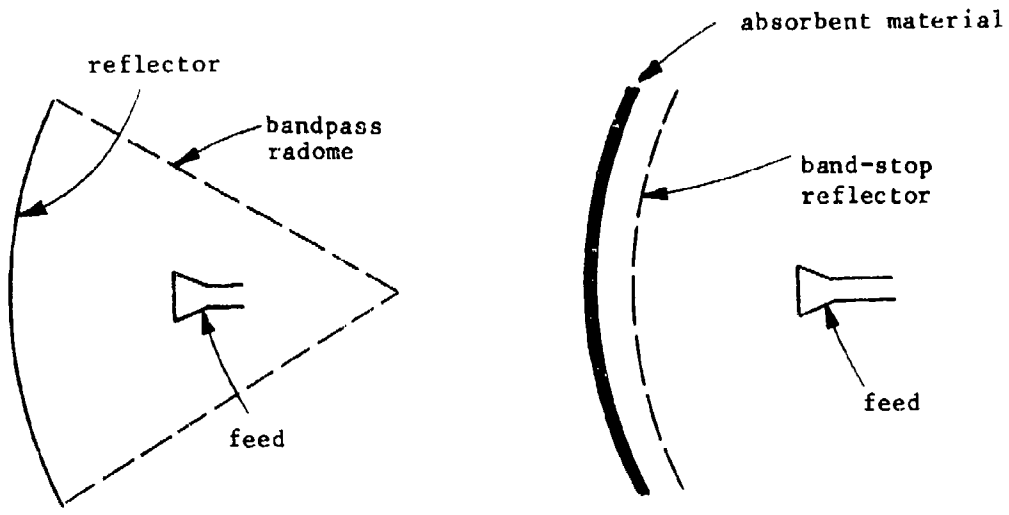

Figure 50. Examples using tuned surfaces.

The bandpass radome is the more desirable, since it tends to work better than the band-stop reflector over a greater range of frequencies. Only the frequencies within the operating band of the radar penetrate the radome from outside; for all (or most) other frequencies, the radome effectively looks like a metallic cone which, as we have seen, is basically a low RCS shape. The bandstop reflector behaves in the opposite manner. At the frequency of operation the reflector is a good one and behaves much like the metallic reflector it replaces. However, it is designed to be essentially transparent at all others so that an incident wave passes through the reflector and is absorbed by the radar absorbent coating placed behind it.

The bandpass radome can be fabricated using printed circuit and etching techniques, but it is still in the development stage and optimum patterns have not yet been fully worked out. The underlying theory is based on array techniques, but is too advanced for presentation here. The theory is developed on the basis of plane (flat) structures and when the flat surface is rolled into a cone, some polarization and

orientation degradation occurs. Nevertheless, the method remains attractive and is likely to be improved as time goes on. Further information is available in references [15] through [19].

IV. RADAR ABSORBING MATERIALS

A. Absorber properties

The theory of radar absorbing materials is complex and over the years literally thousands of pages have been written on the subject comprising hundreds of reports and documents. It would be impossible to explain the details and intricacies of the research that has led to state-of-the-art RAM without resorting to physics and mathematics beyond the scope of this book. Hence the principles will be described using a limited (but necessary) amount of mathematics.

The basic feature of RAM lies in the fact that substances either exist or can be fabricated whose indices of refraction are complex numbers. In the index of refraction, which includes magnetic as well as electric effects, it is the imaginary part that accounts for the loss. At microwave frequencies the loss is due to the finite conductivity of the material as well as a kind of submicroscopic friction experienced by molecules in attempting to follow the alternating fields of an impressed wave. It is customary to lump the effects of all loss mechanisms into the permittivity and permeability of the material, since the engineer is usually only interested in the cumulative effect.

The term "loss" refers to the dissipation of power or energy within the material, quite analogous to the way energy is consumed by a resistor when electric current passes through it. The loss is actually the conversion of electrical energy into heat and although most absorbers do not absorb enough energy to get hot or even detectably warm when illuminated by a radar, this is nevertheless the mechanism by which they operate. If the transmitter were to be brought close enough to the radar absorbing materials, they would assuredly get warm.

The index of refraction is the ratio of the wavenumber describing wave propagation within the material to that of free space and is proportional to the geometric mean of the product of the relative

permeability μ_r and the relative permittivity ε_r:

$$n = k/k_o = \sqrt{\mu_r \varepsilon_r} \tag{24}$$

where k_o is the free space wavenumber. Similarly, μ_r and ε_r also define the intrinsic impedance of the material Z,

$$Z = Z_o \sqrt{\mu_r/\varepsilon_r} \tag{25}$$

where Z_o is the impedance of free space. Both μ_r and ε_r are, in general, complex numbers and it is their imaginary components that account for electromagnetic energy losses. For common dielectrics such as glass, wood, rocks, water, etc., the relative permeability is one.

A normalized impedance η can be defined for a metallic surface coated with a layer of absorbent material,

$$\eta = \sqrt{\frac{\mu_r}{\varepsilon_r}} \tanh(-ik_o d \sqrt{\mu_r \varepsilon_r}) \tag{26}$$

where d is the thickness of the coating. This formula applies to a wave striking the surface at normal incidence and becomes more complicated when the wave arrives at oblique angles. The normalized impedance is used to calculate the reflection coefficient R of the material when covering a metal surface,

$$R = \frac{\eta - 1}{\eta + 1} \tag{27}$$

Since η is a complex number, so is R. It is possible to have nearly 100% reflection if the coating is very thin; for example, if d is very small, then $R \simeq -1$, the negative sign merely indicating a reversal of the sense of polarization of the reflected wave.

In speaking of reflection coefficients, it is customary to ignore the phase angle and to refer only to the "voltage" amplitude $|R|$, so that

the power reflection in decibels is

$$\text{power reflection coefficient in dB} = 20 \log_{10} |R|$$

The objective, of course, is to somehow design the material so that $|R|$ remains as small as possible over as wide a frequency range as possible. No reduction in return is available if $|R| = 1$. It should be noted that unless the material has some loss, the amplitude of the reflection coefficient will be essentially unity, although its phase angle will depend on the electrical thickness of the coating. Thus one of the objectives of RAM design is to provide for sufficient loss over as wide a frequency as possible, thus improving the utility of the material. In the discussion below, the terms "reflection coefficient" and "reflectivity" will be used essentially interchangeably.

B. Pure dielectrics

By "pure dielectrics" we mean absorbing materials having no magnetic losses and for which the loss mechanism is entirely due to electric polarization and conduction losses. Pure dielectrics have been used in radar camouflage applications for several decades and some early designs are still available for routine use. In some the lossy properties are evenly distributed throughout the bulk of the materials and in others the RAM is built up in layers, with the loss being different from layer to layer, but more or less uniform within a given layer.

Carbon has been found to be a very useful material for providing loss because its conductivity is much lower than common metals and is therefore a convenient vehicle with which to dissipate ohmic heating losses. However, its bulk conductivity is still relatively high and it is customarily dispersed in a matrix of almost lossless dielectric material in order to achieve the desired bulk conductivity. It may also be deposited on thin dielectric sheets or paper of the order of 5 mils thick* and used as a Salisbury screen.

*1 mil = 0.001 inch.

1. The Salisbury Screen

The Salisbury screen is the most primitive form of dielectric absorber. For all practical purposes the resistive sheet has no thickness at all and its performance is extremely simple to analyze theoretically. The sheet is spaced a quarter wavelength off the metallic surface it is intended to shield and for maximum performance the sheet resistivity is tailored to that of free space, 377 ohms. However, the quarter wavelength standoff distance is satisfied for only one frequency, consequently the Salisbury screen suffers bandwidth limitations.

The geometry of the Salisbury screen is shown in Figure 51, with the stand-off distance d being fixed at a quarter wavelength at the desired frequency. The resistive sheet is typically mounted on a low dielectric constant spacer, such as a rigid plastic foam or honeycomb structure. The net reflection of energy from this configuration depends on the frequency of the incident wave, the spacing d and the resistivity of the sheet. The reflection coefficient is theoretically zero for a resistivity of 377 ohms per square (i.e., the impedance of free space) and a spacing of a quarter wavelength. In practical situations, of course, the resistivity cannot be controlled this precisely and the incident wavelength may not be exactly four times the stand-off distance. Figures 52 and 53 illustrate the performance that might be expected for several resistivities and spacings.

The screen performance for a 0.5-inch spacing is shown in Figure 52; note that the reflection coefficient reaches its minimum value at a frequency of 5.9 GHz (wavelength = 2 inches). The best performance is obtained for a resistivity of 377 ohms, but the performance is still a respectable -18 dB for a resistivity 20% lower (300 ohms). However, a resistivity of 200 ohms yields barely a -10 dB reflectivity level at the design spacing.

In order to achieve similar performance at a lower frequency, the spacing must be increased because the wavelength becomes longer. The effect is shown in Figure 53 and it will be observed that a pair of nulls now exist, one at a frequency three times the other. The

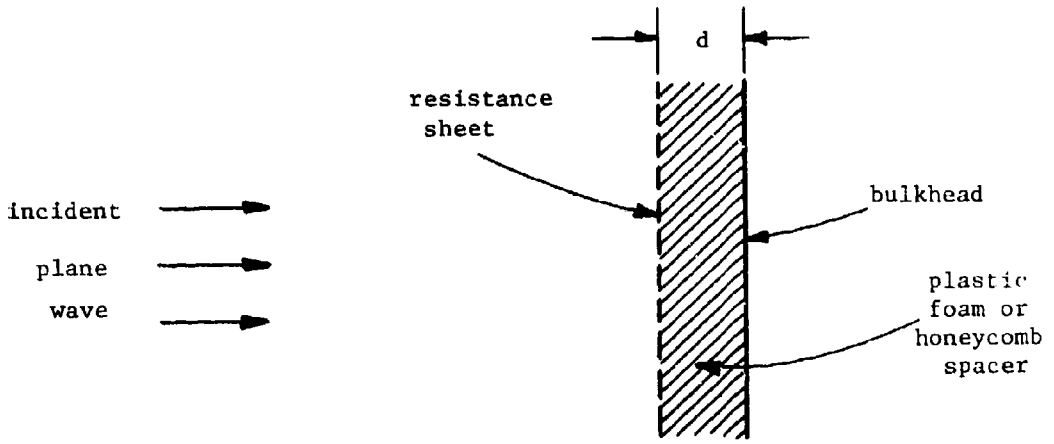

Figure 51. Salisbury screen.

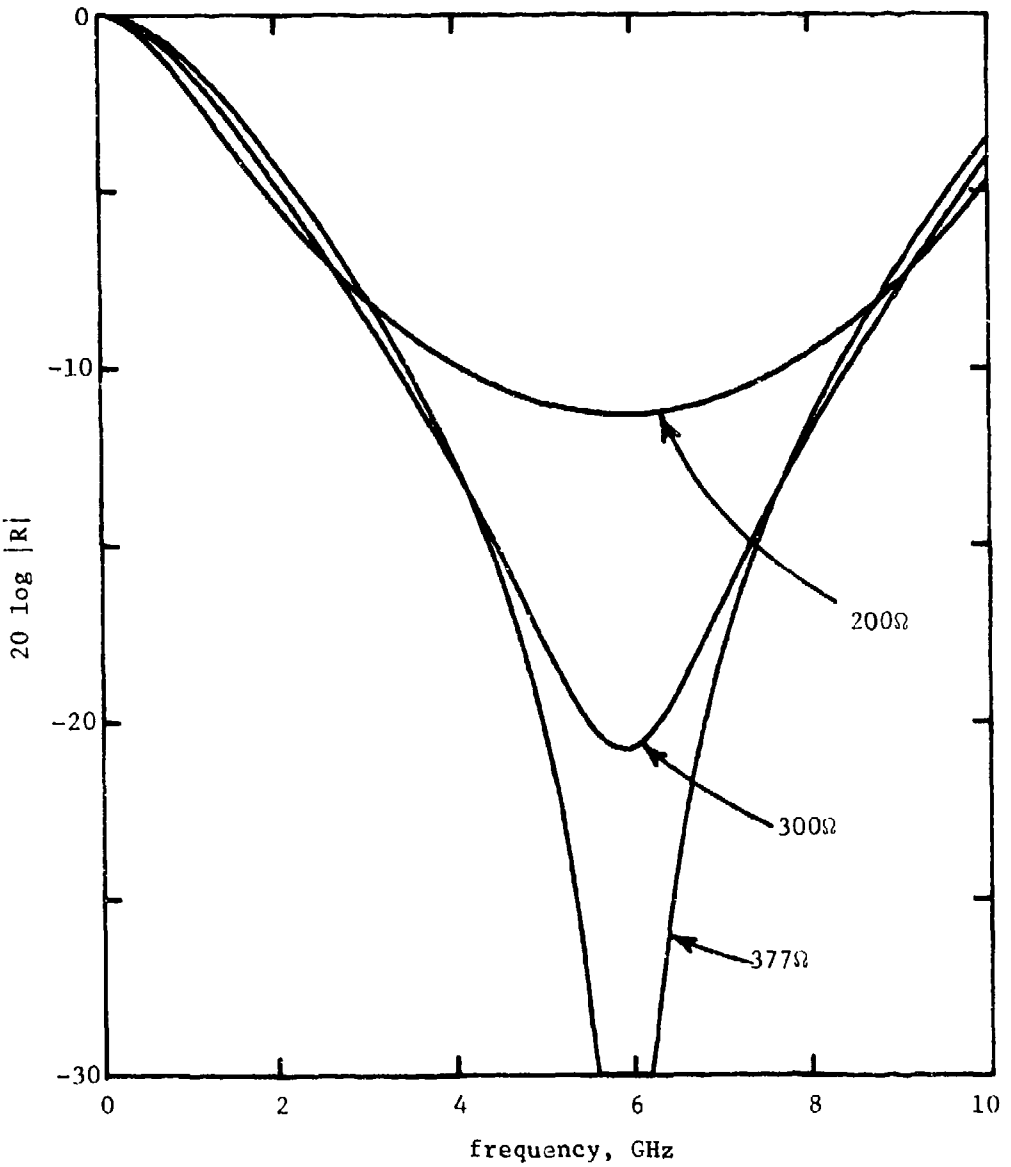

Figure 52. Performance of Salisbury screen for stand-off distance of 0.5 inch.

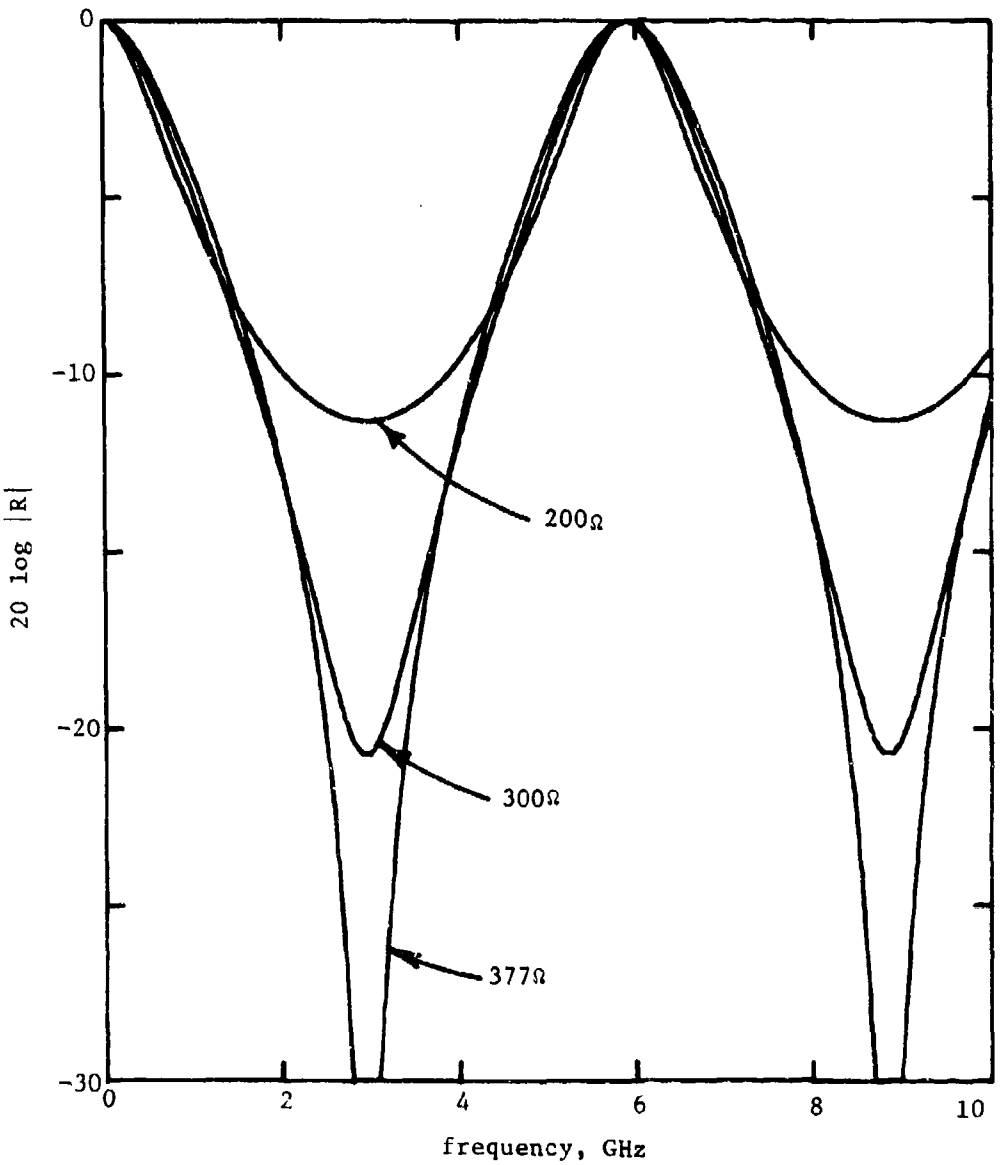

Figure 53. Performance of Salisbury screen for stand-off distance of one inch.

minimum reflectivity levels are the same as those in Figure 52, and it is clear that Figure 52 is merely an expanded portion of Figure 53. The nulls will occur at odd integral multiples of the lowest frequency, which is due to the fact that the design spacing can be any odd multiple of a quarter wavelength.

The Salisbury screen has been used in varying degrees in commercial absorbing materials, but the above characteristics do not necessarily mean that it cannot be used as a lightweight absorber. The rapid oscillations for large spacings would render it ineffective over a wide frequency range, however. In order to maintain the electrical spacing to be a quarter wavelength, the resistive sheet could be mounted over a dielectric layer trimmed to be a quarter wavelength thick within the material, which would be less than the free space wavelength. In this case the sheet resistivity should be pegged at a value near the intrinsic impedance of the material instead of free space.

The bandwidth of a Salisbury screen absorber can be increased by adding more resistive sheets and for optimum performance the resistivity should vary from sheet to sheet, that of the outermost layers being high and that of the innermost layers being low. The increase in bandwidth can be appreciated from inspection of the performance characteristics shown in Figure 54 for hypothetical lay-ups of from one to four sheets. For this illustration the spacing between sheets was fixed at 0.295 inch (a quarter wavelength at 10 GHz). By arbitrarily selecting the -19dB level for gauging the bandwidth, Table III can be constructed; the bandwidth is merely the ratio of the highest

Number of sheets	Bandwidth	Total thickness (inches)
1	1.3:1	0.3
2	1.7:1	0.6
3	3.0:1	0.9
4	4.0:1	1.2

Table III. Bandwidth of multi-sheet resistive absorbers.

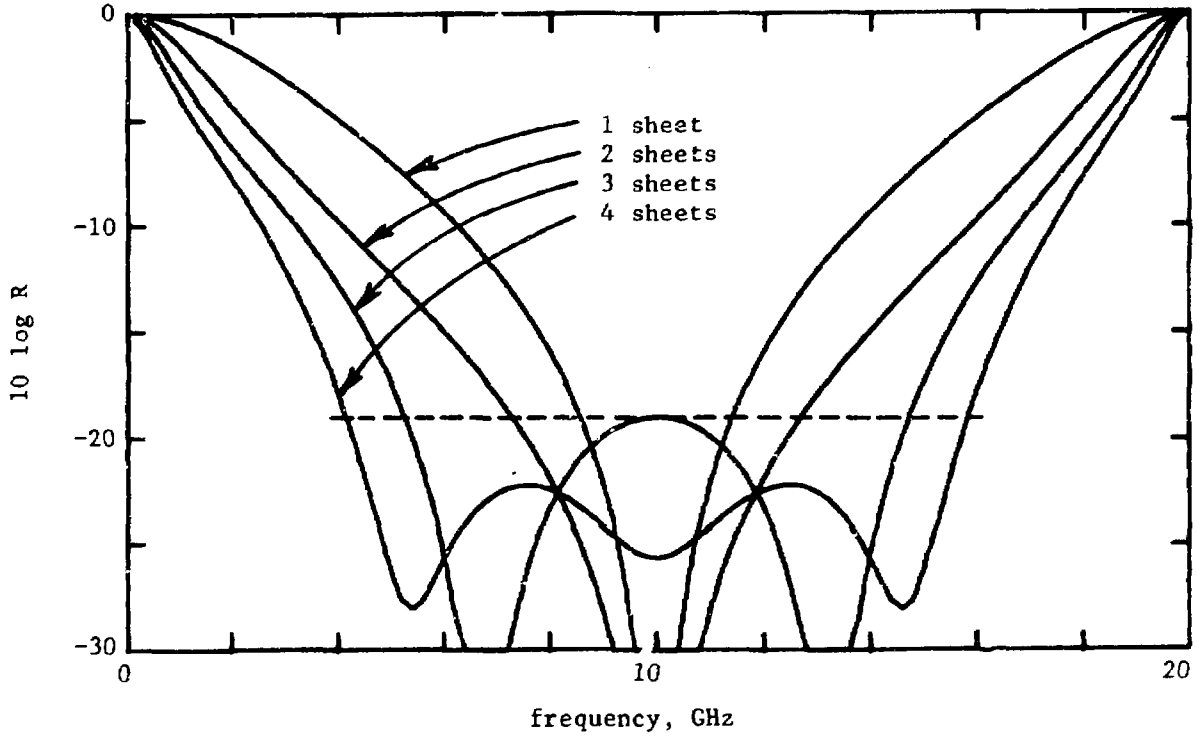

Figure 54. Performance of multiple resistive sheets.

to lowest frequency over which this specified reflectivity level is maintained. Note that a 4-sheet lay-up has more than three times the bandwidth of a single layer, and it is clear that greater bandwidth could be achieved if even more layers were to be added. The price paid to achieve higher bandwidth, however, is an increase in the total thickness of the lay-up.

2. Foam Absorbers

Foam absorbers are typically made of flexible urethane foams, although some low frequency materials have to be fabricated of rigid expanded styrene foams. The flexible urethanes have the advantage that they can be fastened to curved surfaces, although the surface curvature cannot be too small. One type of foam material is based on the Salisbury screen principle; the resistive layer is cemented to one side of a thin slab of foam and a metallic skin to the other. These materials are typically thin, of the order of 1/4 inch or so, and thus find greatest application at relatively high frequencies. They are called resonant foam materials because the foam thickness (i.e., stand-off distance) is crucial in obtaining maximum performance.

Thicker foam materials are commonly made by loading the open cell structure of the foam with carbon particles, "open cell" referring to the fact that a cell within the material is connected to neighboring cells. This is necessary, since in the manufacture of the absorber the foam must act like a sponge and soak up a solution, which would be impossible if it had a closed cell structure. A typical fabrication procedure is to compress a pad or block of foam between a pair of plates, to immerse the pad in a bath containing suspended carbon particles, and then to release the plates and allow the foam to expand. It soaks up the carbon loaded bath solution much as a sponge picks up water. The pad is then removed from the bath and again compressed, forcing out the liquid but leaving the carbon entrapped within the foam's cell structure. The pad can then be dried and subsequently painted or used in the construction of multiple layer materials. It may be possible to include particles having magnetic loss, but whether this is currently done is not clear.

It has been found, and it can be demonstrated theoretically, that if the transition from one medium into another can be accomplished smoothly,

the reflection from the interface between the two media can be minimized. If material properties could be controlled closely enough, this would be done ideally by varying the dielectric constant from a value equal to the impedance of free space at the front of the layer to a value appropriate to zero impedance at the rear where it mounts on the bulkhead. The state-of-the-art has not reached this level of sophistication however, and in practice, the impedance taper is obtained by physically shaping the absorbing material or by stacking up a number of layers in which the intrinsic impedance of each layer is progressively smaller than the previous one, even though the impedance within a given layer is constant through the layer thickness.

The geometrical taper is very common in the foam absorbers, with the pyramidal form being predominant. A side view of the geometry is shown in Figure 55. The depth h of these materials is a function of the lowest frequency at which they must perform and the reflectivity levels that must be attained. Very low frequencies demand very deep materials, and some as deep as h = 12 feet have been produced. However, these are unusual cases and more common sizes are in the 5-inch to 18-inch range. The low reflectivity tends to persist upward through a wide range of frequencies, and levels of -50 dB have been obtained over a 10:1 frequency band. The cost of these radar absorbing materials can be very high; they are customarily used in anechoic chambers and shielded enclosures where high performance is required in radar cross section measurements, antenna pattern work and radio frequency interference (RFI) studies.

Pyramidal absorbers work best when the incident wave arrives in a direction parallel to the symmetry axis of the individual pyramids. As the angle of incidence swings further from this axis, the performance begins to deteriorate. Eventually when the angle gets great enough, reflections from the sides of the pyramid will be picked up and in these cases it would have been better to have used flat (non-pyramidal) materials. This fact induced manufacturers to produce a "squinted" form of pyramidal absorber for a time, such as in Figure 55(b), where the pyramids are angled toward the oblique angle of incidence instead of being erected perpendicular to the bulkhead. Again these found service only in anechoic chambers.

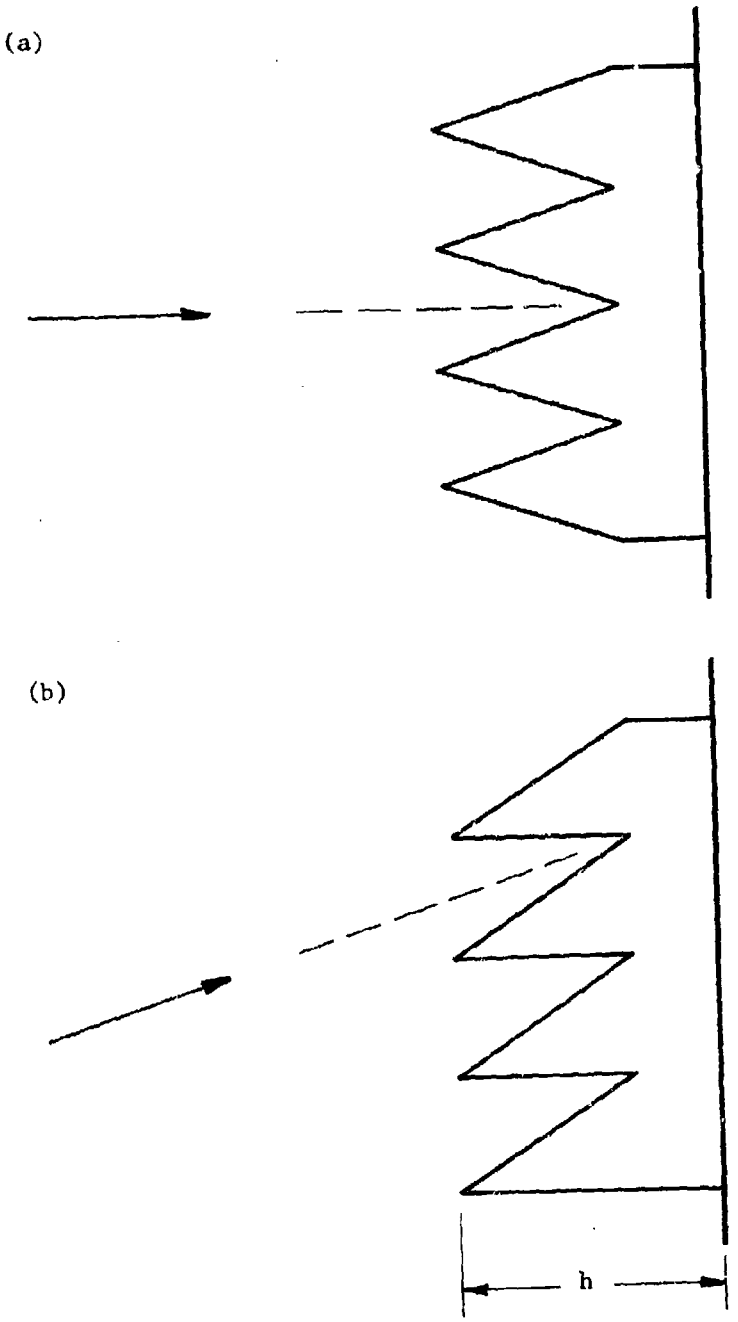

Figure 55. Pyramidal absorbers; a) standard, b) angled

A stratified approximation of a smoothly varying bulk impedance (or resistivity) is sketched in Figure 56. Ideally the variation should be smooth and continuous, with the intrinsic impedance of the material tapering from 377 ohms at the front to zero at the back. This is impossible in practice, but a finite number of layers often produces an acceptable approximation. Some high frequency, multi-layer foam absorbers have only two layers and are relatively thin, while some low frequency RAM has been produced consisting of as many as five layers. These low frequency absorbers can be quite thick (as much as two inches for frequencies near 1 GHz, for example) and are therefore not very flexible. Their performance is in general not as good, pound for pound, as that of the pyramidal type of absorber, but they are less expensive.

3. Hair or Fiber Absorbers

Early in the development of RAM, hair absorbers were common. They were made of animal hair, typically pig bristles obtained from packing houses, fluffed up into a semi-rigid matrix. They are not unlike the padding once used in shipping rooms to pack and protect breakable items. The raw pads are either sprayed with or dipped in a solution bearing dispersed carbon particles and after impregnation they are black, like the flexible urethane foams. The hair absorber can be left in this form after it dries, or can be sprayed a light color (usually white) or each panel can be wrapped in a thin sheet of white vinyl. Neither the paint nor the vinyl seems to affect performance and the light color is mainly for psychological reasons. These materials were widely used in early anechoic chambers and, since a totally black room can be a depressing environment to work in, the light colors improved the performance of personnel. The vinyl covers, it should be mentioned, are easy to clean and therefore facilitate housekeeping.

Hair absorbers are typically produced as panels two feet square and from one to eight inches thick. Each panel is stiffened by a coarse fabric mesh glued to the rear of the panel in the manufacturing process. Their performance improves with increasing thickness and increasing frequency.

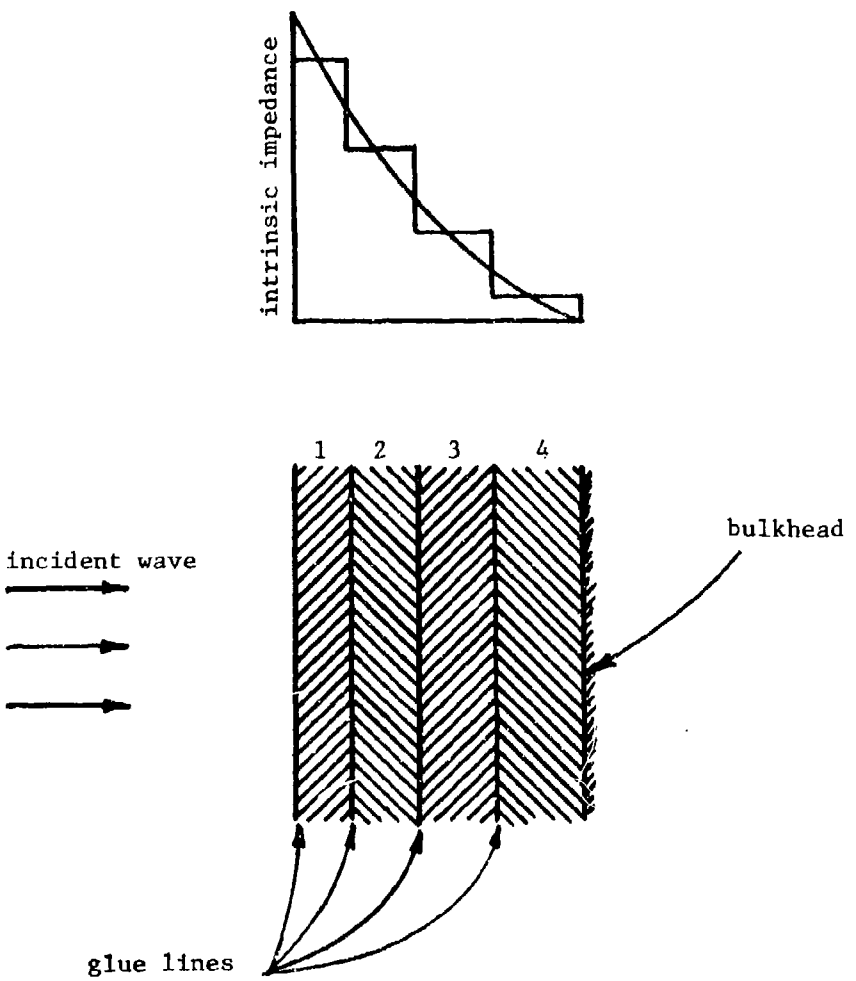

Figure 56. A finite number of layers is an approximation of an ideal continuous variation in impedance from front to back.

C. Magnetic Materials

Magnetic materials generally operate on the principle of magnetic instead of dielectric losses, although there is a small amount of dielectric loss as well. Compounds of iron are usually exploited for these losses, and ferrites and carbonyl iron are common ingredients. Ceramic materials employing ferrites are useful for high temperature applications, provided the ambient temperature remains below the Curie point. When the temperature approaches or exceeds the Curie temperature (usually from 500 to 1000 degrees Fahrenheit) the magnetic properties deteriorate. These ferrite materials are typically sintered in the form of rigid tiles one inch along a side, and application to a surface requires careful consideration of bonding adhesives.

Other methods of manufacture involve embedding the magnetic materials in a flexible matrix of natural or synthetic rubber which can then be glued to the surface to be shielded. Again the method of bonding requires attention. Several firms have developed spray-on materials in which the magnetic "dust" is suspended in an epoxy vehicle. Since the solid particles are heavy, they tend to settle at the bottom of the container used for spraying and constant agitation is required. The lossy coating is built up to the desired thickness by the deposition of several thin layers. Uniform thickness, and therefore uniform properties, are difficult to achieve unless skilled operators are available or can be trained for the task. The material can also be brushed on.

The spray-on RAM [31], also referred to as "iron paint," has the advantage that irregular surfaces can be covered more easily than with the flexible sheets, although singly curved surfaces (cylinders, cones, etc.) are amenable to the use of the sheets. For both forms of material, adequate surface preparation is required or else the absorbing layer may peel off. Since these materials all contain iron in one form or other, they tend to streak rust in a salt water environment. Several versions of the spray-on formulation are available and are marketed under different names: Goodyear calls its product "GRAM"; W.R.D. Corporation's is "ERASE"; North American Rockwell's is the "NR series." It is not known how well ordinary protective paints adhere to these surfaces.

Although magnetic RAM tends to be heavy, its virtue lies in the extended low frequency performance per inch of thickness. Whereas it would require an ordinary dielectric absorber several inches thick to achieve low frequency coverage down to 100 MHz and below, the magnetic materials need be only a tenth as thick (approximately) to achieve comparable performance. The reason for this is that the magnetic losses can be tailored for low frequencies as sketched diagramatically in Figure 57; since the losses tend to increase for the lower frequency via increasing μ_r, the electrical thickness of the material tends to "keep in step" with the frequency, and performance persists for lower frequencies. At the higher frequencies the magnetic properties no longer contribute much to the performance and the dielectric properties (ϵ_r) now account for the loss.

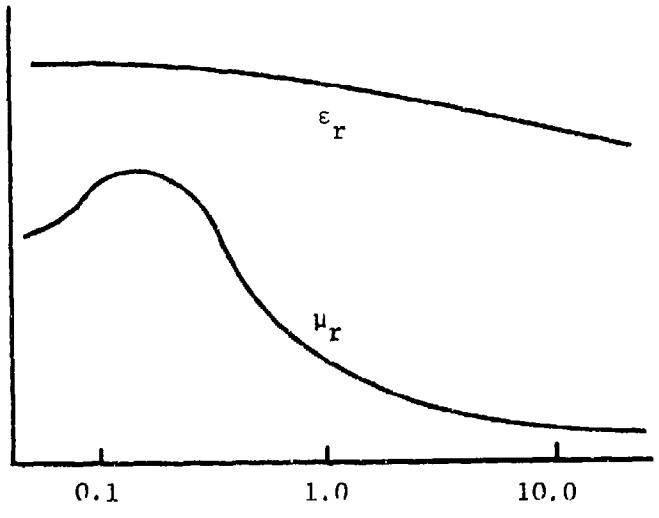

Figure 57. Schematic illustration of the frequency behavior of ferrites.

The performance plot shown in Figure 58 illustrates some of these properties for a hypothetical spray-on material whose magnetic losses increase with decreasing frequency. Note that the layer thickness influences the depth of the null as well as the frequency where the null occurs, much as does a Salisbury screen. However, the nulls are shallower for the thinner layers (t = 0.03 and 0.04 inch) because the loss mechanism is primarily due to dielectric losses. Thicker materials (t = 0.06 and 0.08 inch) have better performance at the lower frequencies because the magnetic losses come into play and the electrical thickness is appropriate to the lower frequencies. Altering the physical formulation of the material can shift these properties and, in fact, some absorbers having quite large bandwidth (of the order of 20 to 1) have been produced.

D. Circuit Analog Materials

Circuit analog (CA) materials are lightweight and depend upon geometrical patterns cut into thin sheets. The concept evolved from the notion of a "tuned" surface, in which a lattice structure is cut into metallic sheets. The precise shape and size of the pattern, which can be in the form of crosses, slots or any of a variety of shapes, dictate whether the surface appears to be inductive or capacitive to an incident plane wave. Since the pattern is cut or etched in a flat sheet, the surface has some reactance, and, in general, the reactance depends on frequency. And since the surface is metallic (although usually mounted on a substrate) there are no losses. This idea is used to produce bandpass radomes, in which a metallic screen can be made to appear nearly transparent at one frequency, but virtually opaque at all others.

Producing the necessary loss can be achieved by using a form of resistive material instead of a metal, and this also imparts some measure of bandwidth. The surface can then be described in terms of a conductance and an admittance, and the sensitivity of the ratio of the two to frequency changes gives the bandwidth. CA materials can be produced having high temperature durability and one of the

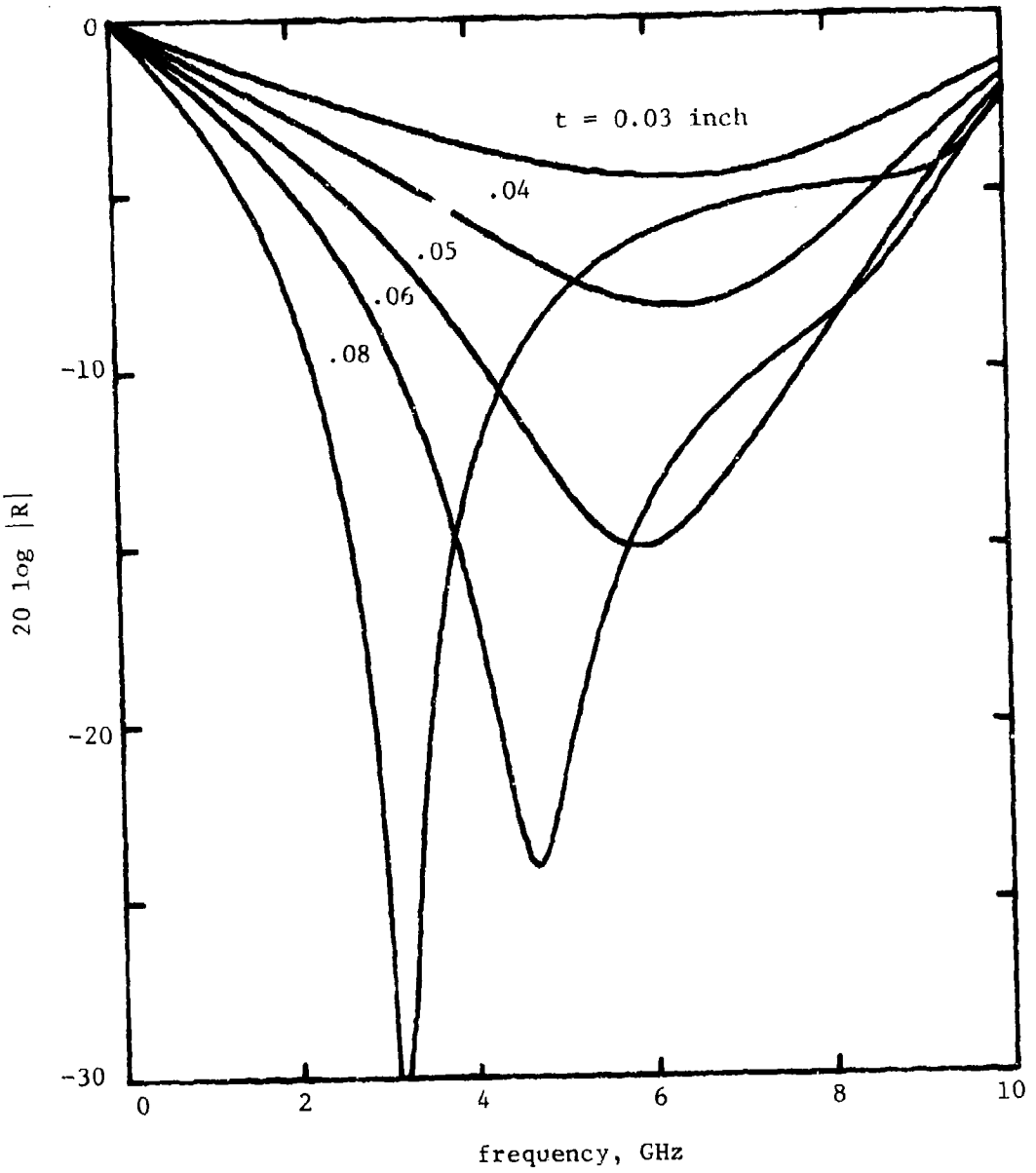

Figure 58. Generalized behavior of spray-on absorber. Layer thickness in inches is the parameter.

first uses was for the inlet ducts of jet aircraft. Layers can be cascaded to achieve improved performance at low frequencies.

E. Hybrid RAM

In a continuing on-going program whose objective is to extend state-of-the-art applications of radar absorbents, the Air Force Avionics Laboratory has evolved methods of designing multiple layer absorbents using existing materials for each layer [32]. The design itself is accomplished by a digital computer using statistical sampling methods; the statistical approach is necessary because the combination of the numbers of layers, layer thicknesses and materials available quickly pyramid to an astronomical number and the fastest computer would have to work continuously for hundreds of years to investigate and evaluate all possible combinations. In order to generate a hybrid RAM design, the computer program uses the measured electrical properties of a few dozen types of materials stored in a "data bank" accessed by the program.

In addition to the properties of what might be called true absorbers, the data bank also contains the properties of low loss, low dielectric constant materials used as spacers. As pointed out earlier in connection with Salisbury screens, it is often necessary to space absorbing layers some distance off the bulkhead or to separate layers. The method of achieving the spacing assumes that the dielectric constant of the interlayer medium is low, and ideally should be identically that of free space. In practice, of course, an actual spacer has a dielectric constant somewhat larger than that of free space (typically from $\epsilon_r \approx 1.05$ to 1.2), and this deviation must be accounted for. Spacer materials can be rigid dielectric forms or honeycomb.

The electrical design constitutes only part of the task. Depending on the type of application, which could include strength and high temperature requirements, a design must satisfy mechanical as well as electrical constraints. The program allows such constraints to be included, although the physical implementation of the design may

be complicated, such as the lay-up of material components on a complex surface to form, say, an engine cowl. The Avionics Laboratory has also developed methods of estimating the production costs of the hybrid RAM treatments and applications, since cost is not a negligible factor in absorber design. Other intricacies of the computer program include the incorporation of the electrical properties of glues and adhesives in the data bank so that an accurate performance prediction can be made of a practical design. A photograph of an actual sample of hybrid RAM may be found in Appendix C.

F. RAM Degradation

The reflectivity level quoted by manufacturers for radar absorbent materials is based on expected or measured performance when the material is applied to a large flat surface viewed at normal incidence. However, it is known that the performance deteriorates for oblique angles of incidence and when the material is used on surfaces with small radii of curvature. Moreover, free space flat plate measurements may show a degradation in comparison to waveguide measurements and this fall-off in performance has been attributed to edge effects [33]. Apparently the only way to compensate for such performance losses is to use a material with a rating better than the particular RCS reduction required.

Predicting the degradation in performance is a challenging theoretical task, but some approximate solutions have been worked out. The amount of flat plate deterioration that will be experienced depends on the size of the plate involved and the intrinsic normal incidence reflectivity of the material used. The better the material, the worse the degradation may be. For example, when mounted on a 10λ by 10λ flat plate, a nominal -30 dB material may degrade to -25 dB (a 5 dB loss), but a nominal -20 dB material may only degrade to -18 dB (a 2 dB loss). Further information may be obtained from Reference [33], which contains both theoretical and experimental assessments of RAM degradation.

When applied to objects with small radii of curvature, such as slender cylinders, the same kind of degradation occurs. An approximate theoretical treatment of the effect is given by Bowman and Weston [34], in which the absorbing layer(s) must be thin and lossy. The degradation

depends on the electrical circumference of the cylinder, the nominal flat plate reflectivity of the material and the incident polarization. A plot of the Bowman-Weston predictions is given in Figure 59 as an example of what might be expected for H-polarization (incident magnetic field parallel to the cylinder axis). Since the deterioration can be severe for very slender cylinders, only modest performance may be expected from otherwise good materials when they are wrapped around small cylinders. Bowman and Weston discuss how the material may be "tuned" for one polarization or the other, but they point out that this cannot be done for both polarizations simultaneously.

G. Absorber Manufacturers

Below is a list of absorbing material manufacturers who constitute the major sources of RAM in the western hemisphere. They are willing to discuss their product lines and will send brochures and specifications upon request.

Emerson & Cunning, Inc.
Canton, Mass. 02021
(617)-828-3300

Rantec Division
Emerson Electric Company
24003 Ventura Blvd.
Calabasas, Calif. 91302
(213)-347-5446

Plessey Microwave Materials
P.O. Box 80845
San Diego, Calif. 92138
(714)-278-6500

WRD Division
Acurex Aerotherm Corp.
485 Clyde Ave.
Mountain View, Calif. 94042
(415)-964-3200

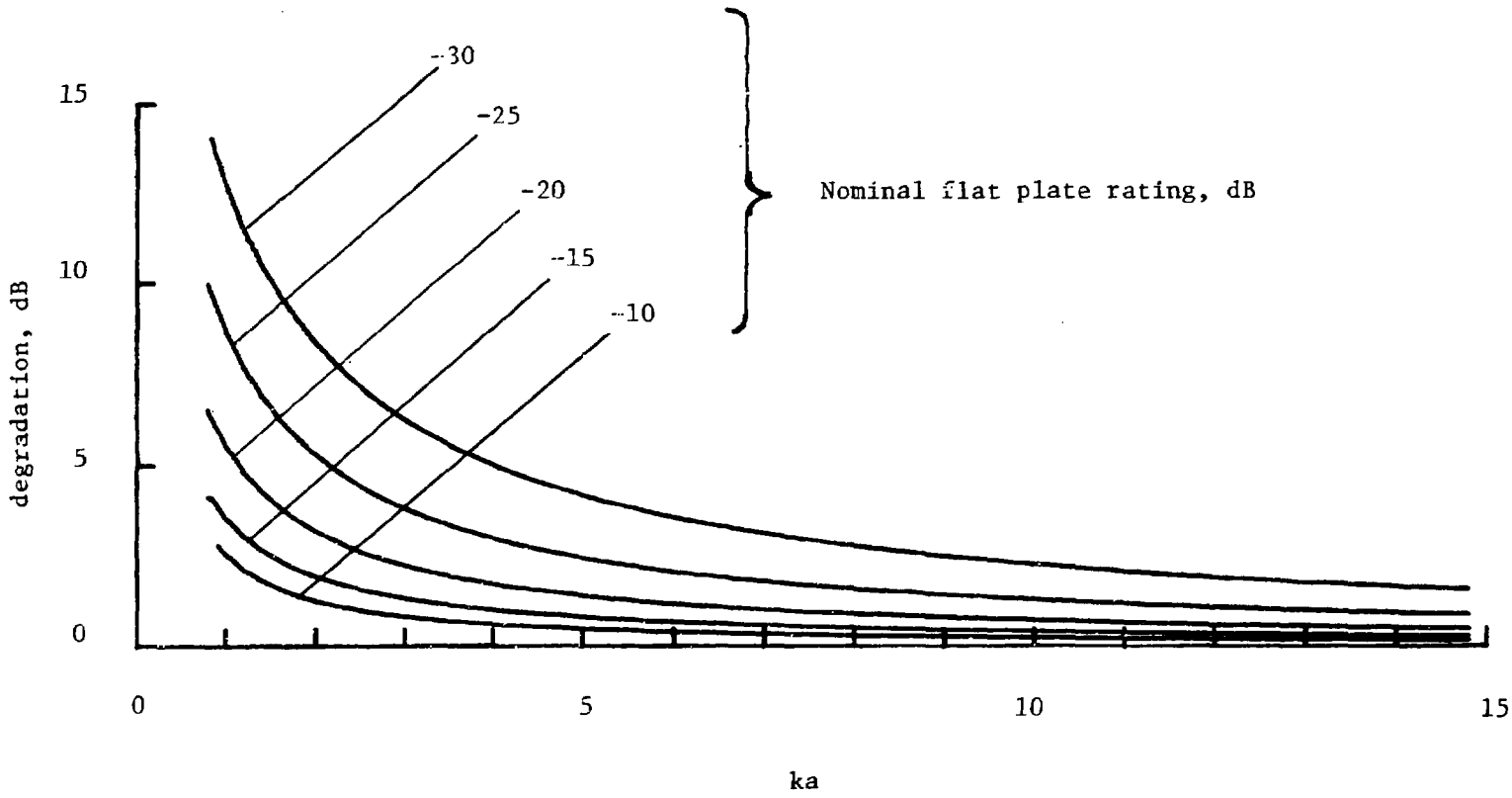

Figure 59. Absorber degradation as a function of cylinder size for H-polarization.

V. TREATMENT OF A SPECIFIC CLASS OF VESSEL

A. Modeling Technique

Previous studies carried out at Georgia Tech [8,14,25] have resulted in mathematical models that can be used to simulate radar performance in a marine environment. These models make it possible to modify radar designs, determine such quantities as radar cross section and received power, and to assess the effects of radar cross section reduction techniques, among other things. The advantages of such modeling is that sea trials or sea tests may be minimized, thereby reducing the cost and time of such exercises. The mathematical models have been verified in numerous field operations and tests, and are therefore useful tools for the specific task of RCS reduction.

These models will be used to demonstrate the importance of the main concepts emphasized in this handbook and examples will be given below for a guided missile cruiser. The model exists in the form of computer codes that account for the earth's curvature, the variation in the atmospheric index of refraction, the sea state, the multipath mechanisms shown in Figure 31 and the details of the actual structure of the ship. A host of results and inter-relationships can be printed out or even drawn by the computer, but only a few examples of the possibilities will be given below.

A time consuming but necessary task in the modeling process is to assemble a list of the dimensions, locations and types of scatterer of which the ship is composed. This list is used by the computer program to determine the composite scattering characteristics of the ship. Obviously many minor details must be omitted, such as small cleats and fittings, and even some sizeable items of deck gear are not included. Accuracy would require that a survey team spend months measuring the ship and consulting loft plans, but this would be a very expensive operation. Consequently the ship's dimensions are typically scaled from small plastic models such as stocked at hobby shops.

If commanded to do so, the computer will draw the composite ship using the data set provided by the user and the broadside view of

Figure 60 is an example. Note that the profile has been represented as a collection of flat plates, cylinders and spheres, with the bulk of the scatterers being flat plates. Amidships the hull is quite flat, hence the plates are relatively large, while near the bow and stern they must be smaller so as to approximate the actual contour of the hull. Profiles below the waterline are omitted from the data set since only those features above the waterline contribute to the scattering.

A different data set is required for a view of the bow, since many of the surfaces seen abeam are not seen from ahead. Figure 61 shows the a bow view of the guided missile cruiser in which some plates are seen to overlap others. The trapezoidal appearance of some of the plates near the waterline is a consequence of viewing rectangular plates from an oblique direction; the data set comprising a description of the vessel allows plates to be tilted or angled away from the vertical, but the plates must be rectangular. Consequently the plates in this view appear to be joined at their bottoms but separated at their tops. This does not affect the accuracy of the predicted results to any significant degree, however.

Each plate or scatterer bears an identification number and if required to do so, the computer program would label each plate with its ID number. Attention is called to the array of 18 rectangles of equal size displayed in two tiers near the center of Figure 61. These plates represent a large single flat plate on the bridge facing forward and in some of the patterns displayed below, this plate will receive special treatment. It is comprised of scatterers 17 through 34.

B. RCSR Treatments

Figure 62 represents the effective radar cross section of the ship of Figures 60 and 61 as a function of azimuth angle in the bow-on region. The radar cross section was calculated for integral values of aspect angle and the datum points generated were connected by straight lines. The lines are intended only to guide the eye from one datum to the next and are thus approximations of the performance that might be measured under actual conditions. A radar frequency of 9.22 GHz was assumed with an antenna height of 100 feet and the ship at a range of 5 nautical miles.

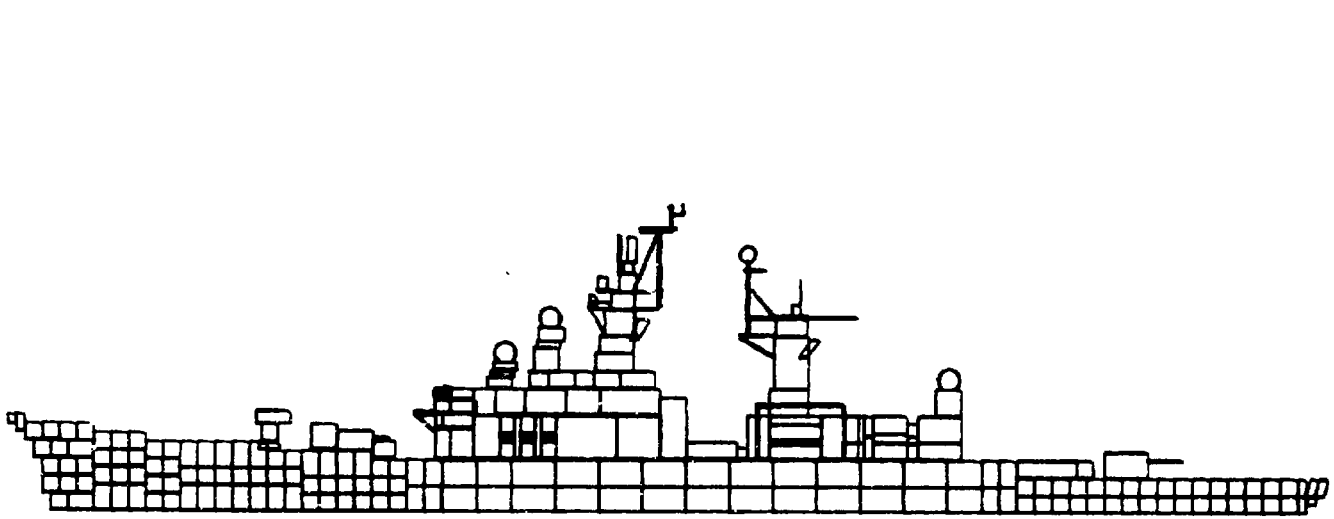

Figure 60. Broadside view of a guided missile cruiser showing the decomposition into scattering elements.

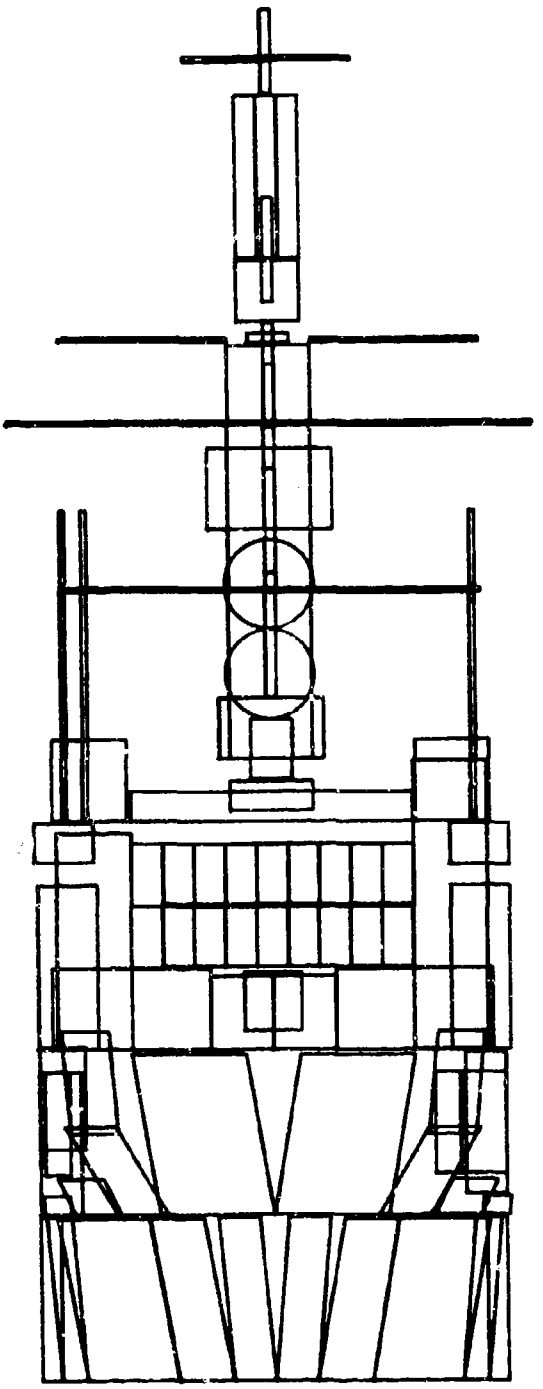

Figure 61. Bow view of guided missile cruiser.

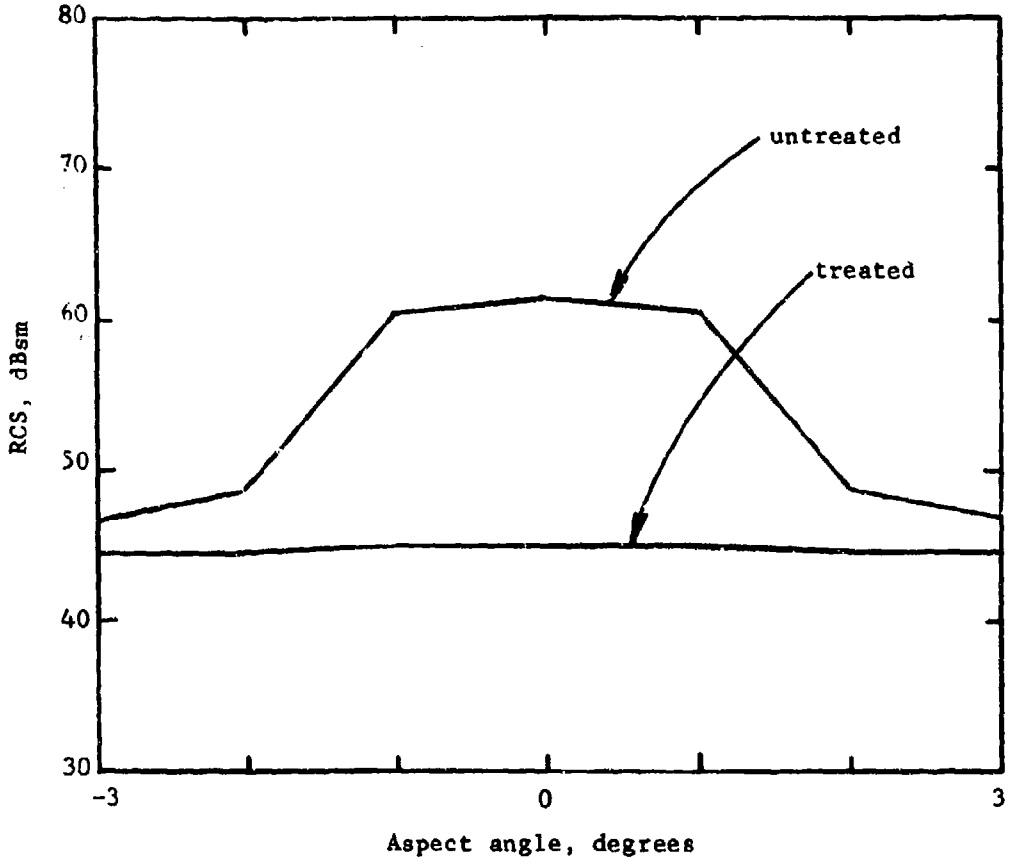

Figure 62. Results of combined effect of three RCS reduction treatments on guided missile cruiser.

The upper trace in Figure 62 represents the RCS of the untreated vessel when seen near bow-on (bow-on is represented by zero aspect angle), while the lower trace shows the effect of the treatment. The reduction is about 18 dB, implying that the return has been reduced by 98.4%.

The reduction was accomplished through the simultaneous application of three techniques. These are as follows:

1. The large forward-facing flat surface on the bridge consisting of the 18 flat plates mentioned earlier has been coated with a radar absorbent material rated at -15 dB at this frequency.

2. The 18 flat plates have been tilted away from the radar by 4 degrees.

3. Those same flat surfaces have been converted into cylinder segments with h/d = 0.3 (see Figure 29).

The ship modeling program also has the capability to display the radar cross section of the ship as a function of range, and this is shown in Figure 63 for the three separate treatments listed above. The dip in the traces at 10 nautical miles is due to the multipath effects diagrammed in Figure 31 and the roll-off beyond 20 nautical miles is due to the gradual disappearance of the ship over the horizon.

The upper trace in Figure 63 represents the behavior of the RCS of the untreated vessel; note that a peak return of 64 dBsm is registered at 15 nautical miles. The lowermost curve represents the effect of tilt; all other things being fixed, the tilting of surfaces away from the vertical is the most effective treatment that can be performed, producing an 18 dB reduction in this instance.

Treating the major scatterers (the large flat surface on the bridge composed of plates 17 through 34) with a -15 dB absorber is the next most effective procedure and yields a 14 dB reduction. The rounding of flat surfaces, although not as influential as the other two treatments, produces a 10 dB reduction, as indeed was predicted on the basis of an extrapolation of Figure 29 for h/d = 0.3. Comparison with Figure 62

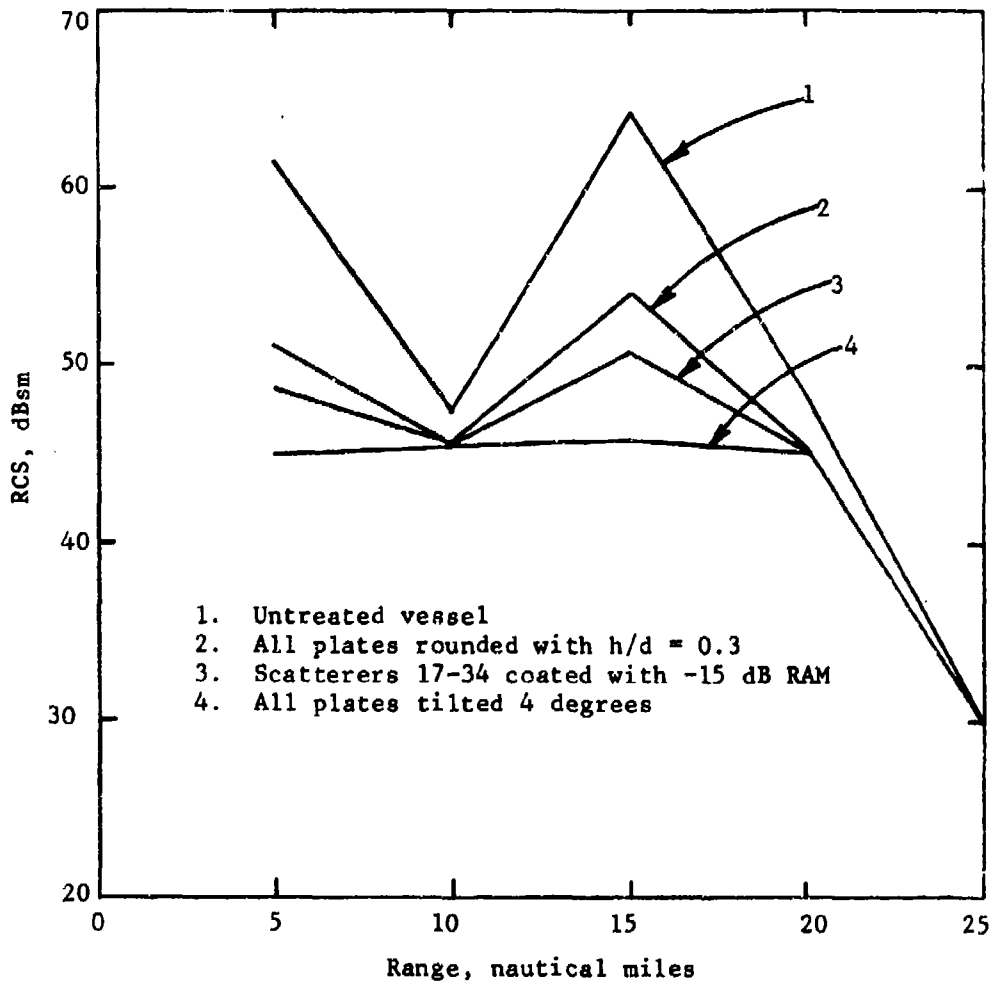

Figure 63. Effects of various treatments for a bow view as a function of range.

indicates that for this particular aspect, tilting the plates provides as much reduction as a combined treatment. However, for other incidence angles (e.g., 4 degrees), treatment other than tilt would prove most effective.

The modeling method can be seen to be a useful tool, since it allows one to ascertain the effects of RCSR treatments quickly at low cost. Moreover, the examples shown in Figures 62 and 63 reinforce the conclusions drawn earlier that tilted or rounded surfaces, together with the use of absorbent materials, represent effective RCSR treatments for conventional surface vessels.

VI. SUMMARY AND CONCLUSIONS

Each class of radar target presents its own particular RCS reduction problem. Radar absorbing materials designed for high speed aircraft must be capable of withstanding substantial mechanical and thermal loads; weight is a primary concern for satellites; techniques used on ships must consider weight, cost and maintainability. Similarly, the tactical mission of a given system greatly influences the tecnniques that may be applied. For example, the upper surfaces of an aircraft are of no concern because the aircraft will seldom be viewed from directly above. In fact, one RCS reduction procedure would be to place the engine inlet, a large source of echo, somewhere on the upper surface of the craft, where it would then be shielded from ground-based radars.

As far as ships are concerned, it must be emphasized that there is no way to make a ship disappear; it is simply too big. However, a great deal can be done to reduce the echo because conventional ship designs are far from optimum from the electromagnetic scattering or radar detectability standpoints. Large surface vessels have a classical "boxy" profile consisting of many flat surfaces that are either vertical or horizontal and that tend to meet at right angles, thus forming corner reflectors. All of these are features that contribute to the large echo.

Two primary methods of treatment for ships are radar absorbing materials and shaping, with shaping being best implemented during the engineering design of the vessel; radar absorbents can be applied in retro-fit applications and, when used in conjunction with good shaping methods, can further reduce the echo. It was shown in Section III that if flat surfaces can be rounded or curved, the return can be reduced, the more curvature the better. However, depending on the parameters of a given tactical encounter and the size of the flat surface, curving the surface may not provide the desired reduction and radar absorbents may have to be used.

Because of the presence of the sea surface, vertical surfaces are particularly objectionable and they should be tilted away from the vertical, preferably either toward or away from the radar. The optimum tilt angle is a function of the angle of arrival of the incident wave, hence a reasonable estimate must be made of this angle. For most threats it appears that a tilt angle of less than 10 degrees is sufficient and if such a tilt is impractical or too difficult to achieve, then screens might be deployed instead. On the other hand, if the deployment of screens reduces deck space too much, then absorbents might be an alternative.

It can be seen that every RCS reduction technique has advantages and disadvantages, and the end result of a treatment is likely to incorporate several of them. Because of the nature of the construction of ships the types of dominant scatterers are relatively few, although the number of such scatterers can be large. Consequently this handbook has focused only these few dominant echo sources and how they may be treated.

APPENDIX A

Bibliography

A. Radar Cross-Section Handbooks

1. J. W. Crispin, Jr. and K. M. Siegel (editors), Methods of Radar Cross Section Analysis, Academic Press, New York and London, 1968.

2. G. T. Ruck (editor), Radar Cross-Section Handbook, Vols. I and II, Plenum Press, New York and London, 1970.

3. J. J. Bowman, T. B. A. Senior and P. L. E. Usleughi, Electromagnetic and Acoustic Scattering from Simple Shapes, North-Holland Publishers, Amsterdam, 1969.

The first is smaller in size and content than the other two. The second is probably the best of the three for the practical engineer and is copiously illustrated. The third contains basic information not always presented in the other two, but is more suited to scholars than the practical engineer. All represent the collective effort of many contributors, both in original work and in surveys of the literature existing at the time of publication.

B. Other Books

4. D. E. Kerr (editor), Propagation of Short Radio Waves, MIT Radiation Laboratory Series, Vol. 13, McGraw-Hill, 1951 (also available in paper-back edition from Dover Publications, Inc., New York). Even after nearly 25 years, this volume remains an excellent reference for propagation effects.

5. P. Beckmann and A. Spizzichino, The Scattering of Electromagnetic Waves from Rough Surfaces, Pergammon Press, New York, 1963. Both theory and experiment are given to describe land and sea clutter.

C. Radar Cross-Section Reduction

6. D. R. Wehner, "Combatant Craft RCS Reduction Guidelincs (U)," Report No. TN2478, Naval Electronics Laboratory Center, 17 September 1973 (Confidential). A review of tactical priorities listing RCS reduction techniques, with emphasis on qualitative (as opposed to quantitative) procedures.

7. J. W. Crispin, Jr. and A. L. Moffett, "The Radar Cross-Section of Surface Effect Ships: the Nature of the Problem," Report No. APL SES 001(QM-72-114), The Johns Hopkins University, Applied Physics Laboratory, December 1972. An exposition of general techniques for RCS prediction and reduction methods as applied to the marine environment.

8. F. B. Dyer, M. T. Tuley and N. T. Alexander, "Methods of Radar Cross-Section Reduction (U)," Final Report on Contract N00039-72-C-1342, Engineering Experiment Station, Georgia Institute of Technology, February 1974 (Secret). A specific RCS reduction problem was attacked.

D. RCS Measurements of Ships

9. H. A. Corriher, Jr., B. O. Pyron, R. D. Wetherington and A. B. Abeling, "Radar Reflectivity of Sea Targets (U)," Vol. II, Final Report on Contract Nonr-991(12), Engineering Experiment Station, Georgia Institute of Technology, 30 September 1967 (Sercet).

10. John C. Daley, "Radar Cross-Sections of Ships," Sixteenth Annual Tri-Service Radar Symposium Record, prepared for the Air Force Avionics Laboratory by the University of Michigan under Contract F33615-70-C-1071, September 1970 (Secret), pp 595-616.

11. E. E. Maine, Jr. and F. D. Queen, "Radar Cross-Section of Surface Ships (U)," Sixteenth Annual Tri-Service Radar Symposium Record, prepared for the Air Force Avionics Laboratory by the University of Michigan under Contract F33615-70-C-1071, September 1970 (Secret), pp 617-640.

12. F. D. Queen and E. E. Maine, Jr., "Radar Cross-Sections of Surface Ships at Grazing Incidence (U)," Report No. 7338, Naval Research Laboratory, Washington, D. C. 18 November 1971 (Confidential) AD 518 382L.

13. Ir. H. Sittrop, "An Introduction to Radar Signatures of a Van Speyk-class Frigate. Part I: X-Band Characteristics. Part II: Ku-Band Characteristics," Report PHL 1974-20, Physics Laboratory, National Defense Research Organization, the Hague, The Netherlands, July 1974 (Secret).

E. RCS Reduction of Antennas

14. F. B. Dyer, M. J. Gary and W. S. Foster, "Radar Cross-Section Reduction of Antennas (U)," Final Report on Subcontract 600023 with the Applied Physics Laboratory, The Johns Hopkins University under Contract N00017-72-C-4401, Engineering Experiment Station, Georgia Institute of Technology, December 1973 (Secret).

15. C. D. Mentzer and B. A. Munk, "Resonant Metallic Radome (U)," Report No. 2382-21, AFAL-TR-70-86, ElectroScience Laboratory, Ohio State University, December 1970 (Secret) AD 509 525.

16. E. L. Pelton, "Radar Cross-Section Control by Use of a Methallic Radome (U)," Report No. 2989-13, AFAL-TR-73-96, ElectroScience Laboratory, Ohio State University, March 1973 (Secret) AD 525 55L.

17. E. L. Pelton and B. A. Munk, "A Streamlined Metallic Radome," IEEE Trans. on Ant. and Prop., Vol. AP-22, November 1974, pp 799-803.

18. B. A. Munk, R. J. Luebbers and R. D. Fulton, "Transmission through a Two-Layer Array of Loaded Slots," IEEE Trans. on Ant. and Prop., Vol. AP-22, November 1974, pp 804-809.

19. R. J. Luebbers and B. A. Munk, "Cross Polarization Losses in Periodic Arrays of Loaded Slots," IEEE Trans. on Ant. and Prop., Vol. AP-23, March 1975, pp 159-164.

F. Sea Clutter

20. C. I. Beard, I. Katz and L. M. Spetner, "Phenomenological Vector Model of Microwave Reflection from the Ocean," IRE Trans. on Ant. and Prop., Vol. AP-4, March 1956, pp 162-167.

21. C. I. Beard, "Coherent and Incoherent Scattering of Microwaves from the Ocean," IRE Trans. on Ant. and Prop., Vol. AP-9, September 1961, pp 470-483.

22. L. M. Spetner, "Incoherent Scattering of Microwaves from the Ocean," Radio Science, Volume 10, June 1975, pp 585-587.

23. D. E. Barrick and W. H. Peake, "Scattering from Surfaces with Different Roughness Scales: Analysis and Interpretation," Report BAT-197A-10-2, Battelle Memorial Institute, 1 November 1967 (Unclassified) AD 662 751.

24. J. W. Wright, "Backscattering from Capillary Waves with Application to Sea Clutter," IEEE Trans. on Ant. and Prop., Vol. AP-14, September 1974, pp 667-672.

25. S. P. Zehner, M. J. Gary, W. M. O'Dowd, Jr. and F. B. Dyer, "RTDA Feasibility Study (U)," Technical Report No. 1 on Contract N00039-73-C-0676, Engineering Experiment Station, Georgia Institute of Technology, November 1973 (Secret).

26. M. W. Long, R. D. Wetherington, J. L. Edwards and A. B. Abeling, "Wavelength Dependence of Sea Echo," Final Report on Project A-840, Engineering Experiment Station, Georgia Institute of Technology, 15 July 1965.

G. General Interest

27. R. G. Kouyoujian and L. Peters, Jr., "Range Requirements in Radar Cross-Section Measurements," Proceedings of the IEEE, Vol. 53, August 1965, pp 920-928.

28. N. I. Durlach, "Influence of the Earth's Surface on Radar," Technical Report No. 373 under Contract AF19(628)500, MIT Lincoln Laboratory, 18 January 1965, AD 627 635.

29. J. B. Keller, "Diffraction by an Aperture," Journal of Applied Physics, Vol. 28, April 1957, pp 426-444.

30. J. W. Crispin, Jr. and A. L. Maffett, "Radar Cross-Section Estimation for Simple Shapes," Proceedings of the IEEE, Vol. 53, August 1965, pp 833-848.

31. M. Abramowitz and I. A. Stegun, Handbook of Mathematical Functions, National Bureau of Standards, Ninth Printing, November 1970.

32. L. E. Carter and C. H. Kruger, Jr., "Design of Radar Absorbent Materials (U)," Technical Report AFAL-TR-74-14, Air Force Avionics Laboratory, Air Force Systems Command, Wright-Patterson Air Force Base, Ohio, February 1974. AD 530 925 (Secret).

33. R. E. Hiatt, E. F. Knott and T. B. A. Senior, "A Study of VHF Materials and Anechoic Rooms," Report No. 5391-1-F, University of Michigan Radiation Laboratory, February 1963.

34. J. J. Bowman and V. H. Weston, "The Effect of Curvature on the Reflection Coefficient of Layered Absorbers," IEEE Transactions on Ant. and Prop., Vol. AP-14, November 1966, pp 760-767.

35. M. T. Tuley, W. M. O'Dowd and F. B. Dyer, "Radar Cross-Section Reduction of Ships (U)," Final Technical Report on Contract N00039-C-0676, Engineering Experiment Station, Georgia Institute of Technology, April 1975 (Secret).

36. R. C. Johnson, H. A. Ecker and R. A. Moore, "Compact Range Techniques and Measurement," IEEE Trans. on Ant. and Prop., Vol. AP-17, September 1969, pp 568-576.

INDEX

Unclassified

SECURITY CLASSIFICATION OF THIS PAGE *(When Data Entered)*

REPORT DOCUMENTATION PAGE		READ INSTRUCTIONS BEFORE COMPLETING FORM
1. REPORT NUMBER	2. GOVT ACCESSION NO. AD-A099 566	3. RECIPIENT'S CATALOG NUMBER
4. TITLE *(and Subtitle)* RCSR GUIDELINES HANDBOOK		5. TYPE OF REPORT & PERIOD COVERED Technical Report
		6. PERFORMING ORG. REPORT NUMBER EES/GIT A-1560-001-TR-P2
7. AUTHOR(s) E. F. Knott		8. CONTRACT OR GRANT NUMBER(s) N00039-73-C-0676
9. PERFORMING ORGANIZATION NAME AND ADDRESS Systems and Techniques Laboratory, Engineering Experiment Station, Georgia Institute of Technology Atlanta, Georgia 30332		10. PROGRAM ELEMENT, PROJECT, TASK AREA & WORK UNIT NUMBERS Mod. P00007
11. CONTROLLING OFFICE NAME AND ADDRESS Department of Navy Naval Electronic Systems Command Washington, D. C. 20360		12. REPORT DATE 1 April 1976
		13. NUMBER OF PAGES viii + 140
14. MONITORING AGENCY NAME & ADDRESS *(if different from Controlling Office)*		15. SECURITY CLASS. *(of this report)*
		15a. DECLASSIFICATION DOWNGRADING SCHEDULE

16. DISTRIBUTION STATEMENT *(of this Report)*

17. DISTRIBUTION STATEMENT *(of the abstract entered in Block 20, if different from Report)*

18. SUPPLEMENTARY NOTES

Georgia Tech Project A-1560-001

19. KEY WORDS *(Continue on reverse side if necessary and identify by block number)*

Radar
Radar Cross Section
Radar Cross Section Reduction
Surface vessels

20. ABSTRACT *(Continue on reverse side if necessary and identify by block number)*

This handbook is intended as a primer for people involved in ship architecture and design but who are not necessarily familiar with radar detectability factors. Its scope is therefore broad, but its depth is limited. Methods for reducing radar ship echo are described and demonstrated.

DD FORM 1 JAN 73 1473 EDITION OF 1 NOV 65 IS OBSOLETE

Unclassified

SECURITY CLASSIFICATION OF THIS PAGE *(When Data Entered)*

cont

Modern surface ships are far from optimum shapes from the radar echo standpoint. They typically have many flat horizontal and vertical surfaces meeting at right angles, all of which constitute strong radar reflectors. Major improvements (reductions) in detectability can be made using a few simple techniques:

(1) replacing flat surfaces with curved surfaces;
(2) tilting upright surfaces away from the vertical;
(3) angling flat surfaces at other than 90 degrees;
(4) using screens;
5. installing radar absorbent materials.

Although these concepts are simple, we realize that incorporating them in ship design is not so simple. Each imposes its own brand of penalty, not the least of which is cost. Nevertheless, if dececctability is to be reduced, the penalties must be paid.